UNIVERSITY OF CALIFORNIA

Santa Barbara

The Effect of Growth Differentiation Factor 6 on the Epithelial to Mesenchymal Transition in Retinal Pigmented Epithelium

A dissertation submitted in partial satisfaction of the requirements for the degree Doctor of Philosophy in Molecular, Cellular, and Developmental Biology

By

Amanda Mae Hurley Timm

Committee in charge:

Professor Pete J. Coffey, Co-Chair

Professor Dennis O. Clegg, Co-Chair

Professor Anthony De Tomaso

Professor Stuart Feinstein

June 2019

The dissertation of Amanda Mae Hurley Timm is approved.

Anthony De Tomaso

Stuart Feinstein

Dennis O. Clegg, Committee Co-Chair

Pete J. Coffey, Committee Co-Chair

May 2019

The Effect of Growth Differentiation Factor 6

on the Epithelial to Mesenchymal Transition

in Retinal Pigmented Epithelium

By
Amanda Mae Hurley Timm

Acknowledgements

First and foremost, I would like to thank the principle investigator of my project, Dr. Pete J. Coffey. His encouragement, support, and guidance made this work possible. Having a PI who believes in you and wants you to succeed makes graduate school an easier place. I would also like to express my gratitude for my co-advisor Dr. Dennis O. Clegg. His mentorship was invaluable during my time in graduate school. I would also like to thank my committee members Dr. Stuart Feinstein and Dr. Anthony De Tomaso for their guidance and insight on my project.

I express my deepest appreciation to Dr. Monte J. Radeke. His patience, supervision, and assistance transformed me from an inquisitive student into the scientist I am today. I would also like to thank Carolyn M. Radeke for all of her technical expertise and support throughout the years. Dr. Rachael Warrington and Lindsay Bailey-Steinitz made coming into lab a fun, enjoyable experience and I thank them for all of their knowledge. My friends and family have been a huge support system over the years and have been pillars of strength and encouragement.

Finally, I would like to thank my husband, Robert, for all of his assistance. He supported me throughout this entire process and believed in me even when I did not believe in myself. This is as much yours as it is mine.

VITA of Amanda Mae Hurley Timm

May 2019

EDUCATION

Ph.D. University of California, Santa Barbara 2019
Major: Molecular, Cellular, and Developmental Biology

M.A. University of California, Santa Barbara 2017
Major: Molecular, Cellular, and Developmental Biology

Certification in Management Practice University of California, Santa Barbara 2017
Major: Technology Management

B.S. University of California, Davis 2010
Major: Biochemistry and Molecular Biology

RESEARCH EXPERIENCE

University of California, Santa Barbara **Graduate Research Assistant** 2013- Present
The Effect of Growth Differentiation Factor 6 on the Epithelial to Mesenchymal Transition in Retinal Pigmented Epithelium.
Dr. Pete J. Coffey, *peter.coffey@lifesci.ucsb.edu*

Cedars-Sinai Medical Center **Research Associate II** 2010-2013
Characterization of neural Stem cell growth and differentiation. Therapeutic use of GDNF-secreting neural progenitors in Amyotrophic Lateral Sclerosis.
Dr. Clive N. Svendsen; *clive.svendsen@cshs.org*

PUBLICATIONS

Gowing G, Shelley B, Staggenborg K, **Hurley A**, Avalos P, Victoroff J, Latter J, Garcia L, Svendsen CN. Glial cell line-derived neurotrophic factor-secreting human neural progenitors show long-term survival, maturation into astrocytes, and no tumor formation following transplantation into the spinal cord of immunocompromised rats. Neuroreport. 2014; 25(6):367-72.

Ebert A, Shelley B*, **Hurley A***, Onorati M*, Castiglioni V*, Patitucci T, Svendsen S, Mattis V, McGivern J, Schwab A, Sareen D, Kim HW, Cattaneo E, Svendsen C. EZ Spheres: A stable and expandable culture system for the generation of pre-rosette multipotent stem cells from human ESCs and iPSCs. Journal of Stem Cell Research. 2013;10(3):417-27. *Contributed equally

ABSTRACTS

Hurley A, Radeke M, Coffey P (April 2018). Growth Differentiation Factor 6 (GDF6) promotes irreversible epithelial to mesenchymal transition in retinal pigmented epithelial cells. Talk given at the Neuroscience Research Symposium, UCSB, Santa Barbara, California

Hurley A, Radeke M, Coffey P (October 2017). Growth Differentiation Factor 6 (GDF6) plays an integral role in irreversible epithelial to mesenchymal transition in retinal pigmented epithelial cells. Poster presented at the Southern California Biomedical Sciences Graduate Student Symposium, Cedars-Sinai Medical Center, Los Angeles, California.

Hurley A, Radeke M, Coffey P (April 2017). Growth Differentiation Factor 6 (GDF6) plays an integral role in irreversible epithelial to mesenchymal transition in retinal pigmented epithelial cells. Talk given at the Biology of Regenerative Medicine Conference, Wellcome Center in Hinxton, England.

Hurley A, Radeke M, Coffey P (May 2016). Growth Differentiation Factor 6 (GDF6) is a novel inducer of the epithelial-to-mesenchymal transition in retinal pigmented epithelial cells. Poster presented at ARVO, Seattle, Washington.

Hurley A, Shelley B, Castiglioni V, Onorati M, Svendsen S, Patitucci T, Mattis V, Sareen D, Kim HW, Heins B, McGivern J, Schwab A, Cattaneo E, Ebert A, Svendsen C (October 2012). EZ spheres: A characterization of a stable and expandable culture system for neural stem cells derived from hESC and hiPSC cultures. Poster presented at the Sociey for Neuroscience, New Orleans, Louisiana.

AWARDS & FELLOWSHIPS

The Jean Devlin Award in Pharmacology
The George & Joy Rathmann Fellowship
The Amgen Fellowship
The Charles A. Storke II Fellowship

TEACHING EXPERIENCE

University of California, Santa Barbara — Teaching Assistant — 2015
Course: Molecular Genetics of Prokaryotes

University of California, Santa Barbara — Teaching Assistant — 2013
Course: Introductory Biology I - Laboratory

ABSTRACT

The Effect of Growth Differentiation Factor 6 on the Epithelial-to-Mesenchymal Transition in Retinal Pigmented Epithelium

By

Amanda Mae Hurley Timm

As retinal pigmented epithelium (RPE) cells are passaged, they undergo an irreversible epithelial-to-mesenchymal transition (EMT). We have shown previously that growth differentiation factor 6 (*GDF6*), a member of the transforming growth factor-beta (TGFβ) family, is highly upregulated in RPE cells that have lost the capacity to obtain an epithelial phenotype. We hypothesize that *GDF6* plays an integral role in the irreversible transition of an RPE cell from an epithelial state to a mesenchymal state.

To test this hypothesis, we overexpressed *GDF6* in differentiation competent RPE and assessed the effects on phenotype and gene expression. To evaluate what receptors and signaling pathways might mediate GDF6's effects, cells were also treated with an Alk5 inhibitor (Repsox), an Alk2/3/6 inhibitor (LDN-193189), or both in combination. Passage 0 RPE transduced with *GDF6* produce significantly less pigmentation than cells infected with an empty vector control. This reduction in pigmentation is accompanied with a change in cell morphology; the control cells maintain a cuboidal morphology and the *GDF6* expressing cells have a spindle-like morphology. Quantitative PCR analysis reveals that RPE cells transduced with *GDF6* significantly upregulate known EMT markers like *ACTA2*, *CTGF*, and *COL1A1* and downregulate classical RPE markers such as *LRAT* and *PMEL* compared to control cells. Both RepSox and LDN-193189 have the ability to reverse the *GDF6* phenotype.

While the phenotype is recovered, RNA-seq analysis reveals *GDF6*-mediated regulation of genes that are unaffected by inhibitors, such as *TGFβ1*, *MSX2*, and *CDH1*.

GDF6 is involved in the EMT process in RPE. We believe GDF6 upregulates *TGFβ1*, which in turn promotes EMT. The ability to revert back to an epithelial cell is inhibited by GDF6. Cells exposed to GDF6 will prematurely undergo EMT, simultaneously downregulating traditional RPE markers while upregulating EMT and wound response markers. Inhibition of the BMP receptors rescues the *GDF6* phenotype, therefore inhibition of GDF6 may be integral in prolonging the integrity and functional lifespan of the RPE. As such, inhibition of GDF6 may help restore RPE to their epithelial state in diseases which affect RPE such as proliferative vitreoretinopathy and age-related macular degeneration.

TABLE OF CONTENTS

LIST OF FIGURES

LIST OF TABLES

CHAPTER I: Introduction

1.1: Retinal Pigmented Epithelium (RPE)

The retinal pigmented epithelium (RPE) is a monolayer of highly pigmented epithelial cells located in the back of the eye, residing between the photoreceptor layer of the retina and Bruch's membrane (BM). RPE cells have a very distinctive appearance—in addition to the accumulation of melanosomes contributing to the coloring of the cells, the cells are also hexagonal, resulting in a cobblestone-like structure. This monolayer is polarized, with the apical surface of the cells containing two types of microvilli and the basal surface containing multiple invaginations [1]. The apical side of the monolayer interacts with photoreceptor outer segments while the basal side faces the fenestrated choroid. RPE cells are vital in maintaining the homeostasis of the eye primarily through providing a barrier between the choroid and the retina, acting as a support cell by providing and transporting nutrients as well as phagocytosing photoreceptor outer segments, and by participating in the visual cycle [2, 3].

1.1.1: Barrier Function

A terminal maturation of the RPE, along with BM and choroidal blood vessels, establishes the outer blood-retina barrier (oBRB) [4]. The formation of this barrier is key for the regulation of nutrients and waste between the retina and choroid. One of the crucial features of oBRB development is the establishment of tight junctions, which not only maintains the polarity of the cells but also limits paracellular movement of ions and water across the monolayer [5]. The barrier ability of tight junctions allows for a concentration

gradient to be established between the apical and basal side of the monolayer [6]. The permeability of tight junctions is not the only way to move solutes from one side of the oBRB to the other; solutes can move through the oBRB using facilitated diffusion, active transport, transcytosis, or solute modification [7].

RPE barrier function is essential for transport from the blood to the retina and from the subretinal space to the blood. The oBRB, specifically the RPE layer, allows for absorption of fluid from the subretinal space, preventing retinal edema and detachment [7-9]. Glucose, retinal, and fatty acids are all taken up from the blood by the RPE and transported to the photoreceptors [2]. Breakdown or dysfunction of the oBRB can cause an imbalance of ions and nutrients in both the choroid and retina. The loss of a barrier cell layer is thought to be the root cause of many diseases in the eye, such as diabetic retinopathy and age-related macular degeneration (AMD) [10, 11]. A functioning barrier is necessary not only for disease prevention but also for the RPE cells to perform vital functions like nutrient regulation and participation in the visual cycle.

1.1.2: Support

RPE cells support both the photoreceptors in the neural retina and the endothelial and immune cells of the choroid. One way in which the RPE provide support is through polarized secretion of proteins and growth factors. RPE apically secrete matrix metalloproteinases, hyaluronan, αB crystallin, and pigment epithelium-derived factor (PEDF) [12]. PEDF is critical in maintaining the health of normal retinas through its neuroprotective, antiangiogenic, and anti-senescent functions [13]. Loss or altered expression of PEDF has been associated with the pathogenesis of AMD, so correct

expression by RPE is crucial in maintaining a healthy eye [14]. Basolateral secretion of growth factors and proteins from the RPE include fibroblast growth factor 5 (FGF-5), endothelin I, cystatin C, and vascular endothelial growth factor (VEGF) [12]. VEGF is a vascular permeability and angiogenesis factor and is essential in maintaining the fenestrated choriocapillaris [15, 16]. Breakdown of the RPE barrier may lead to the expression of VEGF in the subretinal space which causes neovascularization within the retina, leading to blindness [17]. Secretion of polarized growth factors and proteins is just one way in which the RPE support the surrounding tissue.

Another way the RPE provide support to neighboring cells is through phagocytosis of photoreceptor outer segments. RPE, due to their senescent nature and support of multiple photoreceptors per cell, are considered to be the most phagocytic cell in the body [18]. Photoreceptors are constantly forming new outer segment disks and elongating their outer segments. The RPE, in turn, remove the most distal tip of the outer segment, participating in the outer segment renewal process [19]. Defects in the phagocytic ability of RPE impair retinal function and can lead to complete retinal degeneration and blinding disorders such as retinitis pigmentosa [20, 21]. RPE cells are central in the support and maintenance of the photoreceptors, and this dependent relationship is necessary for processing visual cues.

1.1.3: Visual Cycle

The RPE are essential components of the visual cycle as they re-isomerize all-trans-retinal (vitamin A) to 11-cis retinal [2]. Phototransduction begins with the absorption of light by visual pigments (rhodopsin and cone opsins) in the photoreceptors, where capture of light results in the isomerization of 11-cis retinal to all-trans retinal [22]. Lecithin retinol

acyltransferase (LRAT) helps the RPE uptake retinoids from both the choroid and the photoreceptors, and retinoid isomerase (RPE65) catalyzes all-trans retinal to 11-cis retinal [23]. The cycling of vitamin A analogs between RPE and photoreceptor cells replenishes 11-cis retinal for sustained phototransduction [24]. Dysfunction in the pathway, either in RPE or photoreceptors, has been linked to numerous blinding disorders [22].

1.1.4: Age-Related Defects

RPE have been known to undergo a variety of age-related changes, including loss of melanin granules, the formation of drusen, microvilli atrophy, and accumulation of lipofuscin, among other changes [25]. As RPE density decreases by up to 0.3% a year, the RPE struggle to maintain a proper barrier function, increasing their size to fill the gaps [26, 27]. If the wound is too large to fill, RPE will attempt to proliferate to close the wound [28]. Aged RPE have shown defects in repairing large holes in the monolayer and instead undergo atrophy or a fibrotic mesenchymal differentiation [29, 30]. AMD, the most common blinding disorder in the developed world, is directly associated with aging of the RPE [31].

1.2: Epithelial-to-Mesenchymal Transition (EMT)

The epithelial-to-mesenchymal transition (EMT) is a phenomenon in which stationary epithelial cells take on a mobile mesenchymal-like state. EMT transforms the cell through disruption of their cell-cell junctions, loss of apical-basal polarity, the disintegration of the underlying basement membrane, and reorganization of the extracellular matrix (ECM) [32, 33]. One of the hallmarks of EMT is the repression of E-cadherin (CDH1), occludins, and cytokeratins and activation of N-cadherin (CDH2) and vimentin (VIM), converting the cell from a cuboidal morphology to a spindle-shaped cell [32, 34]. This

transition allows for the resulting cell to be migratory and invasive, a trait needed in development and wound healing but unwanted in cancer. This process was initially called a transformation, indicating that the process was not reversible [35]. However, another phenomenon, known as the mesenchymal-to-epithelial transition (MET), led to a change in terminology to transition, indicating the potential for the process to be reversed [36, 37]. EMT is subdivided into three types: EMT during development (Type 1), EMT during wound healing and fibrosis (Type 2), and EMT in cancer (Type 3).

1.2.1: Type 1 EMT

Type 1 EMT is found during implantation, embryogenesis, and organ development of an organism [38]. Gastrulation of the embryo is the first instance of EMT as cells from the epiblast form the primitive streak, which undergoes EMT to form mesoderm and endoderm [39]. Neural crest cells, which can give rise to melanocytes and the peripheral nervous system, undergo EMT from the dorsal neural epithelium, allowing cells to migrate before differentiation [34]. Subsequent rounds of EMT are then initiated to form other mesodermal structures such as cardiac valves and the secondary plate [40].

1.2.2: Type 2 EMT

Wound healing and organ fibrosis is Type 2 EMT, or EMT that occurs after development. In Type 2 EMT, epithelial cells become myofibroblasts in order to repair injured tissues; if the wound is small it is reparative fibrosis, but if there is chronic injury and inflammation the myofibroblasts can cause progressive fibrosis and lead to organ destruction [41]. EMT is a necessary process to repair a disrupted epithelial layer; however aberrant wound healing can lead to disease. Fibrotic diseases of the kidney and lung as well

as fibrotic diseases of the eye, including AMD, are induced by Type 2 EMT [38, 42]. Growth factors such as fibroblast growth factor 2 (FGF-2), epidermal growth factor (EGF), and transforming growth factor-beta (TGFβ) have been known to induce EMT and are often expressed by inflammatory cells [36]. Inhibition of these growth factors, primarily TGFβ, is a target for the prevention of fibrosis [34].

1.2.3: Type 3 EMT

Metastasis of cancer is related to the migration and invasion of cancerous cells into other tissues. Type 3 EMT is linked with cancer progression from normal epithelium to invasive carcinoma [38]. Unlike internal induction of EMT in development, cancer cells are believed to undergo EMT based on external factors [43]. Metastasis can be broken down into five steps: invasion, intravasation, systemic transport, extravasation, and colonization [43]. Early-stage carcinomas are generally in an epithelial state and take on more mesenchymal features as tumor progression continues [32]. However, there is doubt and skepticism about the role of EMT in cancer, especially because metastases often appear histologically identical to the original tumor [44]. In order for the metastases to be identical, the tumor cells must undergo an EMT in order to migrate to their new location, and then undergo MET to revert to an epithelial state [45]. This phenomenon has been observed in colorectal cancer, providing proof to the hypothesis that EMT of cancerous cells leads to metastasis [46]. Understanding both EMT and MET are necessary to understand and prevent the spread of cancer.

1.2.4: Mesenchymal-to-Epithelial Transition (MET)

The mesenchymal-to-epithelial transition is the opposite of EMT, lending to the reversibility of the phenomenon. Mesenchymal cells can achieve apicobasal polarity through the establishment of tight junctions and expression of epithelial markers like CDH1 [32]. MET is present in morphogenesis and organogenesis, pairing with EMT to create multiple cell types [37]. Specifically, MET is critical in somitogenesis, cardiogenesis, and hepatogenesis [47]. Additionally, the reprogramming of fibroblasts to induced pluripotent stem cells requires MET [48]. MET is also an essential part of successful wound healing, as the epithelial layer needs to reestablish itself after closing the wound [32]. Understanding the mechanisms behind EMT and MET can prove helpful when trying to prevent aberrant wound healing and in stopping cancer progression.

1.3: Transforming Growth Factor-Beta (TGFβ) Superfamily

Over 30 secreted dimeric ligands comprise the TGFβ superfamily, and it is grouped into multiple subfamilies: the TGFβ protein family, bone morphogenic protein (BMP) family, growth differentiation factor (GDF) family, activin and inhibin family, glial cell-derived neurotrophic factor (GDNF) family, as well as anti-Mullerian hormone (AMH) and nodal [49]. All members of the superfamily are synthesized as a large precursor molecule, with the pro-domain undergoing cleavage to produce an active ligand. The TGFβ proteins and GDF8 are different from the rest of the family in that they are secreted as an inactive precursor and are subsequently cleaved into a latent and mature peptide which remains covalently attached to prevent unwanted signaling through the receptor [50]. The active domains of

the TGFβ superfamily proteins contain six intra-strand disulfide bonds, forming a characteristic “cysteine knot” folding motif [50].

The ligands bind to serine/threonine kinase receptors located on the cell surface. There are two groups of receptors that the TGFβ superfamily can bind to: type I receptors (Activin-like kinase; Alk) and type II receptors. The receptors form heterotetrameric complexes of two type I and two type II receptors upon binding of the dimeric protein [51]. The close interaction of the receptors promotes type II receptor phosphorylation of the type I receptor, which then goes on to phosphorylate members of the receptor-activated Smad (R-Smad) family [51]. Though there is a high diversity of ligands, there are few receptors to interact with; only five type I receptors and seven type II receptors are present in mammals [52]. This sameness leads to differing affinities for receptors and multiple combinations of receptors, which can help explain the diversity in signaling responses to TGFβ superfamily members [50, 53, 54]. Additionally, the TGFβ superfamily can also participate in non-canonical signaling through the mitogen-activated kinase (MAPK) pathways, Rho-like GTPase pathways, and phosphatidylinositol-3-kinase/AKT pathways [55, 56].

1.3.1: TGFβ Proteins

TGFβ1, TGFβ2, and TGFβ3 are the three isomers that make up the TGFβ subfamily of proteins. These three proteins are synthesized as pre-pro-peptides that contain a signal peptide, a latency associated peptide (LAP), and the active peptide. Before secretion, the TGFβ proteins form a pro-peptide homodimer containing two LAP chains and two active peptide chains [57]. The LAP chains are separated from the active peptides by the enzyme

furin in the Golgi apparatus and proceed to form a large latent TGFβ complex, facilitating the export of TGFβ out of the cell [57, 58].

The TGFβ proteins are secreted in an inactive form and must be converted to a biologically active form. Several molecules have been hypothesized to activate the TGFβ isoforms, including plasmin, thrombospondin-1 (TSP-1), reactive oxygen species, changes in pH, and the integrin $\alpha_v\beta_6$ [58, 59]. Once the protein is in its active form, it can interact with its receptors and participate in signal transduction. TGFβ proteins often signal through the canonical type I receptor Alk5 but have been known to signal through Alk1 in endothelial cells [60, 61]. Canonical TGFβ signaling results in the phosphorylation of the R-Smad2/3.

TGFβ proteins play many roles in the eye, from development to disease. TGFβ signaling is necessary in retinal development as it protects retinal neurons from programmed cell death [62]. Proper differentiation of lens epithelial cells also requires TGFβ signaling as prevention of signaling causes nuclear cataracts [63]. However, various fibrotic eye diseases and EMT of RPE is associated with TGFβ signaling in the mature eye [64]. TGFβ expression has been directly linked to the wet form of AMD, choroidal neovascularization (CNV), as well as proliferative vitreoretinal diseases [65, 66]. Inhibition of TGFβ proteins may be critical in preventing blinding disorders of the eye.

1.3.2: Bone Morphogenic Proteins (BMPs) and Growth Differentiation Factors (GDFs)

BMPs and GDFs constitute the largest TGFβ subfamily with over 20 different proteins. The subfamily is further divided into at least four subgroups based on sequence similarity: BMP2/4, BMP5/6/7/8, BMP9/10, and BMP12/13/14 (GDF 5/6/7) [67, 68]. The prodomain does form a complex with the BMP peptide to exit the cell but unlike TGFβ

proteins, does not need to be activated in the extracellular matrix (ECM) [69]. This complex allows for sequestration of BMPs in the ECM, and complete activity may require the release of the protein from the ECM [68]. BMPs can signal through three different type I receptors Alk3 (BMP type 1A receptor; BMPR1A), Alk 6 (BMP type 1B receptor; BMPR1B), or Alk2 (type 1A activin receptor; ActRIA) and three type 2 receptors BMPR2 (BMP type 2 receptor), type 2A activin receptor (ActRIIA), and ActRIIB (type 2B activin receptor) [67]. Binding and phosphorylation of these receptors result in the phosphorylation of (R)-Smad1/5/9.

Proper development of the eye requires both positive and negative regulation of BMP signaling [70]. BMP4 controls the patterning of the dorsoventral axis of the retina; BMP4 expression results in dorsal features and inhibition of expression, possibly through antagonists ventroptin or noggin, produces ventral features [71]. BMP4 and BMP7 both induce optic cup formation and lens induction [67]. Disease of the mature eye often results from expression of BMPs, similar to what is seen with TGFβ proteins. For example, GDF5 and BMP7 have been affiliated with osseous metaplasia, or bone development in the eye [72].

1.3.3: Activins and Inhibins

Activins and inhibins encompass another prominent subfamily of the TGFβ superfamily. Both share a common β subunit, of which four isomers exist. Activins are composed of a homodimer of β subunits and inhibins are a heterodimer of α and β subunits. As seen with other TGFβ family members, synthesis of activins and inhibins includes the creation of a pro-peptide, cleavage of the pro-domain from the active peptide, and complex formation to shuttle the protein out of the cell, protecting the active protein

dimer from degradation in the ECM [73]. The ligands can bind to two different type II receptors (ActRIIA or ActRIIB) which induces binding to the type I receptors Alk4 or Alk7 [74]. Phosphorylation of (R)-Smad 2/3 occurs upon phosphorylation of the type I receptor.

As seen with the other TGFβ superfamily members, both eye development and disease of the eye involves activin signaling. Activin signaling promotes eye field specification and differentiation of retinal progenitor cells from embryonic stem cells [75]. However, activin is a potent inducer of mesenchyme and thus linked with many fibrotic diseases of the eye [76, 77]. In CNV, an increase in activin expression correlates with an increase in vascular endothelial growth factor (VEGF), a known marker of the disease [78]. Activin A is also found to be involved in proliferative vitreoretinal diseases, regulating tissue fibrosis and angiogenesis [79].

1.3.4: Canonical Signaling

The canonical signaling pathway of the TGFβ superfamily involves phosphorylation of Smad proteins (Figure 1.1). Smad proteins can be classified into three groups: R-Smads, common-mediator Smads (Co-Smads), and inhibitory Smads (I-Smads). R-Smads consist of Smad1, Smad2, Smad3, Smad5, and Smad9 (also known as Smad8), Smad4 is a Co-Smad, and I-Smads include Smad6 and Smad7 [80, 81]. The combination of type I and type II receptors determine what ligand binds and what R-Smads are phosphorylated. The type II receptor is constitutively active, and ligand binding induces recruitment and subsequent phosphorylation of serine and threonine residues on the type I receptor [82].

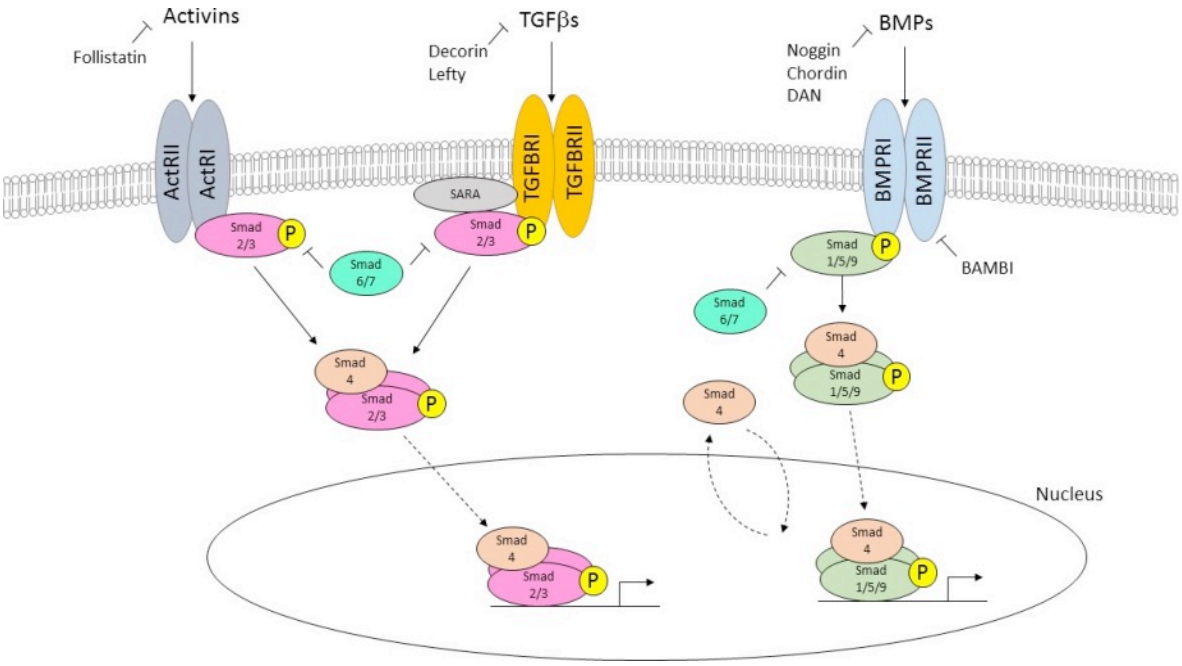

Figure 1.1. Canonical signaling of the TGFβ superfamily. Upon binding of the ligand to the appropriate type II receptor, phosphorylation of the type I receptor occurs, inducing phosphorylation of the receptor-activated Smads (Smad2/3 or Smad1/5/9). The phosphorylated Smad proteins then form a heterotrimeric complex with the co-Smad Smad4, allowing for transport into the nucleus where the Smad proteins can bind to DNA and affect gene transcription.

R-Smads (Smad 1/2/3/5/9) are recruited to the type I receptor where phosphorylation occurs at the extreme C termini, allowing for heterotrimeric complex formation with other Smads and with Smad 4, a mediator Smad [83]. Activated Alk4/5/7 phosphorylate Smad2/3 while Alk1/2/3/6 phosphorylate Smad1/5/9 [84]. Smad2/3 proteins remain accessible to the receptors through immobilization by the Smad anchor for receptor activation (SARA), and phosphorylation of the proteins causes dissociation of Smad2/3 from the SARA complex [85, 86]. Smad4 has a nuclear import signal, thus enabling the newly formed heterotrimeric complex to enter the nucleus where the Smad proteins can bind to DNA and affect gene transcription [87].

I-Smads are directly induced by and mediate negative feedback in TGFβ signaling [83]. I-Smads can directly block signaling through competitive inhibition of the type I receptor sites with R-Smads [88]. Indirect methods of silencing Smad signaling include prevention of heterotrimeric complex formation with R-Smads and co-Smads, transcriptional regulation in the nucleus, and down-regulation of type I receptors [89]. Diseases associated with fibrosis, autoimmune disorders, and cancer are linked to dysregulation of Smad signaling [90-92].

1.3.5: Inhibitors

In addition to the inhibitory Smads, a number of ligands can modulate Smad signaling. Decorin (DCN) is a proteoglycan found in the ECM and is primarily synthesized by fibroblasts, smooth muscle cells, and stressed vascular endothelial cells [93]. DCN antagonizes members of the receptor tyrosine kinase (RTK) family such as EGFR, insulin-like growth factor receptor I (IGF-IR), and hepatocyte growth factor receptor (Met) and has been observed to sequester growth factors, including TGFβ1 [93]. DCN is thought to disrupt TGFβ signaling through an increase in calcium signaling, which causes activation of calmodulin-dependent protein kinase II and subsequent phosphorylation of Smad2 at a negative regulatory site [94]. Another inhibitor of TGFβ protein signaling is the morphogen lefty. Lefty can inhibit Smad2 phosphorylation as well as downstream signaling events, like the formation of the heterotrimeric complex with Smad4 and nuclear localization, without upregulating inhibitory Smads [95].

While activin signaling induces phosphorylation of the same Smad proteins as TGFβ signaling (Smad2/3), inhibition occurs by a different mechanism. Follistatin (FST) complexes

with activin and covers its receptor binding domain, preventing binding to the type II receptor and inhibiting signaling [96]. FST has the highest affinity for activin but has also been observed to bind with myostatin (GDF8) and BMP2/4/6/7 [97]. The BMP antagonist noggin also inhibits through direct binding. Noggin can bind to and inactivate BMPs by blocking the binding sites to both the type I and type II receptor, similar to FST [98, 99]. Chordin, another BMP antagonist, blocks the receptor binding sites of BMPs by forming a horseshoe-shaped complex around the BMP [100, 101].

The differential screening-selected gene in neuroblastoma (DAN) family is comprised of seven BMP antagonists: Nbl1, uterine sensitization-associated gene 1 (USAG-1), Coco, Cerberus, sclerostin (SOST), Gremlin, and Gremlin-2 [102]. Different members of the family exhibit differing affinity for the BMP ligands; Gremlin, Coco, and Gremlin-2 all show preference to BMP2/4/7 whereas Nbl1 has an affinity for BMP2/4 and GDF5 [102]. Unlike Noggin whose antagonistic region for BMP7 lies within its N-terminus, DAN family members inhibit BMPs through amino acids located in their DAN domains [103, 104]. The mechanism of action of BMP inhibition by the DAN family is still undetermined, but it is likely to prevent binding of BMPs to their receptors by blocking the receptor binding sites and forming a complex with the ligand.

1.4: An in vitro Model for EMT in RPE

The culture of RPE *in vitro* can elucidate mechanisms of diseases like AMD and provide the potential for new therapeutics through drug screening. In order to understand disease pathology and progression, a model for the disease must be established. Radeke *et al*. (2015), was able to induce a mesenchymal transition in RPE using a passaging model

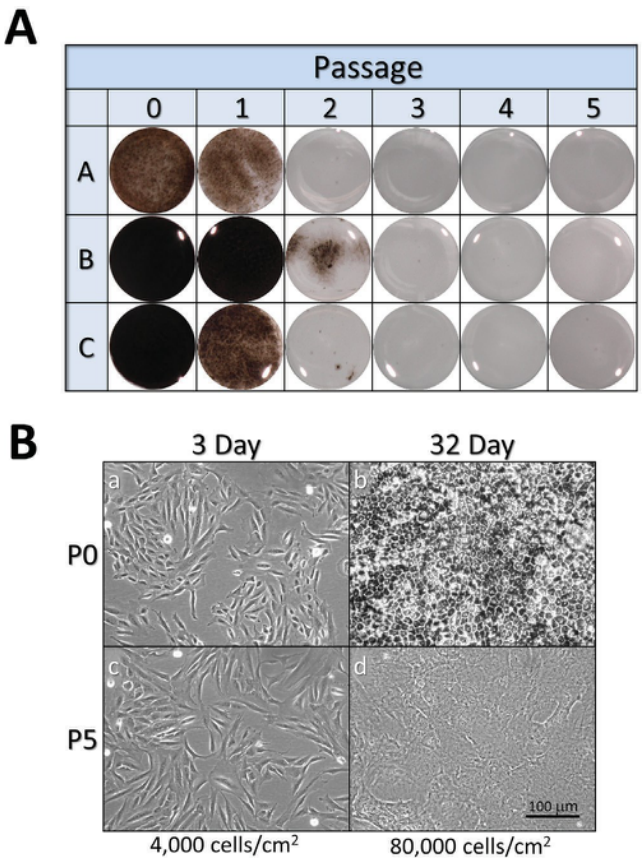

Figure 1.2. Sustained subconfluent culture reduces the differentiation capabilities of RPE. (A) Whole-mount images of 3 RPE donors that were serially passaged. At each passage, RPE were plated at 80,000 cells/cm^2 and allowed to differentiate for 64 days. (B) Phase contrast images of Passage 0 (P0) and passage 5 (P5) RPE. RPE were plated at a low density (4,000 cells/cm^2) and imaged after 3 days or plated at a high density (80,000 cells/cm^2) and imaged after 32 days of differentiation. Images were reproduced from a previous publication [105].

simulating a chronic wound response [105]. They found that constant subconfluent culture reduced the ability for RPE to differentiate, with the RPE losing their ability to pigment after a couple of passages (Figure 1.2 A). By passage 5 (P5), RPE were no longer able to maintain their RPE phenotype, instead exhibiting mesenchymal traits like a spindle-like shape and loss of a cuboidal morphology (Figure 1.2 B). Interestingly, passage 0 (P0) RPE (RPE that can differentiate into a healthy monolayer) and P5 RPE have similar morphologies after three days when plated at a low density, suggesting that both passages of RPE undergo EMT.

However, the P0 cells can undergo MET and regain their epithelial phenotype when induced to differentiate.

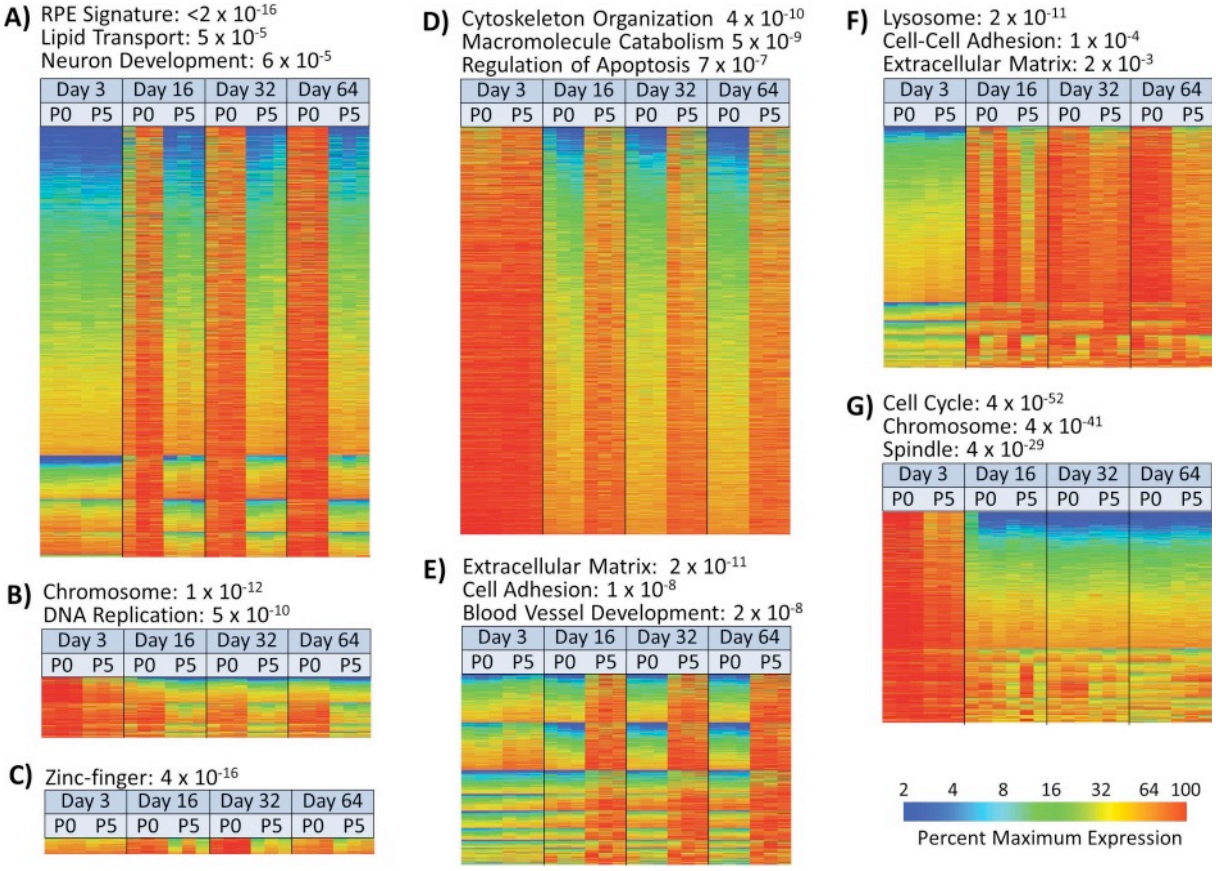

Figure 1.3. Transcriptome profiling and cluster analysis of P0 and P5 RPE. Microarray analysis was performed on P0 or P5 RPE plated at a low density (4,000 cells/cm^2) and harvested after 3 days or plated at a high density (80,000 cells/cm^2) and allowed to differentiate for 16, 32, or 64 days before harvesting. Genes were placed into clusters using AutoSOME 2.1, and individual clusters were manually placed into larger expression groups. The color scale indicates the expression level as a percentage of the maximum expression value for the gene. Images were reproduced from a previous publication [105].

This led Radeke *et al*. (2015) to further investigate the differences between P0 and P5 RPE, specifically the changes in gene expression between the two populations [105]. Transcriptome profiling revealed that nearly two-thirds of genes were differentially expressed with a fold change greater than or equal to two between the two passages

(Figure 1.3). Clustering analysis revealed classes of genes specific to either P0 or P5 RPE. Clusters A-C are comprised of genes specific to P0 cells and/or normal RPE differentiation; these genes fall into categories such as RPE differentiation, neuron development, DNA replication, and zinc finger proteins. Cluster D showcases genes relating to EMT as both P0 and P5 RPE express these genes while they have a mesenchymal appearance (3 days), but P0 RPE begin to downregulate these genes upon initiation of differentiation. Cluster E is one of the most interesting clusters as it highlights genes specific to P5 RPE maturation where cells exhibit a terminal, fibrotic EMT phenotype. This cluster includes genes related to the ECM, blood vessel development, and cell adhesion.

In order to provide a therapeutic approach for diseases in which RPE undergo EMT, we need to understand what causes RPE to be pushed towards a fibrotic state, preventing the cells from undergoing MET. Radeke *et al*. (2015) examined the genes in clusters D and E, looking for genes that were not present in the P0 population but were highly expressed in P5 RPE [105]. TGFβ family members were given special attention as mesenchymal RPE given A-83-01, a TGFβ type I receptor inhibitor (Alk4/5/7), were able to undergo MET and differentiate into a healthy RPE monolayer, suggesting members the TGFβ family inhibit MET in RPE (Figure 1.4). *TGFβ1* and *TGFβ2* were both present in P5 RPE, but they did not exhibit a large increase in expression levels as a function of passage (Figure 1.5). However, growth and differentiation factor 6 (*GDF6*/*BMP13*) exhibited an expression profile matching the requirements for an inhibitor of RPE differentiation: no expression in P0 RPE and high expression in P5 RPE. This makes *GDF6* an ideal candidate to target to promote healthy RPE differentiation in passaged cells.

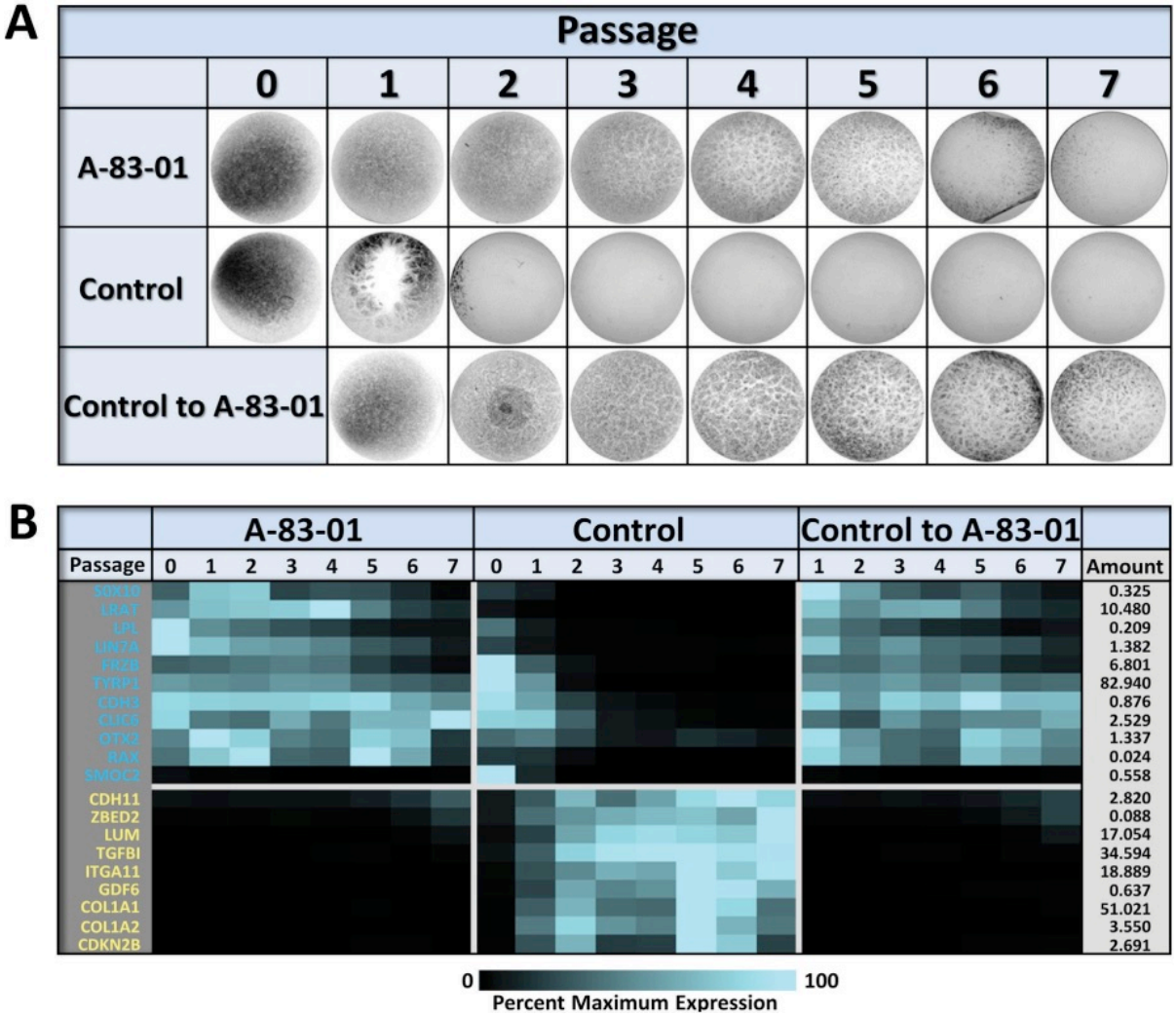

Figure 1.4. Inhibition of TGFβ signaling extends and restores the RPE phenotype. (A) Whole culture photographs of differentiated RPE. RPE were serially passaged and supplemented with 500 nM of the TGFβ inhibitor A-83-01 or normal media. Cells were plated at a high density (80,000 cells/cm^2) at each passage and allowed to differentiate for 32 days. RPE passaged in normal media were also placed into a media containing A-83-01 and allowed to differentiate. (B) RT-qPCR analysis of healthy RPE (blue gene symbols) and RPE wound response (yellow gene symbols). The blue color scale indicates the percent maximum expression of the gene, with the maximum normalized amount listed in the right column titled "Amount". Images were reproduced from a previous publication [105].

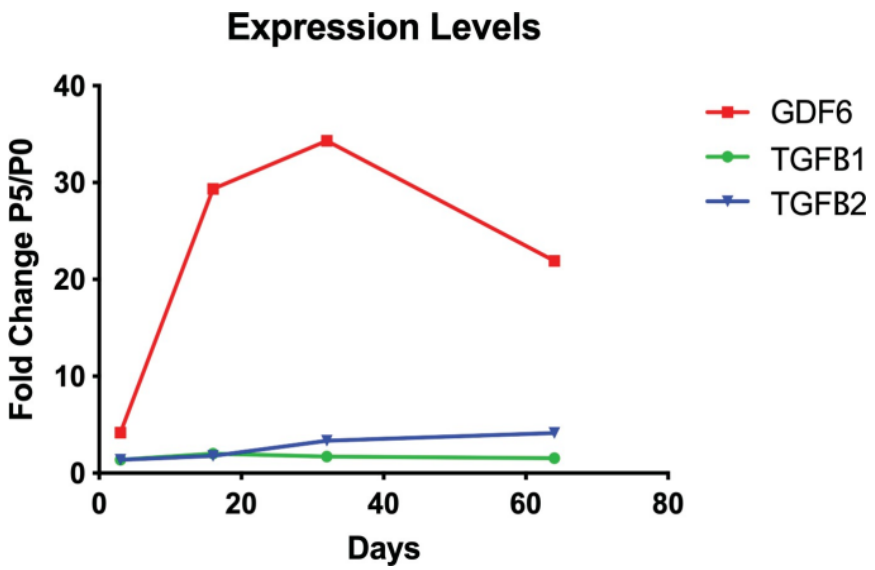

Figure 1.5. Change in expression levels of selected TGFβ family members over time. The fold change of genes in P5 RPE to P0 RPE at different time points of differentiation was determined. Figure was generated with data supplied from a previous publication [105].

1.5: Growth Differentiation Factor 6 (GDF6)

Growth differentiation factor 6 (GDF6/BMP13) is a member of the bone morphogenic protein subfamily, participating in canonical Smad1/5/9 phosphorylation. GDF6 was first discovered, along with GDF5 and GDF7, to have a role in limb alterations and tendon formations, hence its membership in the BMP family [106, 107]. GDF6 is required in the proper development of an organism, as *GDF6* mutants exhibit a fusion in the carpel and tarsal elements, proposing GDF6 is essential for separation of early embryonic condensation units into separate skeletal elements [108]. Mutations in *GDF6* have been observed in Klippel-Feil Syndrome, a disease in which anterior and cervical vertebrae are fused [109]. Induction of *THBS4*, a tendon marker, occurs in the presence of GDF6, transforming cells into collagen-secreting fibroblasts [110]. Multiple synostoses syndrome, a disease involving

joint defects and sometimes progressive deafness, is also correlated with mutations in *GDF6* [111-113].

In addition to the joint and tendon formation commonly associated with BMPs, *GDF6* has also proved to be important in retinal development. Both microphthalmia and anophthalmia have been linked to defects in *GDF6*, and *GDF6* knockout mice exhibit defects in neural tube formation, loss of key retinal genes *PAX6* and *NCAM*, and increased apoptosis in the retina [114, 115]. *GDF6* helps pattern the dorsoventral axis in the retina and is required for proper photoreceptor development and differentiation [116]. *GDF6* is needed in the healthy development of the eye but may become harmful post-development.

1.6: Specific Goals

The goal of my Ph.D. research is to dissect RPE EMT and understand the underlying mechanisms in order to prevent disease.

1. In the first experimental chapter, chapter three, we address the involvement of *GDF6* in RPE EMT.
2. The fourth chapter investigates if inhibition of GDF6 can prevent EMT in RPE.
3. The mechanism of GDF6 in RPE is evaluated in the final experimental chapter five.

Together the findings in this dissertation provide insight into the role of *GDF6* in RPE and possible ways to prevent fibrotic EMT.

1.7: References

1. Boulton, M. and P. Dayhaw-Barker, *The role of the retinal pigment epithelium: topographical variation and ageing changes.* Eye (Lond), 2001. **15**(Pt 3): p. 384-9.
2. Strauss, O., *The Retinal Pigment Epithelium*, in *Webvision: The Organization of the Retina and Visual System [Internet].* F.E. Kolb H, Nelson R, Editor. 2011, University of Utah Health Sciences Center.

3. Simo, R., et al., *The retinal pigment epithelium: something more than a constituent of the blood-retinal barrier--implications for the pathogenesis of diabetic retinopathy.* J Biomed Biotechnol, 2010. **2010**: p. 190724.
4. Benedicto, I., et al., *Concerted regulation of retinal pigment epithelium basement membrane and barrier function by angiocrine factors.* Nat Commun, 2017. **8**: p. 15374.
5. Rizzolo, L.J., *Development and role of tight junctions in the retinal pigment epithelium.* Int Rev Cytol, 2007. **258**: p. 195-234.
6. Rahner, C., et al., *The apical and basal environments of the retinal pigment epithelium regulate the maturation of tight junctions during development.* J Cell Sci, 2004. **117**(Pt 15): p. 3307-18.
7. Rizzolo, L.J., et al., *Integration of tight junctions and claudins with the barrier functions of the retinal pigment epithelium.* Prog Retin Eye Res, 2011. **30**(5): p. 296-323.
8. Negi, A. and M.F. Marmor, *The resorption of subretinal fluid after diffuse damage to the retinal pigment epithelium.* Invest Ophthalmol Vis Sci, 1983. **24**(11): p. 1475-9.
9. Chihara, E. and N. Nao-i, *Resorption of subretinal fluid by transepithelial flow of the retinal pigment epithelium.* Graefes Arch Clin Exp Ophthalmol, 1985. **223**(4): p. 202-4.
10. Xu, H.Z. and Y.Z. Le, *Significance of outer blood-retina barrier breakdown in diabetes and ischemia.* Invest Ophthalmol Vis Sci, 2011. **52**(5): p. 2160-4.
11. Cunha-Vaz, J., *The Blood-Retinal Barrier in the Management of Retinal Disease: EURETINA Award Lecture*, in *Ophthalmologica*. 2017, (c) 2017 S. Karger AG, Basel.: Switzerland. p. 1-10.
12. Kay, P., Y.C. Yang, and L. Paraoan, *Directional protein secretion by the retinal pigment epithelium: roles in retinal health and the development of age-related macular degeneration.* J Cell Mol Med, 2013. **17**(7): p. 833-43.
13. Zhu, D., et al., *Polarized secretion of PEDF from human embryonic stem cell-derived RPE promotes retinal progenitor cell survival.* Invest Ophthalmol Vis Sci, 2011. **52**(3): p. 1573-85.
14. Farnoodian, M., et al., *Expression of pigment epithelium-derived factor and thrombospondin-1 regulate proliferation and migration of retinal pigment epithelial cells.* Physiol Rep, 2015. **3**(1).
15. Blaauwgeers, H.G., et al., *Polarized vascular endothelial growth factor secretion by human retinal pigment epithelium and localization of vascular endothelial growth factor receptors on the inner choriocapillaris. Evidence for a trophic paracrine relation.* Am J Pathol, 1999. **155**(2): p. 421-8.
16. Saint-Geniez, M., et al., *An essential role for RPE-derived soluble VEGF in the maintenance of the choriocapillaris.* Proc Natl Acad Sci U S A, 2009. **106**(44): p. 18751-6.
17. Okamoto, N., et al., *Transgenic mice with increased expression of vascular endothelial growth factor in the retina: a new model of intraretinal and subretinal neovascularization.* Am J Pathol, 1997. **151**(1): p. 281-91.

18. Mazzoni, F., H. Safa, and S.C. Finnemann, *Understanding photoreceptor outer segment phagocytosis: use and utility of RPE cells in culture.* Exp Eye Res, 2014. **126**: p. 51-60.
19. Young, R.W. and D. Bok, *Participation of the retinal pigment epithelium in the rod outer segment renewal process.* J Cell Biol, 1969. **42**(2): p. 392-403.
20. Bok, D. and M.O. Hall, *The role of the pigment epithelium in the etiology of inherited retinal dystrophy in the rat.* J Cell Biol, 1971. **49**(3): p. 664-82.
21. Gal, A., et al., *Mutations in MERTK, the human orthologue of the RCS rat retinal dystrophy gene, cause retinitis pigmentosa.* Nat Genet, 2000. **26**(3): p. 270-1.
22. Thompson, D.A. and A. Gal, *Vitamin A metabolism in the retinal pigment epithelium: genes, mutations, and diseases.* Prog Retin Eye Res, 2003. **22**(5): p. 683-703.
23. Kiser, P.D., M. Golczak, and K. Palczewski, *Chemistry of the retinoid (visual) cycle.* Chem Rev, 2014. **114**(1): p. 194-232.
24. Fulton, B.S. and R.R. Rando, *Biosynthesis of 11-cis-retinoids and retinyl esters by bovine pigment epithelium membranes.* Biochemistry, 1987. **26**(24): p. 7938-45.
25. Gu, X., et al., *Age-related changes in the retinal pigment epithelium (RPE).* PLoS One, 2012. **7**(6): p. e38673.
26. Panda-Jonas, S., J.B. Jonas, and M. Jakobczyk-Zmija, *Retinal pigment epithelial cell count, distribution, and correlations in normal human eyes.* Am J Ophthalmol, 1996. **121**(2): p. 181-9.
27. Boulton, M., M. Roanowska, and T. Wess, *Ageing of the retinal pigment epithelium: implications for transplantation.* Graefes Arch Clin Exp Ophthalmol, 2004. **242**(1): p. 76-84.
28. Stern, J. and S. Temple, *Retinal pigment epithelial cell proliferation.* Exp Biol Med (Maywood), 2015. **240**(8): p. 1079-86.
29. Zarbin, M.A., *Progressive RPE atrophy around disciform scars*, in *Br J Ophthalmol*. 2006: England. p. 396-7.
30. Friedlander, M., *Fibrosis and diseases of the eye.* J Clin Invest, 2007. **117**(3): p. 576-86.
31. Wong, W.L., et al., *Global prevalence of age-related macular degeneration and disease burden projection for 2020 and 2040: a systematic review and meta-analysis.* Lancet Glob Health, 2014. **2**(2): p. e106-16.
32. Dongre, A. and R.A. Weinberg, *New insights into the mechanisms of epithelial-mesenchymal transition and implications for cancer.* Nat Rev Mol Cell Biol, 2019. **20**(2): p. 69-84.
33. Lamouille, S., J. Xu, and R. Derynck, *Molecular mechanisms of epithelial-mesenchymal transition.* Nat Rev Mol Cell Biol, 2014. **15**(3): p. 178-96.
34. Thiery, J.P., et al., *Epithelial-mesenchymal transitions in development and disease.* Cell, 2009. **139**(5): p. 871-90.
35. Hay, E.D., *An overview of epithelio-mesenchymal transformation.* Acta Anat (Basel), 1995. **154**(1): p. 8-20.
36. Kalluri, R. and E.G. Neilson, *Epithelial-mesenchymal transition and its implications for fibrosis.* J Clin Invest, 2003. **112**(12): p. 1776-84.

37. Pei, D., et al., *Mesenchymal-epithelial transition in development and reprogramming.* Nat Cell Biol, 2019. **21**(1): p. 44-53.
38. Kalluri, R. and R.A. Weinberg, *The basics of epithelial-mesenchymal transition.* J Clin Invest, 2009. **119**(6): p. 1420-8.
39. Acloque, H., et al., *Epithelial-mesenchymal transitions: the importance of changing cell state in development and disease.* J Clin Invest, 2009. **119**(6): p. 1438-49.
40. Yang, J. and R.A. Weinberg, *Epithelial-mesenchymal transition: at the crossroads of development and tumor metastasis.* Dev Cell, 2008. **14**(6): p. 818-29.
41. Tennakoon, A.H., et al., *Pathogenesis of Type 2 Epithelial to Mesenchymal Transition (EMT) in Renal and Hepatic Fibrosis.* J Clin Med, 2015. **5**(1).
42. Ghosh, S., et al., *A Role for betaA3/A1-Crystallin in Type 2 EMT of RPE Cells Occurring in Dry Age-Related Macular Degeneration.* Invest Ophthalmol Vis Sci, 2018. **59**(4): p. Amd104-amd113.
43. Tsai, J.H. and J. Yang, *Epithelial-mesenchymal plasticity in carcinoma metastasis.* Genes Dev, 2013. **27**(20): p. 2192-206.
44. Tarin, D., E.W. Thompson, and D.F. Newgreen, *The fallacy of epithelial mesenchymal transition in neoplasia.* Cancer Res, 2005. **65**(14): p. 5996-6000; discussion 6000-1.
45. Lee, J.M., et al., *The epithelial-mesenchymal transition: new insights in signaling, development, and disease.* J Cell Biol, 2006. **172**(7): p. 973-81.
46. Vincan, E. and N. Barker, *The upstream components of the Wnt signalling pathway in the dynamic EMT and MET associated with colorectal cancer progression.* Clin Exp Metastasis, 2008. **25**(6): p. 657-63.
47. Sipos, F. and O. Galamb, *Epithelial-to-mesenchymal and mesenchymal-to-epithelial transitions in the colon.* World J Gastroenterol, 2012. **18**(7): p. 601-8.
48. Li, R., et al., *A mesenchymal-to-epithelial transition initiates and is required for the nuclear reprogramming of mouse fibroblasts.* Cell Stem Cell, 2010. **7**(1): p. 51-63.
49. Knight, P.G. and C. Glister, *TGF-beta superfamily members and ovarian follicle development.* Reproduction, 2006. **132**(2): p. 191-206.
50. de Caestecker, M., *The transforming growth factor-beta superfamily of receptors.* Cytokine Growth Factor Rev, 2004. **15**(1): p. 1-11.
51. Heldin, C.H. and A. Moustakas, *Signaling Receptors for TGF-beta Family Members.* Cold Spring Harb Perspect Biol, 2016. **8**(8).
52. Wrana, J.L., *Signaling by the TGFbeta superfamily.* Cold Spring Harb Perspect Biol, 2013. **5**(10): p. a011197.
53. Mazerbourg, S., et al., *Identification of receptors and signaling pathways for orphan bone morphogenetic protein/growth differentiation factor ligands based on genomic analyses.* J Biol Chem, 2005. **280**(37): p. 32122-32.
54. Khalil, A.M., et al., *Differential Binding Activity of TGF-beta Family Proteins to Select TGF-beta Receptors.* J Pharmacol Exp Ther, 2016. **358**(3): p. 423-30.
55. Zhang, Y.E., *Non-Smad Signaling Pathways of the TGF-beta Family.* Cold Spring Harb Perspect Biol, 2017. **9**(2).
56. Zhang, Y.E., *Non-Smad pathways in TGF-beta signaling.* Cell Res, 2009. **19**(1): p. 128-39.

57. Poniatowski, L.A., et al., *Transforming growth factor Beta family: insight into the role of growth factors in regulation of fracture healing biology and potential clinical applications.* Mediators Inflamm, 2015. **2015**: p. 137823.
58. Khalil, N., *TGF-beta: from latent to active.* Microbes Infect, 1999. **1**(15): p. 1255-63.
59. Annes, J.P., J.S. Munger, and D.B. Rifkin, *Making sense of latent TGFbeta activation.* J Cell Sci, 2003. **116**(Pt 2): p. 217-24.
60. Dobolyi, A., et al., *The Neuroprotective Functions of Transforming Growth Factor Beta Proteins*, in *Int J Mol Sci*. 2012. p. 8219-58.
61. Konig, H.G., et al., *TGF-{beta}1 activates two distinct type I receptors in neurons: implications for neuronal NF-{kappa}B signaling.* J Cell Biol, 2005. **168**(7): p. 1077-86.
62. Braunger, B.M., et al., *TGF-beta signaling protects retinal neurons from programmed cell death during the development of the mammalian eye.* J Neurosci, 2013. **33**(35): p. 14246-58.
63. Saika, S., *TGFbeta pathobiology in the eye.* Lab Invest, 2006. **86**(2): p. 106-15.
64. Xu, J., S. Lamouille, and R. Derynck, *TGF-beta-induced epithelial to mesenchymal transition.* Cell Res, 2009. **19**(2): p. 156-72.
65. Kita, T., et al., *Role of TGF-β in proliferative vitreoretinal diseases and ROCK as a therapeutic target.* Proceedings of the National Academy of Sciences, 2008. **105**(45): p. 17504-17509.
66. Wang, X., et al., *TGF-beta participates choroid neovascularization through Smad2/3-VEGF/TNF-alpha signaling in mice with Laser-induced wet age-related macular degeneration.* Sci Rep, 2017. **7**(1): p. 9672.
67. Wang, R.N., et al., *Bone Morphogenetic Protein (BMP) signaling in development and human diseases.* Genes Dis, 2014. **1**(1): p. 87-105.
68. Bragdon, B., et al., *Bone morphogenetic proteins: a critical review.* Cell Signal, 2011. **23**(4): p. 609-20.
69. Sengle, G., et al., *Targeting of bone morphogenetic protein growth factor complexes to fibrillin.* J Biol Chem, 2008. **283**(20): p. 13874-88.
70. Huang, J., et al., *Negative and Positive Auto-Regulation of BMP Expression in Early Eye Development.* Dev Biol, 2015. **407**(2): p. 256-64.
71. Murali, D., et al., *Distinct developmental programs require different levels of Bmp signaling during mouse retinal development.* Development, 2005. **132**(5): p. 913-923.
72. Toyran, S., A.Y. Lin, and D.P. Edward, *Expression of growth differentiation factor-5 and bone morphogenic protein-7 in intraocular osseous metaplasia*, in *Br J Ophthalmol*. 2005. p. 885-90.
73. Namwanje, M. and C.W. Brown, *Activins and Inhibins: Roles in Development, Physiology, and Disease.* Cold Spring Harb Perspect Biol, 2016. **8**(7).
74. Wijayarathna, R. and D.M. de Kretser, *Activins in reproductive biology and beyond.* Hum Reprod Update, 2016. **22**(3): p. 342-57.
75. Bertacchi, M., et al., *Activin/Nodal Signaling Supports Retinal Progenitor Specification in a Narrow Time Window during Pluripotent Stem Cell Neuralization*, in *Stem Cell Reports*. 2015. p. 532-45.
76. Cornell, R.A. and D. Kimelman, *Activin-mediated mesoderm induction requires FGF.* Development, 1994. **120**(2): p. 453-462.

77. Werner, S. and C. Alzheimer, *Roles of activin in tissue repair, fibrosis, and inflammatory disease.* Cytokine Growth Factor Rev, 2006. **17**(3): p. 157-71.
78. Poulaki, V., et al., *Activin a in the regulation of corneal neovascularization and vascular endothelial growth factor expression.* Am J Pathol, 2004. **164**(4): p. 1293-302.
79. Yamamoto, T., et al., *Expression and possible roles of activin A in proliferative vitreoretinal diseases.* Jpn J Ophthalmol, 2000. **44**(3): p. 221-6.
80. Tsukamoto, S., et al., *Smad9 is a new type of transcriptional regulator in bone morphogenetic protein signaling.* Sci Rep, 2014. **4**: p. 7596.
81. Dennler, S. and P. Ten Dijke, *Smad Proteins in TGF-Beta Signaling*, in *Encyclopedia of Cancer*, M. Schwab, Editor. 2011, Springer Berlin Heidelberg: Berlin, Heidelberg. p. 3440-3443.
82. Wrana, J.L., et al., *Mechanism of activation of the TGF-beta receptor.* Nature, 1994. **370**(6488): p. 341-7.
83. Schmierer, B. and C.S. Hill, *TGFbeta-SMAD signal transduction: molecular specificity and functional flexibility.* Nat Rev Mol Cell Biol, 2007. **8**(12): p. 970-82.
84. Wrighton, K.H., X. Lin, and X.H. Feng, *Phospho-control of TGF-β superfamily signaling.* Cell Res, 2009. **19**(1): p. 8-20.
85. Tsukazaki, T., et al., *SARA, a FYVE domain protein that recruits Smad2 to the TGFbeta receptor.* Cell, 1998. **95**(6): p. 779-91.
86. Xu, L., Y.G. Chen, and J. Massague, *The nuclear import function of Smad2 is masked by SARA and unmasked by TGFbeta-dependent phosphorylation.* Nat Cell Biol, 2000. **2**(8): p. 559-62.
87. Shi, Y. and J. Massague, *Mechanisms of TGF-beta signaling from cell membrane to the nucleus.* Cell, 2003. **113**(6): p. 685-700.
88. Hayashi, H., et al., *The MAD-related protein Smad7 associates with the TGFbeta receptor and functions as an antagonist of TGFbeta signaling.* Cell, 1997. **89**(7): p. 1165-73.
89. Miyazawa, K. and K. Miyazono, *Regulation of TGF-beta Family Signaling by Inhibitory Smads.* Cold Spring Harb Perspect Biol, 2017. **9**(3).
90. Walton, K.L., K.E. Johnson, and C.A. Harrison, *Targeting TGF-β Mediated SMAD Signaling for the Prevention of Fibrosis.* Front Pharmacol, 2017. **8**.
91. Malhotra, N. and J. Kang, *SMAD regulatory networks construct a balanced immune system.* Immunology, 2013. **139**(1): p. 1-10.
92. Samanta, D. and P.K. Datta, *Alterations in the Smad pathway in human cancers.* Front Biosci (Landmark Ed), 2012. **17**: p. 1281-93.
93. Neill, T., L. Schaefer, and R.V. Iozzo, *Decorin: a guardian from the matrix.* Am J Pathol, 2012. **181**(2): p. 380-7.
94. Abdel-Wahab, N., et al., *Decorin suppresses transforming growth factor-beta-induced expression of plasminogen activator inhibitor-1 in human mesangial cells through a mechanism that involves Ca2+-dependent phosphorylation of Smad2 at serine-240.* Biochem J, 2002. **362**(Pt 3): p. 643-9.

95. Ulloa, L. and S. Tabibzadeh, *Lefty inhibits receptor-regulated Smad phosphorylation induced by the activated transforming growth factor-beta receptor.* J Biol Chem, 2001. **276**(24): p. 21397-404.
96. Hashimoto, O., et al., *A novel role of follistatin, an activin-binding protein, in the inhibition of activin action in rat pituitary cells. Endocytotic degradation of activin and its acceleration by follistatin associated with cell-surface heparan sulfate.* J Biol Chem, 1997. **272**(21): p. 13835-42.
97. Harrington, A.E., et al., *Structural basis for the inhibition of activin signalling by follistatin.* Embo j, 2006. **25**(5): p. 1035-45.
98. Zimmerman, L.B., J.M. De Jesus-Escobar, and R.M. Harland, *The Spemann organizer signal noggin binds and inactivates bone morphogenetic protein 4.* Cell, 1996. **86**(4): p. 599-606.
99. Groppe, J., et al., *Structural basis of BMP signaling inhibition by Noggin, a novel twelve-membered cystine knot protein.* J Bone Joint Surg Am, 2003. **85-A Suppl 3**: p. 52-8.
100. Piccolo, S., et al., *Dorsoventral patterning in Xenopus: inhibition of ventral signals by direct binding of chordin to BMP-4.* Cell, 1996. **86**(4): p. 589-98.
101. Troilo, H., et al., *Nanoscale structure of the BMP antagonist chordin supports cooperative BMP binding.* Proc Natl Acad Sci U S A, 2014. **111**(36): p. 13063-8.
102. Nolan, K. and T.B. Thompson, *The DAN family: modulators of TGF-beta signaling and beyond.* Protein Sci, 2014. **23**(8): p. 999-1012.
103. Groppe, J., et al., *Structural basis of BMP signalling inhibition by the cystine knot protein Noggin.* Nature, 2002. **420**(6916): p. 636-42.
104. Sun, J., et al., *BMP4 activation and secretion are negatively regulated by an intracellular gremlin-BMP4 interaction.* J Biol Chem, 2006. **281**(39): p. 29349-56.
105. Radeke, M.J., et al., *Restoration of mesenchymal retinal pigmented epithelial cells by TGFβ pathway inhibitors: implications for age-related macular degeneration.* Genome Med, 2015. **7**(1): p. 58.
106. Storm, E.E., et al., *Limb alterations in brachypodism mice due to mutations in a new member of the TGF beta-superfamily.* Nature, 1994. **368**(6472): p. 639-43.
107. Wolfman, N.M., et al., *Ectopic induction of tendon and ligament in rats by growth and differentiation factors 5, 6, and 7, members of the TGF-beta gene family.* J Clin Invest, 1997. **100**(2): p. 321-30.
108. Settle, S.H., Jr., et al., *Multiple joint and skeletal patterning defects caused by single and double mutations in the mouse Gdf6 and Gdf5 genes.* Dev Biol, 2003. **254**(1): p. 116-30.
109. Tassabehji, M., et al., *Mutations in GDF6 are associated with vertebral segmentation defects in Klippel-Feil syndrome.* Hum Mutat, 2008. **29**(8): p. 1017-27.
110. Berasi, S.P., et al., *Divergent activities of osteogenic BMP2, and tenogenic BMP12 and BMP13 independent of receptor binding affinities.* Growth Factors, 2011. **29**(4): p. 128-39.
111. Wang, J., et al., *A New Subtype of Multiple Synostoses Syndrome Is Caused by a Mutation in GDF6 That Decreases Its Sensitivity to Noggin and Enhances Its Potency as a BMP Signal.* J Bone Miner Res, 2016. **31**(4): p. 882-9.

112. Terhal, P.A., et al., *Further delineation of the GDF6 related multiple synostoses syndrome.* Am J Med Genet A, 2018. **176**(1): p. 225-229.
113. Drage Berentsen, R., et al., *A Novel GDF6 Mutation in a Family with Multiple Synostoses Syndrome without Hearing Loss.* Mol Syndromol, 2019. **9**(5): p. 228-234.
114. Hanel, M.L. and C. Hensey, *Eye and neural defects associated with loss of GDF6.* BMC Dev Biol, 2006. **6**: p. 43.
115. Asai-Coakwell, M., et al., *GDF6, a novel locus for a spectrum of ocular developmental anomalies.* Am J Hum Genet, 2007. **80**(2): p. 306-15.
116. Asai-Coakwell, M., et al., *Contribution of growth differentiation factor 6-dependent cell survival to early-onset retinal dystrophies.* Hum Mol Genet, 2013. **22**(7): p. 1432-42.

CHAPTER II: Materials and Methods

2.1: Lentivirus Production

Human growth differentiation factor 6 (*GDF6*) open reading frame (ORF) was obtained from GeneCopia (Rockville, MD, USA). The ORF was cloned into the LeGO-iCer vector (Addgene, Cambridge, MA, USA). Guide RNA (gRNA) vectors were generated by cloning in gRNA sequences determined using guide design tools from the Zhang lab (crispr.mit.edu) into a donor plasmid (Addgene #46918). The packaging plasmids pMD2.G, pMDLg/pRRE, and pRSV-R (Addgene) were used in conjunction with the cloned GDF6 LeGO-iCer vector, a LeGO-iV2 vector as a control, or the gRNA vectors to generate lentiviral particles from HEK293T cells. Lentiviral particles were harvested and concentrated using PEG-it™ (System Biosciences, Mountain View, CA, USA) and titered per fluorescent expression levels in retinal pigmented epithelial cells (RPE) using flow cytometry. Expression of *GDF6* was verified using real-time quantitative PCR (RT-qPCR).

2.2: Lentiviral Transduction and Cell Culture

Fetal RPE cells were obtained from a working cell bank described in Radeke *et al.* [1]. Passage 0 human fetal RPE were plated on Matrigel (Corning, Corning, NY, USA) coated plates at 20,000 cells/cm^2 in a base media without hydrocortisone containing 5% heat-inactivated fetal calf serum (Miller media) [2] or Miller media supplemented with 0.1mM RepSox (Cayman Chemical, Ann Arbor, MI, USA), 200nM LDN-193189 (LDN) (Cayman Chemical), or both. The following day the cells were transduced with the appropriate lentiviral vector (multiplicity of infection [MOI] = 0.4 – 0.5 for each vector) supplemented with polybrene (Millipore Sigma, Billerica, MA, USA) at a concentration of 10 µg/mL. After

24 hours, the viral media was replaced with fresh Miller media and appropriate supplementation. 48 hours post-transduction the cells were lifted using Accumax (Innovative Cell Technologies, San Diego, CA, USA) and sorted based on fluorophore expression using fluorescent activated cell sorting (FACS). After sorting, the cells were seeded at 80,000 cells/cm^2 on Matrigel-coated plates and allowed to differentiate for 32 days. During differentiation, Miller media and appropriate supplementation were replaced every 2-3 days. After 32 days cells were imaged and RNA was harvested using the NucleoSpin RNA Kit (Takara, Mountain View, CA, USA) following manufacturer's instructions.

2.3: Pigmentation Analysis

4X montage images were obtained using a Cytation 5 Imager (BioTek, Winooski, VT, USA). Images were automatically stitched together using the Gen5 Imager Software (BioTek) and imported into Matlab (MathWorks, Natick, MA, USA) to calculate the percent of the image that was pigmented. Briefly, images were cropped to the same size and binarized using a thresholding mechanism. The number of black pixels and white pixels were determined and transformed into percentages.

2.4: Real-time Quantitative PCR (RT-qPCR)

Real-time Quantitative PCR (RT-qPCR) was performed using PrimeTime® PCR Assays (Integrated DNA Technologies Inc, Coralville, IA, USA). The iScript cDNA Synthesis Kit (Bio-Rad, Hercules, CA, USA) was used to generate cDNA from total RNA. For each gene of interest, RT-qPCR was carried out in triplicate using iTaq Universal Probes Supermix (Bio-Rad) using the following thermal cycle profile: 95^{o}C for 1 min, 45 x (95^{o}C for 5 s, 60^{o}C for 1

min). Gene expression levels were normalized to the geometric mean of three housekeeping genes (RPLP0, RPS2, and UBB).

2.4.1: RT-qPCR Probes

Gene	**IDT Assay ID**	**Gene**	**IDT Assay ID**
ACTA2	Hs.PT.56a.2542642	NOG	Hs.PT.58.27300029.g
APOE	Hs.PT.56a.3799446	OTX2	Hs.PT.58.46695245
CDH3	Hs.PT.58.39234242	PMEL	Hs.PT.58.18690699
COL1A1	Hs.PT.58.15517795	RPLP0	Hs.PT.39a.22214824
CTGF	Hs.PT.58.14485164.g	RPS2	Hs.PT.58.22843181
DCN	Hs.PT.58.38497176	SERPINF1	Hs.PT.58.20553847
GDF6	Hs.PT.56a.20193545	SMOC2	Hs.PT.56a.20763253
ITGA11	Hs.PT.58.39995058	SPP1	Hs.PT.58.19252426
LIN7A	Hs.PT.58.2551960	TGFB1	Hs.PT.58.39813975
LRAT	Hs.PT.56a.39384980	TGFB2	Hs.PT.58.24824921
LUM	Hs.PT.56a.39858305	TGFBI	Hs.PT.56a.40018323
MAN1C1	Hs.PT.58.4817967	TYRP1	Hs.PT.58.423853
MITF	Hs.PT.56a.38853705	UBB	Hs.PT.58.4937882

Gene	**Primer 1**	**Primer2**	**Probe**

LPL	5’-GGACTGAGAGT GAAACCCATAC-3’	5’-TGTGGAAACTTC AGGCAGAG-3’	5’-/56-FAM/AATGGGATG/ZEN /TTCTCACTCTCGGCC/3IABkFQ/-3’

2.5: RNA-Sequencing (RNA-seq) and Transcriptome Analysis

RNA-sequencing (RNA-seq) libraries were prepared using the Ion AmpliSeq™ Transcriptome Human Gene Expression Kit (ThermoFisher, Waltham, MA, USA). Libraries were prepared using the Ion AmpliSeq Library Preparation on the Ion Chef System (ThermoFisher). Briefly, RNA was diluted to 1ng/uL, and a reverse transcriptase reaction was performed. The cDNA reaction was then loaded onto a primer plate, and the Ion Chef automatically prepared the libraries. The libraries were quantified by qPCR and diluted to 100 pM using the Ion Library TaqMan™ Quantitation Kit (ThermoFisher). The libraries were then loaded onto sequencing chips via the Ion Chef system and sequenced using an Ion Torrent next-generation sequencer (ThermoFisher). The resulting sequences were automatically aligned to the human genome using the ampliSeqRNA plugin [3].

The dataset was normalized using the trimmed mean of the M-values method [4]. Genes were based on read counts per million (RPM) ≥ 1 in two or more samples, and differential expression and statistical analysis were performed using edgeR [5]. Heat maps were generated by averaging technical replicates together, and the Log2 ratio of GDF6 to control cells was determined for each biological pair. The average of all three pairs was taken, and the genes were ranked based on highest expression in GDF6 cells. Cluster analysis was performed using AutoSOME 2.1 on data that was Log2 transformed and centered on the midpoint of the range (500 ensemble runs, P=0.03, unit variance, sum of

squares = 1, and precision settings) [6]. Individual clusters were assigned to more general groups based on visual examination of the expression patterns. Gene ontology enrichment analysis was determined using DAVID Bioinformatics Resources 6.8 with default settings [7] and the ToppFun Application of the ToppGene Suite with default settings [8].

2.6: Recombinant Gdf6 (rmGdf6) Treatment

Recombinant mouse Gdf6 (rmGdf6) (R&D Systems, Minneapolis, MN) was reconstituted according to manufacturer's instructions in 4mM HCl with 0.1% bovine serum albumin to a final concentration of 300 μg/mL (22 mM). RPE were plated at 80,000 cells/cm^2 in Miller media supplemented with 3 μg/mL (219 uM) rmGdf6, 200nM LDN, or both. Media was changed every other day for 14 days at which time cells were imaged, and RNA was harvested for RT-qPCR analysis. For the dose-response experiments, passage 0 RPE were plated at 80,000 cells/cm^2 and supplemented with various amounts of rmGdf6 for 14 days, with media being replaced every other day for 14 days. At this point, cells were imaged and RNA was harvested as before for RT-qPCR analysis.

2.7: Smad Phosphorylation Assay

RPE were plated at a concentration of 20,000-30,000 cells/cm^2 on Matrigel-coated plates. The following day cells were placed in a Miller media without serum for 5 hours. After 5 hours of serum-starvation, appropriate inhibitor molecules (DMSO, RepSox, or LDN) were added to the media and allowed to incubate for one hour. Following this small molecule incubation, RPE were challenged with 1 μg/mL (73 μM) rmGdf6 or TGFβ1 (R&D Systems) for 30 minutes, rinsed in phosphate buffered saline (PBS), harvested in Laemmli Sample Buffer, and boiled at 95^oC for 10 min. Samples were stored at -20^oC until analysis.

2.8: Western Blot Analysis

Samples were harvested in Laemmli Sample Buffer and denatured using 10% TCEP (ThermoFisher) at 95^{o}C for 10 minutes. The total cell lysate was loaded on to an AnyKD™ Criterion™ TGX™ Precast Midi Protein Gel (Bio-Rad), and proteins were separated by one-dimensional sodium dodecyl sulfate-polyacrylamide gel electrophoresis (SDS-PAGE) under reducing conditions. Proteins were transferred to polyvinylidene fluoride (PVDF) membrane (Bio-Rad). The membranes were blocked in light soymilk (commercial grade) containing 0.1% Tween-20 (Promega, Madison, WI, USA) for 30 minutes at room temperature [9]. Membranes were incubated in primary antibody overnight at 4^{o}C, washed 5 times in Tris-buffered saline containing 0.1% Tween 20 (TBST), and incubated in secondary antibodies conjugated to horseradish peroxidase for one hour at room temperature. The membranes were washed 5 times with TBST and one time with TBS before developing with SuperSignal™ West Femto Maximum Sensitivity Substrate (ThermoFisher) on a ChemiDoc Imager (Bio-Rad).

Primary Antibodies Used:

Antibody	Dilution	Company

Anti-PhosphoSmad 1/5/9	1:1000	Cell Signaling Technologies 13820
Anti-PhosphoSmad 2/3	1:1000	Cell Signaling Technologies 8828
Anti-GDF6	1:1000	Sigma-Aldrich PRS4691
Anti-Ubi-1	1:1000	Thermo Fisher

Secondary Antibodies Used:

Antibody	Dilution	Company
Goat anti-Rabbit HRP	1:10000	Pierce 31466
Goat anti-Mouse HRP	1:500	ThermoFisher 32430

2.9: LDN Passaging

Passage 0 RPE were plated at 4,000 cells/cm^2 in Miller media, with half the samples supplemented with 200nM LDN. At approximately 80% confluence, the cells were passaged by enzymatically dissociating using Accumax and re-seeding at 4,000 cells/cm^2. At the time of re-seeding, a portion of cells was plated at 80,000 cells/cm^2 and allowed to differentiate for 32 days. After 32 days of differentiation, cells were imaged and RNA was harvested as before for RT-qPCR analysis.

2.10: Generation of CRISPR Knock-in Cell Line

Induced pluripotent stem cells (iPSCs) were generated from the lab's working cell bank of fetal RPE using ReproRNA-OKSGM (Stemcell Technologies, Vancouver, Canada) per manufacturer's instructions. The methods published by He *et al*., 2016 were followed to generate a KRAB-dCas9 knock-in iPSC cell line through non-homologous end joining (NEHJ)

[10]. KRAB-dCas9-P2A (Addgene # 60954) was cloned into the double cut NH-donor plasmid (Addgene #83576) between the IRES and GFP. To deliver and transiently express the plasmids required for NHEJ, cells were electroporated to deliver 4 plasmids (Addgene #41815, #83576, #83809, and the donor plasmid) into an iPS cell line. The cells were then expanded and subjected to a series of three FACS selection sorts to ensure purity before differentiation into RPE. The site-specific insertion was confirmed using PCR.

The protocol for differentiation of iPSCs into RPE was adapted from Idelson *et al*., 2009 [11]. Briefly, iPSCs were plated on Matrigel coated plates in TeSR-E8 (Stemcell Technologies) and cells were then directed towards an RPE fate. Once differentiated, iPSC-RPE were dissociated using protease digestion and pure populations were isolated based on RPE cell surface markers and pigmentation using FACS (Coffey Lab, unpublished protocol).

2.11: CRISPRi Knockdown in RPE

iPS-RPE stably expressing dCas9 were transduced with gRNA vectors targeting the transcription start site (TSS) of *GDF6* or a control gene (UBE4A). The cells were sorted on mCherry expression 3 days after infection. Cells were plated at 5,000 cells/cm^2 in Miller media without serum. At approximately 80% confluence, the cells were passaged by enzymatically dissociating using Accumax and re-seeded at 5,000 cells/cm^2. At the time of re-seeding, a portion of cells was plated at 80,000 cells/cm^2 and allowed to differentiate for 32 days. After 32 days of differentiation, cells were imaged, and RNA was harvested as before for RT-qPCR analysis.

2.12: Proteome Profile Assay

To determine differences in receptor activation, a Human Proteome Phospho-Kinase Array (R&D Systems) was followed according to manufacturer's instructions. Briefly, RPE were plated at a concentration of 20,000-30,000 cells/cm^2 on Matrigel-coated plates. The following day cells were placed in Miller media without serum for 5 hours. After 5 hours of serum-starvation, appropriate inhibitor molecules (DMSO or RepSox and LDN) were added to the media and allowed to incubate for one hour. Following this small molecule incubation, RPE were challenged with 1 μg/mL (73 μM) rmGdf6. RPE were lysed at a concentration of $1x10^7$ cells/mL and protein concentration was quantified using a DC™ protein assay (Bio-Rad). 600 μg of total protein extract was applied to the membranes. The membranes were treated with appropriate antibody cocktails and secondary antibodies. Chemiluminescence was read in a Bio-Rad ChemiDoc Imager from 30 seconds to 4 minutes, and spot pixel intensity was quantified using ImageJ software.

2.13: References:

1. Radeke, M.J., et al., *Restoration of mesenchymal retinal pigmented epithelial cells by TGFβ pathway inhibitors: implications for age-related macular degeneration.* Genome Med, 2015. **7**(1): p. 58.
2. Maminishkis, A., et al., *Confluent monolayers of cultured human fetal retinal pigment epithelium exhibit morphology and physiology of native tissue.* Invest Ophthalmol Vis Sci, 2006. **47**(8): p. 3612-24.
3. Broeckel, W.L., et al., *Comprehensive evaluation of AmpliSeq transcriptome, a novel targeted whole transcriptome RNA sequencing methodology for global gene expression analysis.* BMC Genomics, 2015. **16**(1): p. 1069.
4. Robinson, M.D. and A. Oshlack, *A scaling normalization method for differential expression analysis of RNA-seq data.* Genome Biol, 2010. **11**(3): p. R25.
5. McCarthy, D.J., Y. Chen, and G.K. Smyth, *Differential expression analysis of multifactor RNA-Seq experiments with respect to biological variation.* Nucleic Acids Res, 2012. **40**(10): p. 4288-97.

6. Cooper, A.M.N. and B. James, *AutoSOME: a clustering method for identifying gene expression modules without prior knowledge of cluster number.* BMC Bioinformatics, 2010. **11**(1): p. 117.
7. Huang da, W., B.T. Sherman, and R.A. Lempicki, *Systematic and integrative analysis of large gene lists using DAVID bioinformatics resources.* Nat Protoc, 2009. **4**(1): p. 44-57.
8. Chen, J., et al., *ToppGene Suite for gene list enrichment analysis and candidate gene prioritization.* Nucleic Acids Res, 2009. **37**(Web Server issue): p. W305-11.
9. Galva, C., C. Gatto, and M. Milanick, *Soymilk: an effective and inexpensive blocking agent for immunoblotting.* Anal Biochem, 2012. **426**(1): p. 22-3.
10. He, X., et al., *Knock-in of large reporter genes in human cells via CRISPR/Cas9-induced homology-dependent and independent DNA repair.* Nucleic Acids Res, 2016. **44**(9): p. e85.
11. Idelson, M., et al., *Directed differentiation of human embryonic stem cells into functional retinal pigment epithelium cells.* Cell Stem Cell, 2009. **5**(4): p. 396-408.

CHAPTER III: The Effect of GDF6 on RPE

3.1: Introduction

Epithelial-to-mesenchymal transition (EMT) is a process in which a polarized, stationary epithelial cell transforms into a migratory, invasive mesenchymal cell [1]. EMT can be classified into three different types of biological processes, resulting in different functional characteristics. Type 1 EMT is found in embryogenesis and gastrulation, helping to form the mesoderm, neural tube, and other various bones and tissues [2, 3]. Type 2 EMT is commonly associated with wound healing and fibrosis, whereas Type 3 EMT is found in cancer and metastasis [1, 4]. EMT, and its converse, the mesenchymal-to-epithelial transition (MET), are necessary for proper development and performance. Disease can occur if these pathways do not function properly.

EMT in the eye is necessary for early development and wound healing, but unregulated EMT can lead to vision issues. Retinal pigmented epithelial (RPE) cells are a polarized, pigmented monolayer of cuboidal cells located behind the retina, performing various essential functions to maintain a healthy environment in the eye [5]. Aberrant wound healing mechanisms can lead to a permanent mesenchymal phenotype in RPE, leading to various blinding disorders such as proliferative vitreoretinopathy (PVR) and choroidal neovascularization (CNV) [6-9]. Previous work by Radeke, *et al*. 2015 established that early passage RPE can undergo EMT and MET *in vitro*, eventually differentiating back into a healthy monolayer. If RPE are passaged under a chronic wounding model, they lose their ability to undergo MET and remain in a mesenchymal, fibrotic state. In order to help

determine why RPE undergo this irreversible EMT after repeated passaging, they analyzed the genetic differences between early passage 0 (P0) and late passage 5 (P5) RPE [10].

Growth and differentiation factor 6 (*GDF6*; *BMP13*) was found to be exclusive to P5 RPE, suggesting it is a contributing factor to irreversible RPE EMT [10]. *GDF6* is a member of the transforming growth factor beta (TGFβ) superfamily and thus it participates in Smad protein phosphorylation. *GDF6* is essential for healthy development as it is involved in ectoderm patterning and proper bone and joint formation [11, 12]. Additionally, *GDF6* is essential for the correct development of the retina through functions like inhibition of apoptosis and differentiation of photoreceptors [13-16]. Though *GDF6* is present during development of the eye, it is noticeably absent in a healthy, mature eye until RPE cells undergo EMT. Here we investigate the role of *GDF6* in RPE EMT by administering GDF6 to RPE and observing phenotypic changes, genotypic changes and Smad protein phosphorylation.

3.2: Results

3.2.1: GDF6 Overexpression Prevents Normal Differentiation in RPE

To investigate the possible role *GDF6* may play in the EMT of RPE, P0 RPE were transfected with a *GDF6* overexpression vector and sorted into a pure population using fluorescence activated cell sorting (FACS) (Figure 3.1). After 32 days in culture, these RPE cells overexpressing *GDF6* (GDF6 RPE) were unable to obtain the normal RPE phenotype, as illustrated in Figure 3.2-A. GDF6 RPE do not exhibit the typical cuboidal, cobblestone RPE morphology, but appear larger and more spindle-like in shape with holes present in the

monolayer. This change in morphology is accompanied by a 35% reduction in pigmentation (Figure 3.2-B).

Overexpressing *GDF6* also has a substantial effect on RPE gene expression. A subset of genes was selected for further analysis based on their expression profile in passaged RPE cells [10]. This quantitative PCR (qPCR) panel includes genes typically upregulated in a late passage, mesenchymal-like RPE as well as genes found in healthy, differentiated RPE. GDF6 RPE upregulate genes found in highly passaged mesenchymal RPE cells and downregulate genes found in healthy RPE (Figure 3.2-C). Notably, GDF6 RPE show increased levels of collagen (*COL1A1*), an extracellular matrix protein that is an abundant component of mesenchymal connective tissue, as well as an increase in *TGFβ2*, a known inducer of EMT. GDF6 RPE display decreased levels of genes found in epithelial cells and low passage RPE, like p-cadherin (*CDH3*), an important cell adhesion protein in RPE, as well as lecithin retinol acyltransferase (*LRAT*), an essential gene involved in retinoid uptake and the visual cycle.

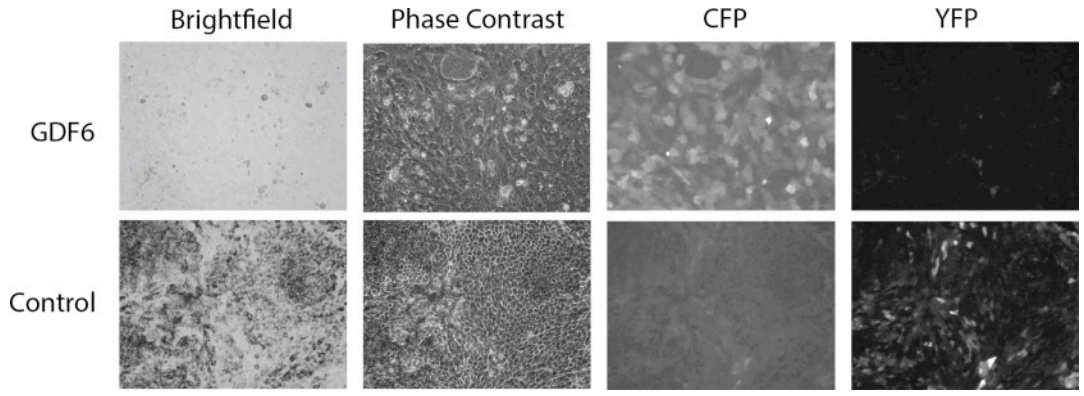

Figure 3.1. RPE have the ability to overexpress *GDF6*. (A) Brightfield, phase contrast, CFP, and YFP images of RPE. RPE were infected with either a construct causing overexpression of *GDF6* and CFP, or an empty vector control that causes overexpression of YFP.

A

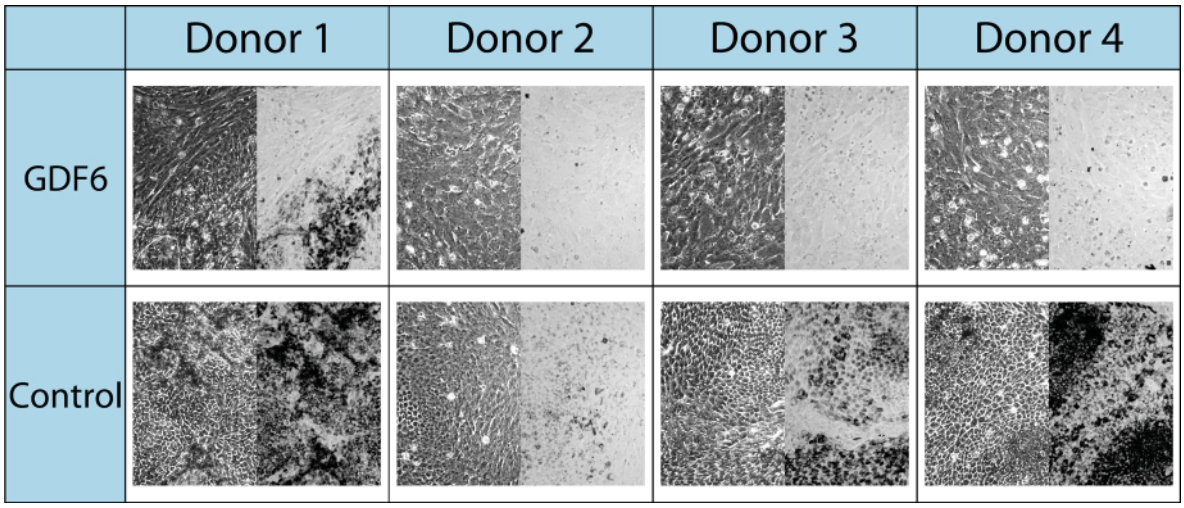

B

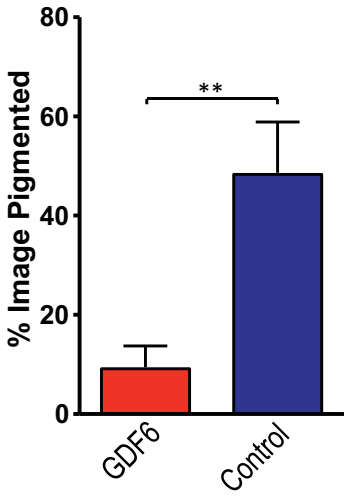

C

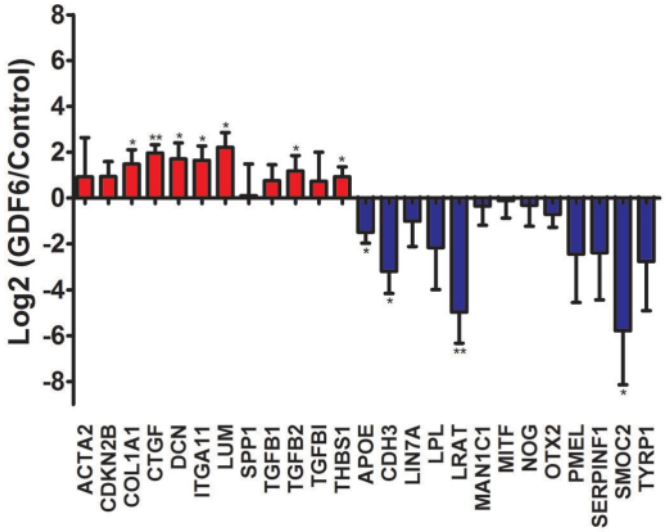

Figure 3.2. *GDF6* overexpression in RPE causes morphological and genotypic changes. (A) Phase contrast (left) and brightfield (right) images of four different RPE lines taken at 10X. Cells were transfected with either *GDF6* or an empty vector construct, sorted, and allowed to differentiate for 32 days. (B) RPE that overexpress *GDF6* lose the ability to pigment. Brightfield montage images were taken of each well, stitched together using the Gen5 program software, and pigmentation was analyzed using the Matlab software package. Statistical significance was determined using the Student's t-test (n=4, **≤0.005). (C) RPE overexpressing *GDF6* upregulate genes related to EMT and a mesenchymal state while downregulating genes found in healthy RPE. Highlighted in red are genes known to increase during RPE passaging while genes in blue are representative of genes found in healthy RPE. A one-sample t-test was used to determine statistical significance (n=4, *≤0.05, **≤0.005).

RNA-sequencing (RNA-seq) can help elucidate the differences between GDF6 RPE and control RPE. We generated libraries from 32-day GDF6 RPE and control RPE cells and determined which genes were differentially expressed. GDF6 RPE have genes that cluster in Extracellular Matrix Organization (n = 35, *P*-value < 1×10^{-14}), EGF-like Domains (n = 30, *P*-value < 1×10^{-9}), and Focal Adhesion (n=24, *P*-value < 1×10^{-5}) while Cell Junction genes (n = 56, *P*-value < 1×10^{-7}) and those involved in Melanin Biosynthesis (n = 4, *P*-value < 1×10^{-3}) and Vision (n = 15, *P*-value < 1×10^{-4}) are all downregulated (Figure 3.3). GDF6 RPE upregulate cadherin 2 (*CDH2*) and cadherin 11 (*CDH11*) along with fibronectin and collagens, while healthy RPE have higher expression levels of *CDH1* and *CDH3* (Table 3.1). Overall, GDF6 RPE cells exhibit dysregulation in greater than 10% of its genes.

3.2.2: GDF6 Has No Effect on Mature RPE

As a member of the TGFβ superfamily, GDF6 is involved in Smad protein phosphorylation, specifically Smad1/5/9 protein phosphorylation [17]. While the effects of GDF6 have been studied in some cell lines [18-22], the effect of GDF6 on RPE has not been previously assessed. We found that undifferentiated, low-density passage 1 (P1) RPE respond to GDF6 through phosphorylation of Smad1/5/9 (Figure 3.4-A). Low-density P5 RPE that have undergone a mesenchymal transition also phosphorylate Smad1/5/9 in the presence of GDF6. LDN-193189 (LDN) is a potent kinase inhibitor of the type 1 BMP Receptor (activin-like kinase (Alk) 2, 3, 6) [23, 24]. We can prevent the response to GDF6 and subsequent phosphorylation of Smad1/5/9 in RPE with the use of LDN, thus making it an active inhibitor of GDF6 signaling. However, the kinase inhibitor of Alk5, RepSox, did not affect the GDF6 stimulation of Smad1/5/9.

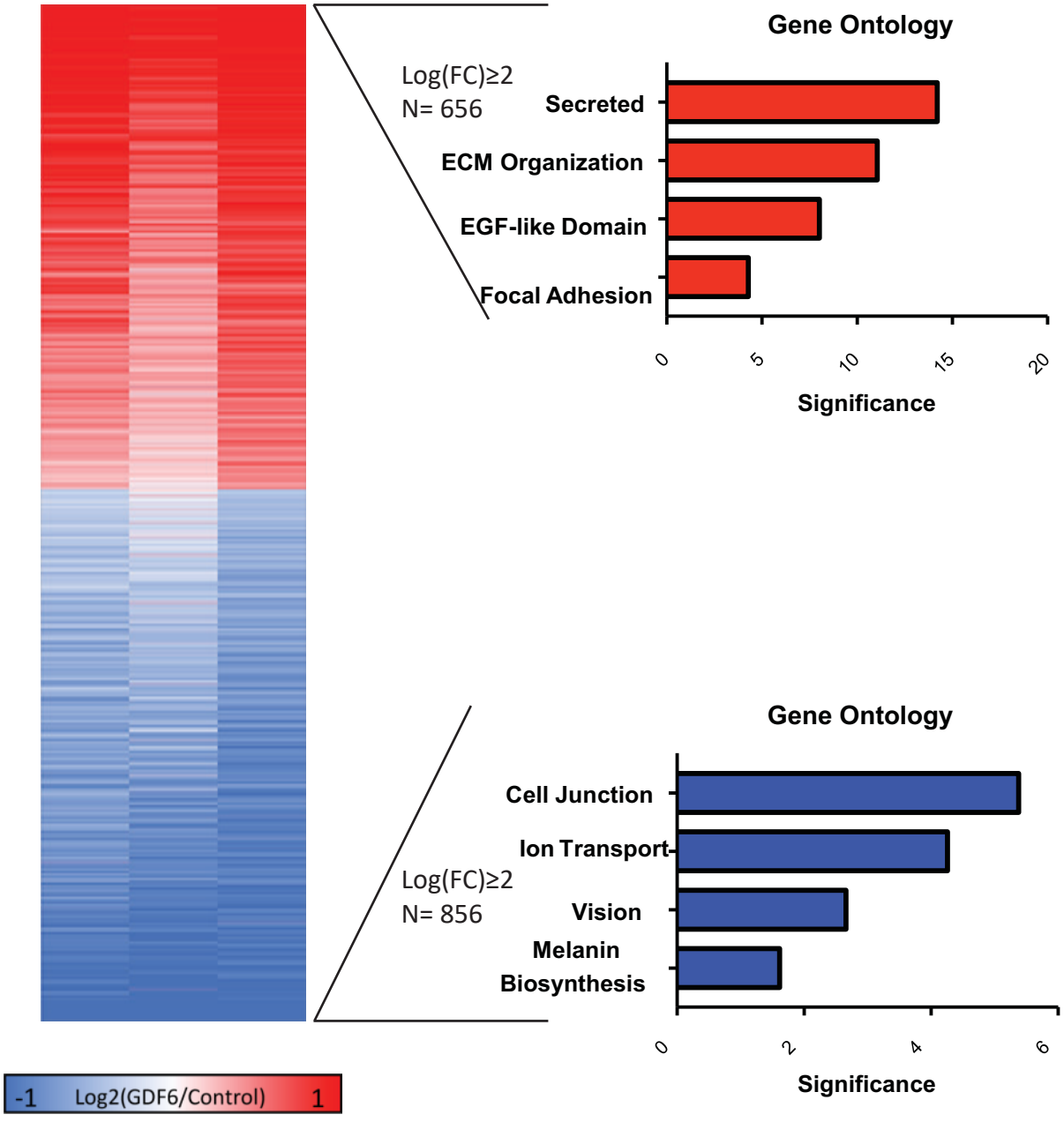

Figure 3.3. *GDF6* overexpression results in 10 % of genes having a 2-fold or greater change in expression. Differentially expressed genes are those with an FDR ≤ 0.01. Gene ontology enrichment analysis was carried out on genes that had a log2 transformed ratio ≥ 2 of GDF6 RPE to control cells. Significance was determined by taking the Log of the reciprocal of the Benjamini p-value.

Table 3.1

Differentially expressed cadherin, collagen, and fibronectin genes in normal and GDF6 RPE.

Gene	logFC	Pvalue	FDR
CDH1	3.145	1.62E-44	1.54E-41
CDH2	-1.445	5.16E-20	6.35E-18
CDH3	2.610	4.83E-57	1.15E-53
CDH7	-1.118	2.67E-04	2.07E-03
CDH8	-1.872	2.67E-08	5.73E-07
CDH10	-1.813	1.99E-08	4.36E-07
CDH11	-2.400	2.24E-17	1.90E-15
CDH19	-1.897	2.59E-07	4.44E-06
COL1A1	-2.348	2.53E-12	1.00E-10
COL1A2	-2.207	1.10E-21	1.67E-19
COL3A1	-2.227	2.52E-22	4.28E-20
COL4A1	-1.358	1.91E-06	2.68E-05
COL4A2	-1.094	8.83E-07	1.33E-05
COL4A4	-0.714	2.47E-03	1.34E-02
COL5A1	-1.648	2.23E-10	6.58E-09
COL5A2	-1.464	1.03E-16	8.43E-15
COL7A1	-1.812	1.82E-11	6.26E-10
COL8A1	-0.395	2.18E-03	1.21E-02
COL9A1	3.575	4.60E-21	6.44E-19
COL14A1	-2.259	1.14E-10	3.54E-09
COL15A1	5.570	1.75E-15	1.20E-13
COL16A1	-0.778	2.16E-05	2.32E-04
COL18A1	0.591	1.80E-04	1.48E-03
COL25A1	-2.651	7.61E-04	5.04E-03
COL27A1	1.225	3.92E-05	3.85E-04
FN1	-2.622	1.12E-14	6.48E-13

The log fold-change of normal/GDF6 is shown. FDR ≤ 0.01.

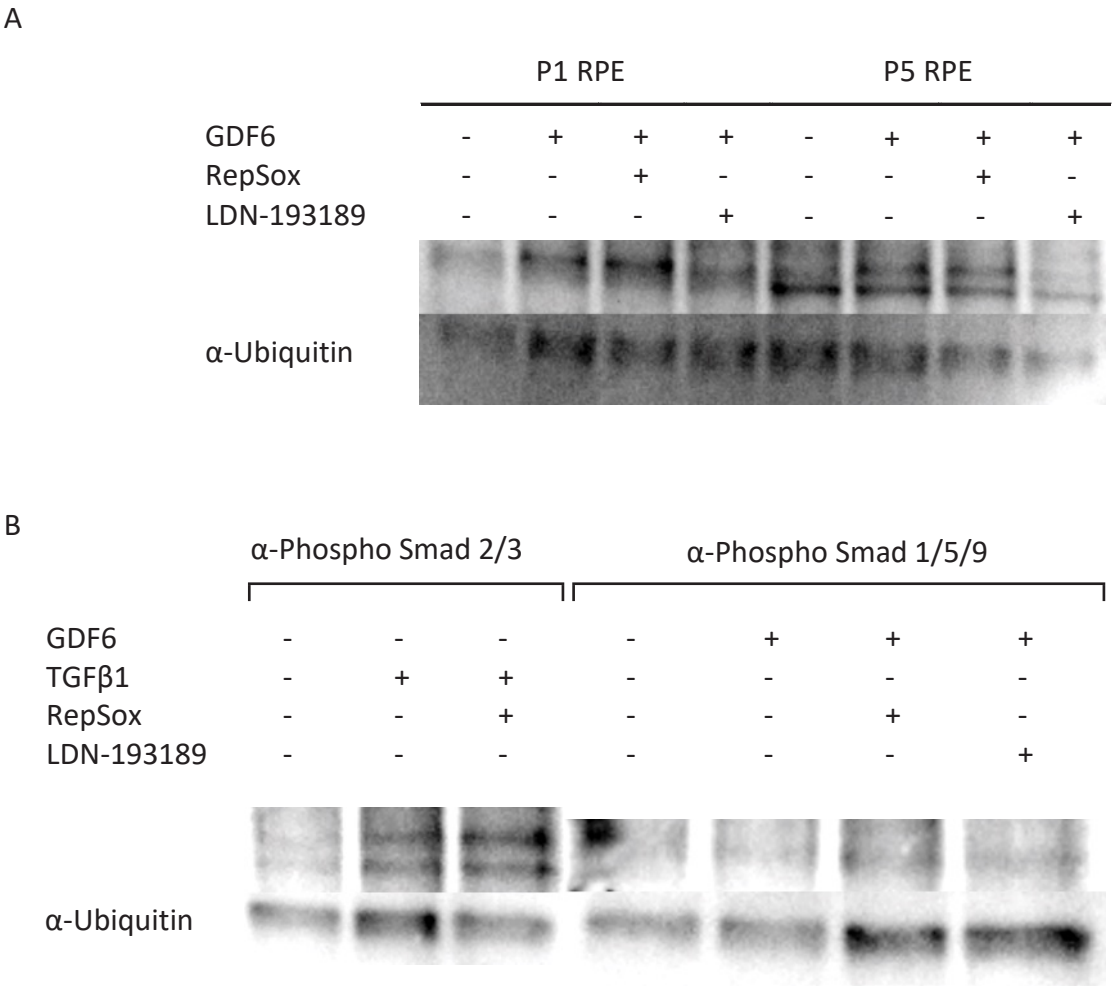

Figure 3.4. Western blots showing phosphorylation of Smad proteins in RPE. (A) Undifferentiated RPE can respond to GDF6. Passage 1 and Passage 5 RPE were treated with 1 µg/mL (73 µM) recombinant mouse GDF6 (rmGDF6) for 30 minutes and phospho-Smad1/5/9 levels were assayed, with α-Ubiquitin serving as a loading control. (B) Mature, differentiated RPE cannot respond to rmGdf6, but can respond to TGFβ1. Passage 0 RPE were differentiated for 4 months on inserts. rmGdf6 or TGFβ1 was applied to both sides of the insert for 30 minutes. Both phospho-Smad2/3 and phospho-Smad1/5/9 levels were assayed with α-Ubiquitin serving as a loading control.

It is possible for GDF6 to induce Smad2/3 phosphorylation as GDF6 binds to the activin receptor 2 (ActRII) B with a high affinity, and ActRIIB can associate with the activin receptor 1 B (ActRIB; Alk4) [25]. However, it is unknown whether GDF6 can produce Smad2/3 signaling in RPE. Previous studies have used cell lines that did not express ActRIB,

whereas RPE cells have high expression levels of this receptor [10, 17]. Due to this combination of receptors, RPE maintain the potential to have GDF6 induce Smad2/3 phosphorylation. We discovered that undifferentiated P0 RPE can participate in canonical Smad2/3 phosphorylation through TGFβ1 stimulation, but GDF6 itself does not induce a similar response (Figure 3.5). GDF6 only initiates Smad1/5/9 signaling in RPE, similar to other cell types.

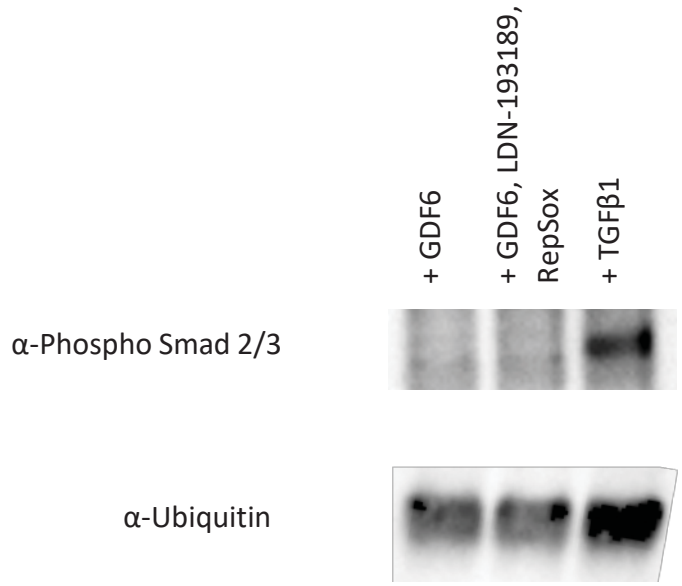

Figure 3.5. GDF6 does not induce Smad2/3 phosphorylation in RPE. Passage 0 RPE were pretreated with LDN and RepSox inhibitors for one hour prior to stimulation with 1 µg/ mL (73 µM) rmGdf6 or 100 ng/mL (4 µM) TGFβ1. Cells stimulated with rmGdf6 show no induction of Smad2/3 phosphorylation whereas cells treated with TGFβ1 induce a robust phosphorylation on Smad2/3.

GDF6 and TGFβ ligands initiate a dissimilar response in RPE based on the maturity and state of differentiation of the cells. Mature P0 RPE cells are unable to undergo Smad1/5/9 phosphorylation in the presence of GDF6 yet retain the ability to be stimulated

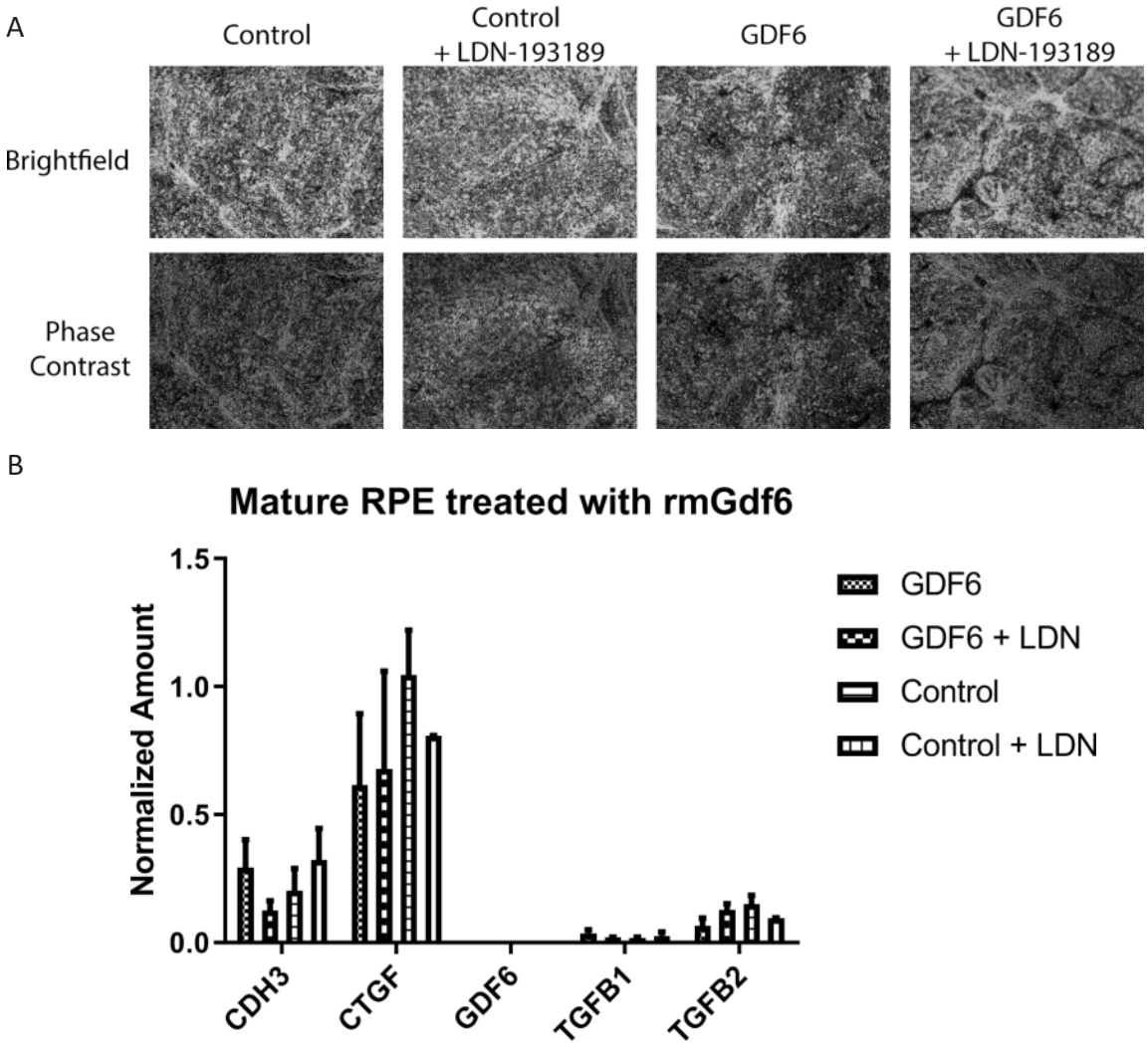

Figure 3.6. GDF6 has no effect on the morphology or gene expression of mature, differentiated RPE. (A) Brightfield and phase contrast 10X images of P0 RPE that have been differentiating for 60 days. Cells received 3 µg/mL (219µM) GDF6 every other day for 14 days. LDN was also administered every other day for 14 days. (B) RT-qPCR analysis of mature, differentiated P0 RPE treated with rmGdf6 for 14 days. Genes that had a significant change in previous overexpression experiments were selected for analysis.

by TGFβ1 (Figure 3.4-B). This absence of an immediate response to GDF6 was intriguing, so we investigated the effect of longer-term exposure to GDF6 on mature, differentiated RPE. After 14 days of administration of recombinant mouse (rmGdf6), the RPE display no overt difference in cell morphology or pigmentation when compared to their control counterparts (Figure 3.6-A). The lack of effect from rmGdf6 exposure remains true when examining any

gene expression changes in cells treated with rmGdf6; RT-qPCR analysis revealed no significant differences in gene expression on the genes which were previously most affected by GDF6 (Figure 3.6-B). It appears GDF6 can only affect RPE if they are in a dedifferentiated, less mature state.

3.2.3: GDF6 Accelerates the Mesenchymal Transition in RPE

As RPE are passaged under a persistent wounding model, they naturally undergo EMT [10]. Though mature P0 RPE treated for 14 days with rmGdf6 showed no phenotypic or genotypic effect, we observed a substantial effect on undifferentiated passage 2 (P2) RPE using the same concentration of rmGdf6. Passage 2 RPE are at a stage where they are beginning to waver between a pigmented, epithelial-like state and a more mesenchymal state, as evidenced in the altered morphology of the control cells seen in Figure 3.7-A. When treated with rmGdf6, the cells exhibit a more severe phenotype than seen in early passage cells. The cells are long and tube-like, with a net-like appearance instead of a spindle-like shape seen in P0 cells treated with GDF6. Looking at a subset of genes most likely to change during passaging, we see GDF6 treatment causes expression of p-cadherin, the most abundant cadherin in RPE, to drop to levels that are undetectable (Figure 3.7-B). As expected, other common EMT markers like connective tissue growth factor (*CTGF*) and *TGFβ2* are upregulated from GDF6 treatment in P2 RPE. There is no significant change in the *TGFβ1* level between P2 cells treated with GDF6 and those not. It is possible that as these RPE are beginning to undergo EMT, *TGFβ1* has reached its maximum expression value, and therefore no increase can be made. Importantly, it appears that the exogenous addition of GDF6 causes an endogenous upregulation of *GDF6* transcripts, suggesting GDF6 participates

in a positive feedback loop for itself (see discussion).

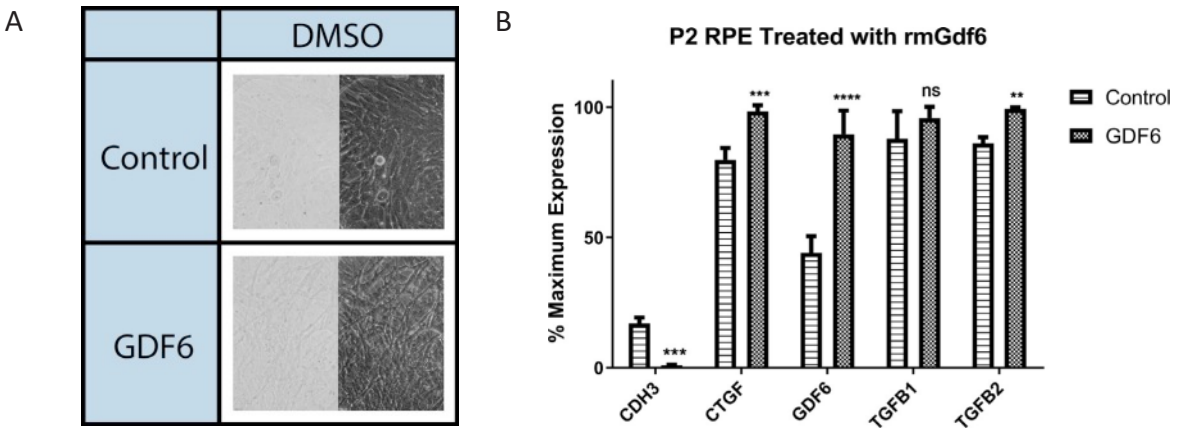

Figure 3.7. GDF6 causes a more severe phenotype on passage 2 RPE. (A) Brightfield and phase contrast 10X images of passage 2 RPE cells treated with 3µg/mL (219 nM) rmGdf6 for 14 days. At P2, the control cells are beginning to undergo EMT, losing the ability to pigment as well as their cobblestone-like phenotype. (B) RT-qPCR analysis of a subset of genes most affected by GDF6. A decrease in epithelial gene expression and an increase in mesenchymal gene expression is expected in P2 RPE. Statistical significance was determined using a 2-way ANOVA with a Bonferroni post-test (** ≤ 0.005, *** ≤ 0.0005, **** < 0.0001).

3.2.4: GDF6 Has a Dose-Dependent Effect on RPE

A dose-dependent effect of *GDF6* on RPE was achieved by plating a known number of cells overexpressing *GDF6* with a known number of control RPE expressing the empty vector. As seen in Figure 3.8, the two populations of cells are mixed and allowed to differentiate for 32 days. RPE cell morphology is altered more as the percentage of *GDF6* positive cells increase. Pigmentation is lost, cell size increases, the cuboidal structure is lost

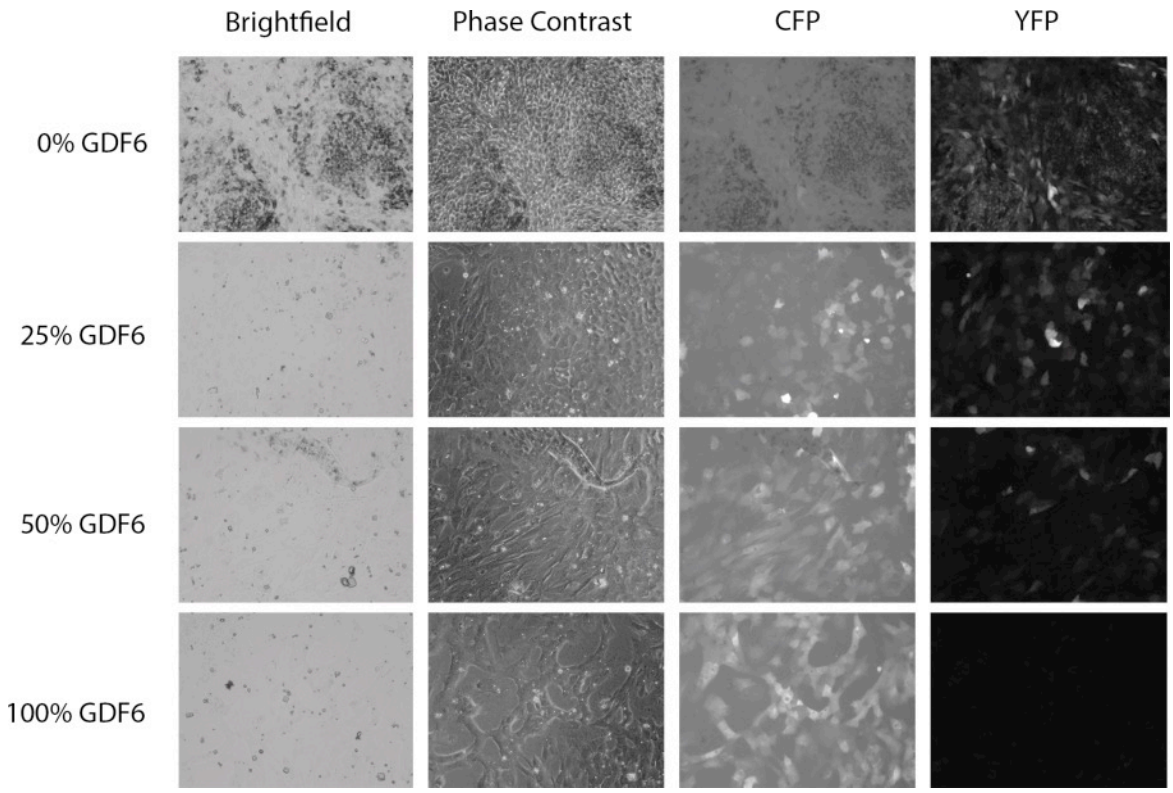

Figure 3.8. Dose-dependent effect of *GDF6* on RPE. A dose-dependent effect of *GDF6* can be observed by combining RPE overexpressing *GDF6* with RPE infected with a control vector. RPE over expressing either *GDF6* or an empty vector control were sorted and plated in to wells as follows: 0% GDF6, 100% Control; 25% GDF6, 75% Control; 50% GDF6, 50% Control; or 100% GDF6, 0% Control. The cells were allowed to differentiate for 32 days at which 10X images were taken. The cells over expressing *GDF6* fluoresce CFP while the control cells fluoresce YFP.

and holes appear in the monolayer. The severity of the phenotype is correlated with an increase in GDF6 expression.

GDF6 has an effect, measured by canonical Smad1/5/9 phosphorylation, on RPE in the micromolar range (Figure 3.9). RPE exposed to nanomolar concentrations of rmGdf6 show a considerable reduction of Smad1/5/9 phosphorylation. This finding led us to investigate the dose-dependent effect of rmGdf6 on P0 RPE. RPE were grown in the

presence of rmGdf6 for 14 days, feeding every other day. This protocol is consistent with what has produced major results in the previous experiments. After 14 days of differentiation, P0 RPE cells are beginning to exhibit characteristics typical of mature RPE, such as pigmentation and a cobblestone appearance. As the concentration of rmGdf6 is increased, the potential of RPE to exhibit these characteristics decreases (Figure 3.10 A). The highest concentration of rmGdf6, (5ug/ml) causes the RPE to look tubular and enlarged, no longer recognizable as an epithelial cell.

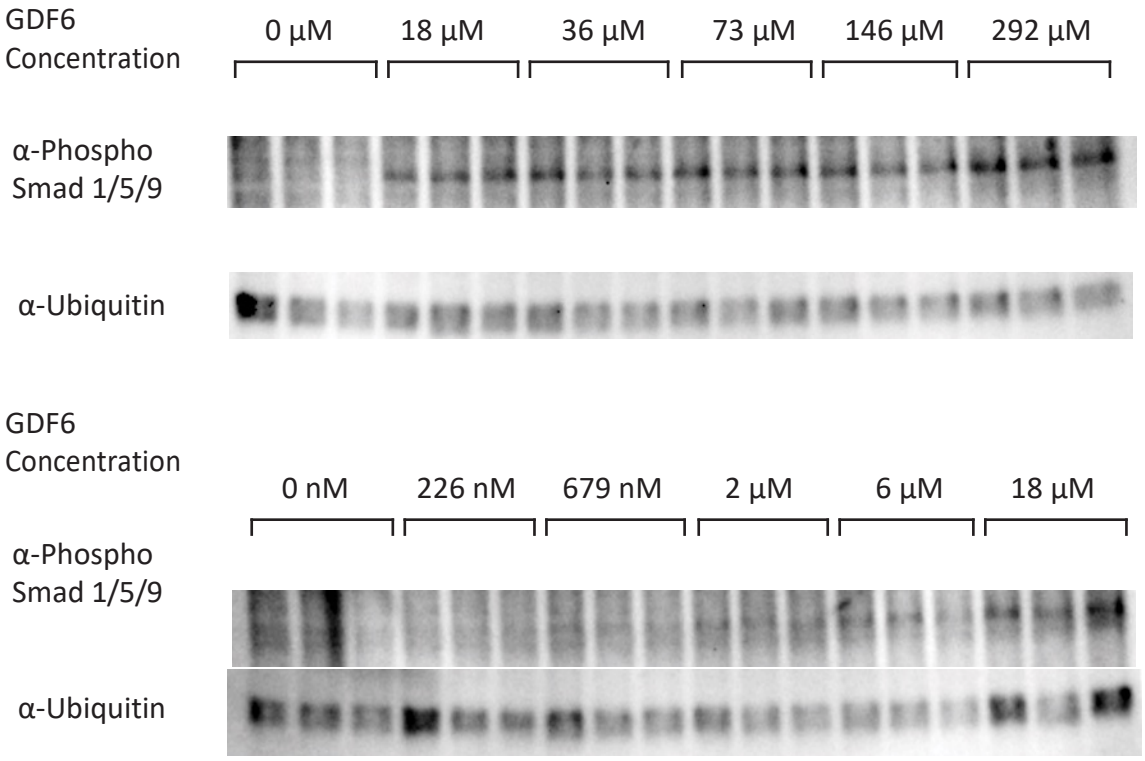

Figure 3.9. GDF6 induces Smad1/5/9 phosphorylation in RPE in micromolar concentrations. rmGdf6 was administered to p0 RPE for 30 minutes. The samples were harvested and assayed for Smad1/5/9 phosphorylation. rmGdf6 administered in the nanomolar range failed to induce phosphorylation, whereas rmGdf6 administered in the micromolar range induced Smad1/5/9 phosphorylation.

Many genes found in mature RPE or RPE with a mesenchymal phenotype also exhibit a dose-dependent response to rmGdf6. As the rmGdf6 concentration increases, we see a corresponding increase in the natural inhibitor of GDF6, Noggin. This dose-dependent effect is also seen with two genes prominent in mesenchymal RPE: Osteopontin (*SPP1*) and *TGFβ1*. Two genes important for RPE function show a dose dependent decrease with rmGdf6. The first is *LRAT*, a critical gene involved in the visual cycle. The second is premelanosome protein (*PMEL*), a gene involved in pigmentation, which appears to be silenced entirely once a particular concentration of GDF6 is reached. Interestingly, adding rmGdf6 to P0 RPE cells does not induce endogenous *GDF6* production as was previously seen in P2 RPE.

A.

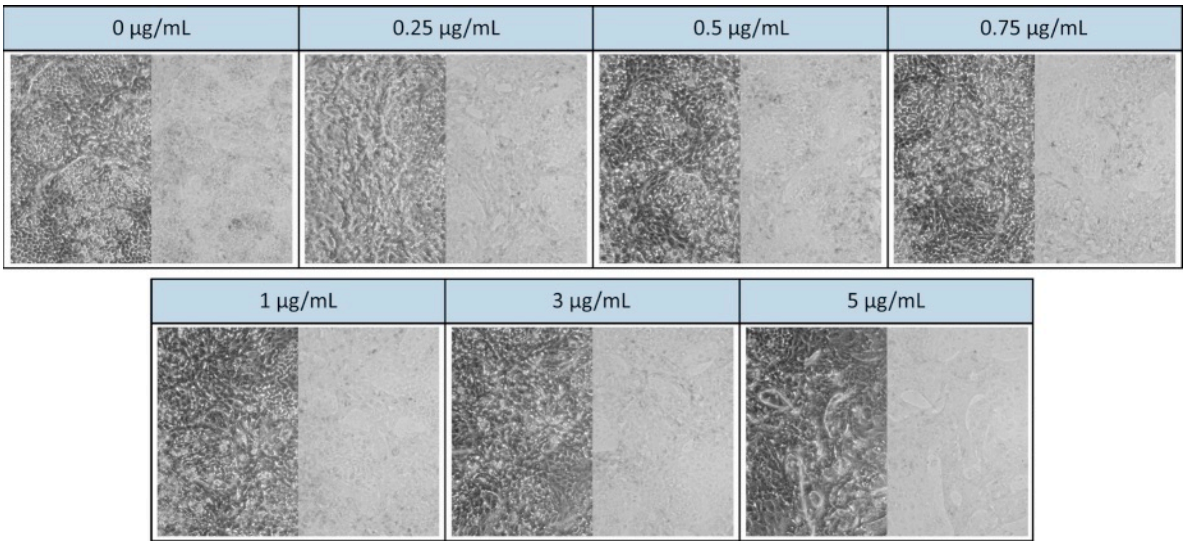

B.

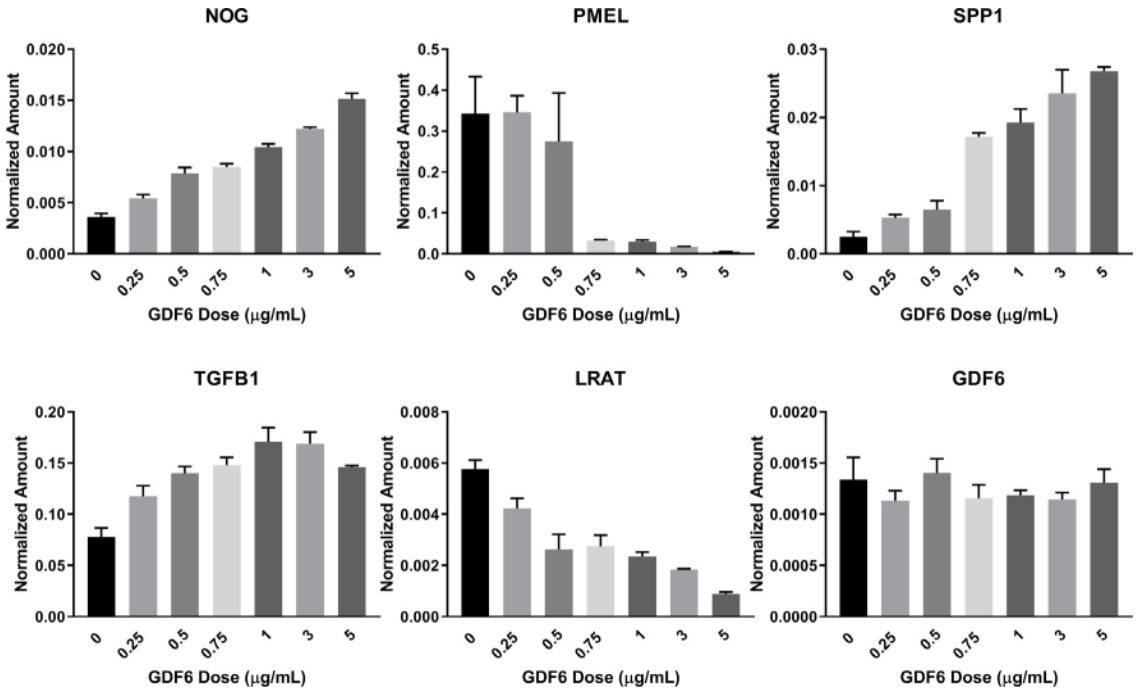

Figure 3.10. rmGdf6 has a dose-dependent effect on RPE. (A) Phase contrast (left) and brightfield (right) 10X images of P0 RPE treated with various amounts of rmGdf6 for 14 days. As the concentration of rmGdf6 increases, the traditional cobblestone phenotype diminishes. At the highest concentration, the cells appear tubular and thin. (B) RT-qPCR analysis of RPE treated with various amounts of rmGdf6 for 14 days. Highlighted are genes that exhibited a dose-like effect when treated with rmGdf6.

3.3: Discussion

RPE must maintain a healthy state, performing their essential barrier and support functions, in order to have healthy vision. When RPE become diseased or damaged, they often undergo an epithelial to mesenchymal transition into a fibrotic cell. This transition, in turn, results in the death of photoreceptors or scarring in the eye leading to blindness. To prevent this detrimental EMT, we must first understand it. *GDF6* is highly upregulated in RPE that have undergone EMT but not expressed in healthy RPE. Thus, *GDF6* became a candidate gene for playing a role in EMT and causing RPE to enter a fibrotic state.

3.3.1: GDF6 Expression Causes RPE to Undergo EMT

We found GDF6 RPE to share many characteristics with P5 RPE (RPE that have undergone an irreversible EMT and begun to form fibrotic cells). Previous work has shown that these highly passaged P5 cells are unable to undergo MET and form a cobblestone monolayer. They exhibit a fibrotic appearance with holes beginning to appear in the monolayer [10]. Additionally, there are substantial changes in gene expression, with P5 RPE downregulating genes found in healthy RPE and upregulating genes related to EMT and a mesenchymal state [10, 26]. One of the genes that exhibited the highest change in RPE gene expression was *GDF6*, with its levels undetectable in P0 RPE and highly expressed in P5 RPE [10]. When we treated early passage RPE with GDF6, we saw the RPE exhibit morphology (loss of a cobblestone phenotype and reduced pigmentation) and changes in gene expression, similar to P5 RPE. The important difference between the two cell populations is that GDF6 RPE undergo EMT without passaging, suggesting *GDF6* is an initiator for terminal EMT in RPE.

There are multiple markers which indicate the transition of epithelial cells into mesenchymal cells, such as changes in cadherin expression, cytoskeletal rearrangement, and an increase in focal adhesions and stress fibers [1, 27-29]. The most characteristic sign that a cell has undergone EMT is the loss of epithelial cadherin (*CDH1*) and upregulation of mesenchymal cadherin (*CDH2*). While RPE express *CDH1*, it has been shown that p-cadherin (*CDH3*) is the most abundant cadherin in mature RPE [30]. GDF6 RPE decrease epithelial cadherins *CDH1* and *CDH3*, indicating the cells are no longer epithelial. CDH11 has been shown to interact with the more traditional mesenchymal n-cadherin (*CDH2*), suggesting *CDH11* expression may also be a marker for a mesenchymal cell [31]. GDF6 RPE show increased transcripts in both mesenchymal cadherins, no longer maintaining the necessary transcripts to form traditional epithelial adherins junctions.

Another common hallmark of EMT is fibronectin expression and changes in the extracellular matrix (ECM). As the cell transitions from a sedentary cell to a motile cell, changes in the ECM need to occur. Collagen is the most abundant fibrin protein in the ECM, followed by elastin and fibronectin (FN) [32, 33]. As cells undergo EMT, they begin to produce larger quantities of these ECM proteins, specifically collagen 1, collagen 3, and FN. This transformed ECM provides a stiffer environment, stimulating directional migration of the cells. GDF6 RPE also upregulate many of these ECM proteins, suggesting the cell has undergone EMT. Additionally, GDF6 RPE upregulate genes related to focal adhesion and stress fibers. Focal adhesions are essential in mediating the effects of the ECM on cell behavior and require cells to spread in order to form [34]. Under extreme conditions, like repetitive passaging or wounding, enhanced ECM crosslinking can lead to aberrant fibrosis,

similar to what is observed in diseases like proliferative vitreoretinopathy [32]. GDF6 may be placing the RPE under constant stress, forcing them to maintain this altered ECM, ultimately resulting in a final mesenchymal state.

In vitro, RPE are coaxed into undergoing EMT through various stressors, such as low density passaging or stimulation with TGFβ ligands [10]. GDF6 RPE undergo EMT without passaging of the cells. This morphological transformation may be similar to what occurs with TGFβ stimulation—the cells spontaneously undergo EMT [35]. When passaged, it is necessary for RPE to proliferate to reach confluence. However, the cells will stop dividing, undergo MET, and initiate differentiation once confluence is established. GDF6 RPE may not be able to undergo MET or halt proliferation. It is possible GDF6 RPE lose their contact inhibition ability and instead continuously proliferate. As the cells differentiate, they begin to grow on top of one another, forming a mesh-like network of cells instead of a nice even layer. BMP proteins have been found to have a multitude of effects in various cell types during development, including but not limited to the regulation of cell proliferation, apoptosis, and migration [36]. GDF6 RPE may upregulate cell cycle genes and proliferation early on, as no apparent upregulation in cell cycle genes is seen at 32 days of differentiation. Analysis of GDF6 RPE at various time points during differentiation can elucidate any potential increases in cell cycle markers. Many epithelial cancer cells will undergo EMT to migrate and invade tissues, resulting in a metastatic phenotype [37]. One of the hallmarks of cancer cells and tumor formation is the loss of cell contact inhibition, instead erroneously proliferating and growing on top of one another, similar to what is seen in GDF6 RPE [38].

TGFβ ligands are known inducers of EMT and a mesenchymal fate in RPE [2, 7, 39]. However, these ligands are likely not responsible for an irreversible EMT in RPE. TGFβ proteins are present in early passage, healthy RPE [10]. It is necessary for these RPE to undergo EMT to reach confluence, but the cells can undergo MET and revert to their epithelial state. GDF6 RPE are unable to undergo MET, suggesting *GDF6* may be inhibiting or preventing that pathway. *GDF6* may not be the primary reason why passaged RPE are unable to undergo MET, but it may interact or activate an inhibitor of the pathway. In order to determine the role *GDF6* has in both EMT and MET, the gene will need to be silenced.

3.3.2: GDF6 Only Affects Wounded RPE

For RPE to undergo EMT, there needs to be some cellular stress or damage to induce a loss of cell-cell contact. Differentiated RPE that maintain cell-cell contacts are resistant to TGFβ2 induced EMT, whereas cells that have lost this contact are especially susceptible to TGFβ2 stimulation [40]. GDF6 RPE also display this phenomenon, suggesting the RPE are resistant to GDF6 stimulation if fully mature, implying that the induction of EMT by TGFβ family members is not possible in healthy RPE monolayers.

When RPE are passaged under a persistent wounding model, the cells begin to express *GDF6* [10]. As the cells become more stressed through passage, they elicit a much stronger response to GDF6 treatment, taking on a myofibroblast phenotype. In this state, exogenous GDF6 exposure results in an endogenous increase in *GDF6* transcripts. *GDF6* then causes the RPE to enter a terminal EMT state, ultimately resulting in fibrosis. This natural upregulation of *GDF6* by RPE may be a protective mechanism. The retina is one of the most metabolically active tissues in the body, and RPE are responsible for processing

and transporting all of these metabolites, which puts high stress on the cell [5]. RPE are exposed to other stressors as well, such as ultraviolet radiation (which can cause DNA double-stranded breaks), and being that they are a somewhat quiescent cell, do not undergo the same rigorous proofreading as cells that regularly divide [41, 42]. RPE that accumulate damage (through inflammatory cytokines, DNA damage, oxidative stress, or other mechanisms) may not be able to perform the multitude of functions required of RPE, so they are transformed into a fibrotic cell instead.

3.3.3: Implications in Disease

EMT of the RPE is a common phenotype found in eye diseases that result in scarring or RPE death, like PVR and CNV [6, 8, 9, 43, 44]. One study has linked a lack of *GDF6* to an increased risk of age-related macular degeneration (AMD), finding elevated levels of *GDF6* mRNA in the mouse retina and protein localization using immunohistochemistry [45]. Our results from this study disagree. First, *GDF6* mRNA is undetectable in healthy mature human RPE. Secondly, an antibody selective for GDF6 has yet to be located. We have found antibodies that can detect GDF6; however, it appears that other proteins are being detected as well. Large amounts of protein are seen in healthy RPE when no mRNA transcripts for *GDF6* exist, suggesting the antibodies are non-specific and potentially recognizing some other, closely related GDF protein.

GDF6 is crucial during early ocular and retinal development, and lack of GDF6 has been associated with microphthalmia, photoreceptor death, and loss of laminar structure [13, 14, 16]. Proper development of the retina requires *GDF6*, but once the eye is fully differentiated, its presence is detrimental. This phenomenon of ligands having opposing

effects over time is well reported in various members of the TGFβ family; loss of TGFβ2 in early development results in altered ocular tissues (such as a thin cornea and immature retina), whereas TGFβ2 expression in the developed eye can result in tissue fibrosis [46].

GDF6 has not been implicated in the pathogenesis of PVR or CNV [47]. Previous studies have shown that once RPE take on a myofibroblast phenotype, levels of *GDF6* gradually decline over time [10]. By the time these diseases have been diagnosed, the RPE have already undergone EMT. It is possible for *GDF6* to be present in early stages of the disease to push RPE into a terminal EMT state and then disappear as it is no longer necessary to maintain the cell in a fibrotic state. We saw that *in vitro* RPE exhibit drastic changes in their gene expression and morphology in only 32 days of GDF6 exposure. It may be that the overexpression of *GDF6* causes higher than normal amounts of GDF6 to be produced, eliciting a more drastic effect on the RPE. Stimulating RPE with recombinant mouse Gdf6 ligand produces the same results, ensuring the effect is not a by-product of overexpression. It would be helpful to determine the endogenous levels of GDF6 in P5 RPE, but a robust antibody is needed to do so. Once this is established, GDF6 can be administered to RPE for different durations to determine at what point they no longer need GDF6 and remain in a mesenchymal state.

3.4: Conclusion

GDF6 RPE display qualities and characteristics of a mesenchymal cell, suggesting the RPE have undergone EMT. This effect is only noticeable on RPE that have lost cell-cell contact, potentially through damage or disease. Inhibition of GDF6 may help prevent diseases like CNV and PVR where EMT of the RPE is a major phenotype. Though a

knockdown is needed to determine its necessity, we have shown that GDF6 is sufficient to cause irreversible EMT in RPE.

3.5: References

1. Kalluri, R. and R.A. Weinberg, *The basics of epithelial-mesenchymal transition.* J Clin Invest, 2009. **119**(6): p. 1420-8.
2. Xu, J., S. Lamouille, and R. Derynck, *TGF-beta-induced epithelial to mesenchymal transition.* Cell Res, 2009. **19**(2): p. 156-72.
3. Thiery, J.P., et al., *Epithelial-mesenchymal transitions in development and disease.* Cell, 2009. **139**(5): p. 871-90.
4. Stone, R.C., et al., *Epithelial-mesenchymal transition in tissue repair and fibrosis.* Cell Tissue Res, 2016. **365**(3): p. 495-506.
5. Strauss, O., *The Retinal Pigment Epithelium*, in *Webvision: The Organization of the Retina and Visual System [Internet].* F.E. Kolb H, Nelson R, Editor. 2011, University of Utah Health Sciences Center.
6. Ohlmann, A., et al., *Epithelial-mesenchymal transition of the retinal pigment epithelium causes choriocapillaris atrophy.* Histochem Cell Biol, 2016. **146**(6): p. 769-780.
7. Casaroli-Marano, R.P., R. Pagan, and S. Vilaro, *Epithelial-mesenchymal transition in proliferative vitreoretinopathy: intermediate filament protein expression in retinal pigment epithelial cells.* Invest Ophthalmol Vis Sci, 1999. **40**(9): p. 2062-72.
8. Chen, Z., Y. Shao, and X. Li, *The roles of signaling pathways in epithelial-to-mesenchymal transition of PVR.* Mol Vis, 2015. **21**: p. 706-10.
9. Hirasawa, M., et al., *Transcriptional factors associated with epithelial-mesenchymal transition in choroidal neovascularization.* Mol Vis, 2011. **17**: p. 1222-30.
10. Radeke, M.J., et al., *Restoration of mesenchymal retinal pigmented epithelial cells by TGFβ pathway inhibitors: implications for age-related macular degeneration.* Genome Med, 2015. **7**(1): p. 58.
11. Chang, C. and A. Hemmati-Brivanlou, *Xenopus GDF6, a new antagonist of noggin and a partner of BMPs.* Development, 1999. **126**(15): p. 3347-57.
12. Settle, S.H., Jr., et al., *Multiple joint and skeletal patterning defects caused by single and double mutations in the mouse Gdf6 and Gdf5 genes.* Dev Biol, 2003. **254**(1): p. 116-30.
13. Asai-Coakwell, M., et al., *GDF6, a novel locus for a spectrum of ocular developmental anomalies.* Am J Hum Genet, 2007. **80**(2): p. 306-15.
14. Asai-Coakwell, M., et al., *Contribution of growth differentiation factor 6-dependent cell survival to early-onset retinal dystrophies.* Hum Mol Genet, 2013. **22**(7): p. 1432-42.
15. Gonzalez-Rodriguez, J., et al., *Mutational screening of CHX10, GDF6, OTX2, RAX and SOX2 genes in 50 unrelated microphthalmia-anophthalmia-coloboma (MAC) spectrum cases.* Br J Ophthalmol, 2010. **94**(8): p. 1100-4.

16. Hanel, M.L. and C. Hensey, *Eye and neural defects associated with loss of GDF6.* BMC Dev Biol, 2006. **6**: p. 43.
17. Mazerbourg, S., et al., *Identification of receptors and signaling pathways for orphan bone morphogenetic protein/growth differentiation factor ligands based on genomic analyses.* J Biol Chem, 2005. **280**(37): p. 32122-32.
18. Chen, L., et al., *Bone Morphogenetic Protein 9 and 13 Induce C3H10T1/2 Cell Differentiation to Cardiomyocyte-Like Cells In Vitro.* Cell Transplant, 2015. **24**(5): p. 909-20.
19. Clarke, L.E., et al., *Growth differentiation factor 6 and transforming growth factor-beta differentially mediate mesenchymal stem cell differentiation, composition, and micromechanical properties of nucleus pulposus constructs.* Arthritis Res Ther, 2014. **16**(2): p. R67.
20. Clendenning, D.E. and D.P. Mortlock, *The BMP ligand Gdf6 prevents differentiation of coronal suture mesenchyme in early cranial development.* PLoS One, 2012. **7**(5): p. e36789.
21. Haddad-Weber, M., et al., *BMP12 and BMP13 gene transfer induce ligamentogenic differentiation in mesenchymal progenitor and anterior cruciate ligament cells.* Cytotherapy, 2010. **12**(4): p. 505-13.
22. Krispin, S., et al., *Growth Differentiation Factor 6 Promotes Vascular Stability by Restraining Vascular Endothelial Growth Factor Signaling.* Arterioscler Thromb Vasc Biol, 2018. **38**(2): p. 353-362.
23. Cuny, G.D., et al., *Structure-activity relationship study of bone morphogenetic protein (BMP) signaling inhibitors.* Bioorg Med Chem Lett, 2008. **18**(15): p. 4388-92.
24. Boergermann, J.H., et al., *Dorsomorphin and LDN-193189 inhibit BMP-mediated Smad, p38 and Akt signalling in C2C12 cells.* Int J Biochem Cell Biol, 2010. **42**(11): p. 1802-7.
25. Berasi, S.P., et al., *Divergent activities of osteogenic BMP2, and tenogenic BMP12 and BMP13 independent of receptor binding affinities.* Growth Factors, 2011. **29**(4): p. 128-39.
26. Shih, Y.H., et al., *Restoration of Mesenchymal RPE by Transcription Factor-Mediated Reprogramming.* Invest Ophthalmol Vis Sci, 2017. **58**(1): p. 430-441.
27. Kalluri, R., *EMT: When epithelial cells decide to become mesenchymal-like cells.* 2009.
28. McCormack, N. and S. O'Dea, *Regulation of epithelial to mesenchymal transition by bone morphogenetic proteins.* Cell Signal, 2013. **25**(12): p. 2856-62.
29. Sun, B.O., et al., *Role of cellular cytoskeleton in epithelial-mesenchymal transition process during cancer progression.* Biomed Rep, 2015. **3**(5): p. 603-610.
30. Yang, X., et al., *Cadherins in the retinal pigment epithelium (RPE) revisited: P-cadherin is the highly dominant cadherin expressed in human and mouse RPE in vivo.* PLoS One, 2018. **13**(1): p. e0191279.
31. Straub, B.K., et al., *A novel cell-cell junction system: the cortex adhaerens mosaic of lens fiber cells.* J Cell Sci, 2003. **116**(Pt 24): p. 4985-95.
32. Frantz, C., K.M. Stewart, and V.M. Weaver, *The extracellular matrix at a glance.* J Cell Sci, 2010. **123**(Pt 24): p. 4195-200.

33. Theocharis, A.D., et al., *Extracellular matrix structure.* Adv Drug Deliv Rev, 2016. **97**: p. 4-27.
34. Chen, C.S., et al., *Cell shape provides global control of focal adhesion assembly.* Biochem Biophys Res Commun, 2003. **307**(2): p. 355-61.
35. Lee, J., M. Ko, and C.K. Joo, *Rho plays a key role in TGF-beta1-induced cytoskeletal rearrangement in human retinal pigment epithelium.* J Cell Physiol, 2008. **216**(2): p. 520-6.
36. Liu, A. and L.A. Niswander, *Bone morphogenetic protein signalling and vertebrate nervous system development.* Nat Rev Neurosci, 2005. **6**(12): p. 945-54.
37. Chaffer, C.L., et al., *EMT, cell plasticity and metastasis.* Cancer Metastasis Rev, 2016. **35**(4): p. 645-654.
38. Ribatti, D., *A revisited concept: Contact inhibition of growth. From cell biology to malignancy.* Exp Cell Res, 2017. **359**(1): p. 17-19.
39. Grisanti, S. and C. Guidry, *Transdifferentiation of retinal pigment epithelial cells from epithelial to mesenchymal phenotype.* Invest Ophthalmol Vis Sci, 1995. **36**(2): p. 391-405.
40. Tamiya, S., L. Liu, and H.J. Kaplan, *Epithelial-mesenchymal transition and proliferation of retinal pigment epithelial cells initiated upon loss of cell-cell contact.* Invest Ophthalmol Vis Sci, 2010. **51**(5): p. 2755-63.
41. Stern, J. and S. Temple, *Retinal pigment epithelial cell proliferation.* Exp Biol Med (Maywood), 2015. **240**(8): p. 1079-86.
42. Patton, W.P., et al., *Comet assay of UV-induced DNA damage in retinal pigment epithelial cells.* Invest Ophthalmol Vis Sci, 1999. **40**(13): p. 3268-75.
43. Yang, S., et al., *Mechanisms of epithelial-mesenchymal transition in proliferative vitreoretinopathy.* Discov Med, 2015. **20**(110): p. 207-17.
44. Zhang, J., et al., *Notch signaling modulates proliferative vitreoretinopathy via regulating retinal pigment epithelial-to-mesenchymal transition.* Histochem Cell Biol, 2017. **147**(3): p. 367-375.
45. Zhang, L., et al., *High temperature requirement factor A1 (HTRA1) gene regulates angiogenesis through transforming growth factor-β family member growth differentiation factor 6.* J Biol Chem, 2012. **287**(2): p. 1520-6.
46. Saika, S., *TGFbeta pathobiology in the eye.* Lab Invest, 2006. **86**(2): p. 106-15.
47. Tosi, G.M., et al., *HTRA1 and TGF-β1 Concentrations in the Aqueous Humor of Patients With Neovascular Age-Related Macular Degeneration.* Invest Ophthalmol Vis Sci, 2017. **58**(1): p. 162-167.

CHAPTER IV: Inhibition of GDF6 Does Not Prevent EMT in RPE

4.1: Introduction

In the previous chapter, we found growth differentiation factor 6 (*GDF6*/*BMP13*), a member of the transforming growth factor-beta (TGFβ) superfamily, to play a role in the epithelial to mesenchymal transition (EMT) of the retinal pigmented epithelium (RPE). Expression of GDF6 resulted in a mesenchymal phenotype of the cells, indicating that *GDF6* is sufficient in inducing EMT in RPE. However, the necessity of *GDF6* in the EMT process remains unknown. Prevention of aberrant wound healing in the RPE is essential to maintain healthy vision. EMT of the RPE is associated with the pathology of various eye diseases, including choroidal neovascularization (wet age-related macular degeneration) or proliferative vitreoretinopathy due to retinal detachment [1, 2].

TGFβ proteins are known inducers of EMT in RPE cells [3, 4]. Recent studies have shown that inhibiting the Smad2/3 TGFβ signaling cascade through the small molecule A-83-01, a TGFβ type I receptor (TGFβRI) activin-like kinase (Alk) 5 inhibitor, prolonged the epithelial state in passaged RPE [5]. This small molecule will not suffice as an inhibitor for GDF6 signaling, as GDF6 operates through the bone morphogenic protein (BMP) receptors Alk3 and Alk6 where it participates in Smad1/5/9 phosphorylation [6]. Dorsomorphin is a small molecule that inhibits the BMP type I receptors Alk2, Alk3, and Alk6, thus inhibiting Smad1/5/9 phosphorylation [7]. Recently, dorsomorphin has shown promiscuity for other Alk receptors, and another small molecule, LDN-193189 (LDN) selectively inhibits Smad1/5/9 phosphorylation [8]. We can utilize these small molecules, along with other silencing techniques, to determine the necessity of GDF6 to initiate RPE EMT.

4.2: Results

4.2.1: Inhibition of Smad 1/5/9 Signaling Does Not Prevent EMT in RPE

One way to block the effects of GDF6 on RPE is to prevent its subsequent signaling cascade. Culturing the cells in the presence of the small molecule LDN achieves silencing of the Alk1, 2, 3, and 6 receptors, thus preventing Smad1/5/9 phosphorylation [8, 9]. As seen in Figure 4.1-A, RPE are unable to maintain their pigmentation and lose their cuboidal shape when passaged, even when cultured with LDN. At passage 7 (P7), the RPE have undergone EMT in every treatment, but there are some differences in the morphology of the cells (Figure 4.1-B). RPE cultured without any inhibitor exhibit the typical appearance of RPE that have undergone EMT: the cells are spindle-like, fibrous, and thin. RPE cultured with LDN, on the other hand, exhibit a different morphology. There are more holes in the monolayer; however, the cells retain more of a spherical shape instead of a spindle shape. While the RPE in either treatment no longer resemble healthy RPE, LDN-treated RPE are not typical of RPE that have undergone EMT.

This difference in phenotype is confirmed by a difference in gene expression (Figure 4.2). LDN suppresses *GDF6* expression levels, thus reducing GDF6 protein expression. Expression levels remain relatively the same for the cell junction gene p-cadherin (*CDH3*) up to passage 5, when *GDF6* expression increases in control cells. As *GDF6* levels rise, *CDH3* levels simultaneously decrease; however, *CDH3* levels remain high in RPE cultured with LDN (where *GDF6* levels are low). LDN appears to inhibit *TGFβ1* expression independent of GDF6

A.

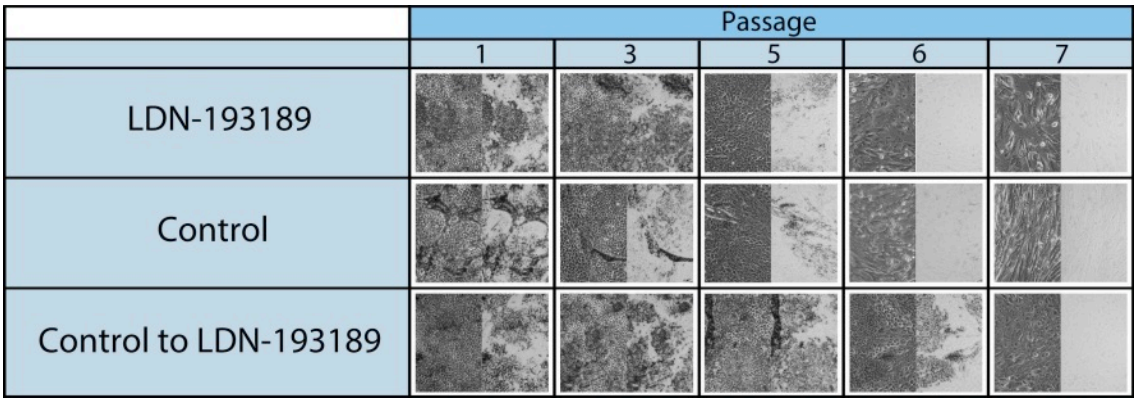

B.

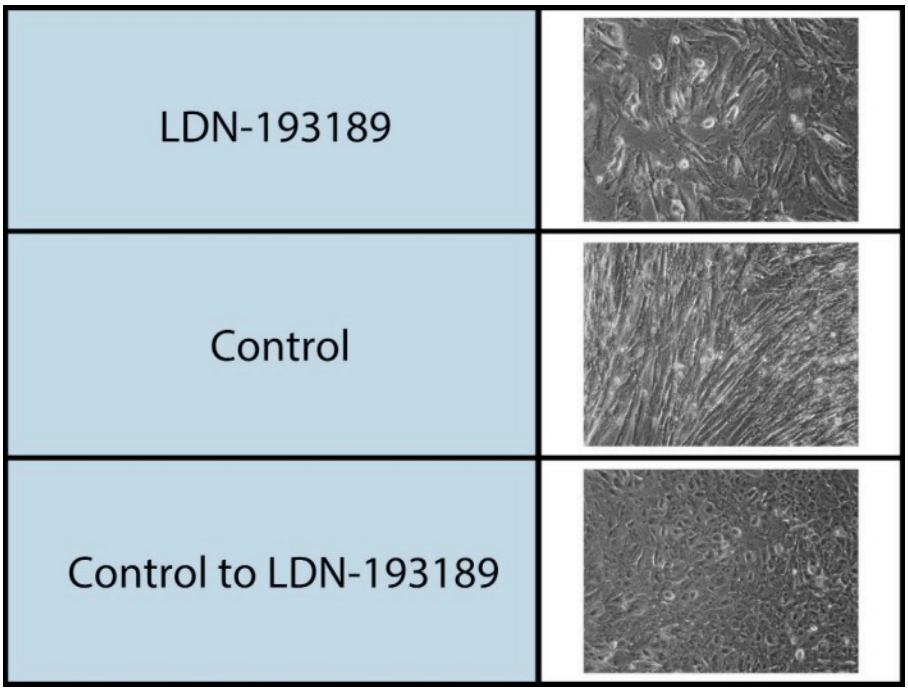

Figure 4.1. RPE passaged in the presence of LDN-193189 (LDN) do not display an extension of the epithelial phenotype. (A) Phase contrast (left) and brightfield (right) 10X images of RPE cultured with LDN. Cells were passaged under a persistent wounding model in the presence of LDN or dimethyl sulfoxide (DMSO) (control). At each passage, a subset of cells was plated at a high density and allowed to differentiate while still in the presence of the inhibitor or DMSO. The control to LDN RPE were passaged in the presence of DMSO but allowed to differentiate in the presence of LDN. (B) Phase contrast 10X images of P7 RPE at each condition. Images were enlarged to show the differences of morphology in each condition.

but does not affect *TGFβ2* levels. The morphological differences observed in P7 cells likely contribute to these differences in gene expression. Inhibiting GDF6 signal transduction does not prevent EMT in RPE, but it does create a difference in what type of mesenchymal cell the RPE become.

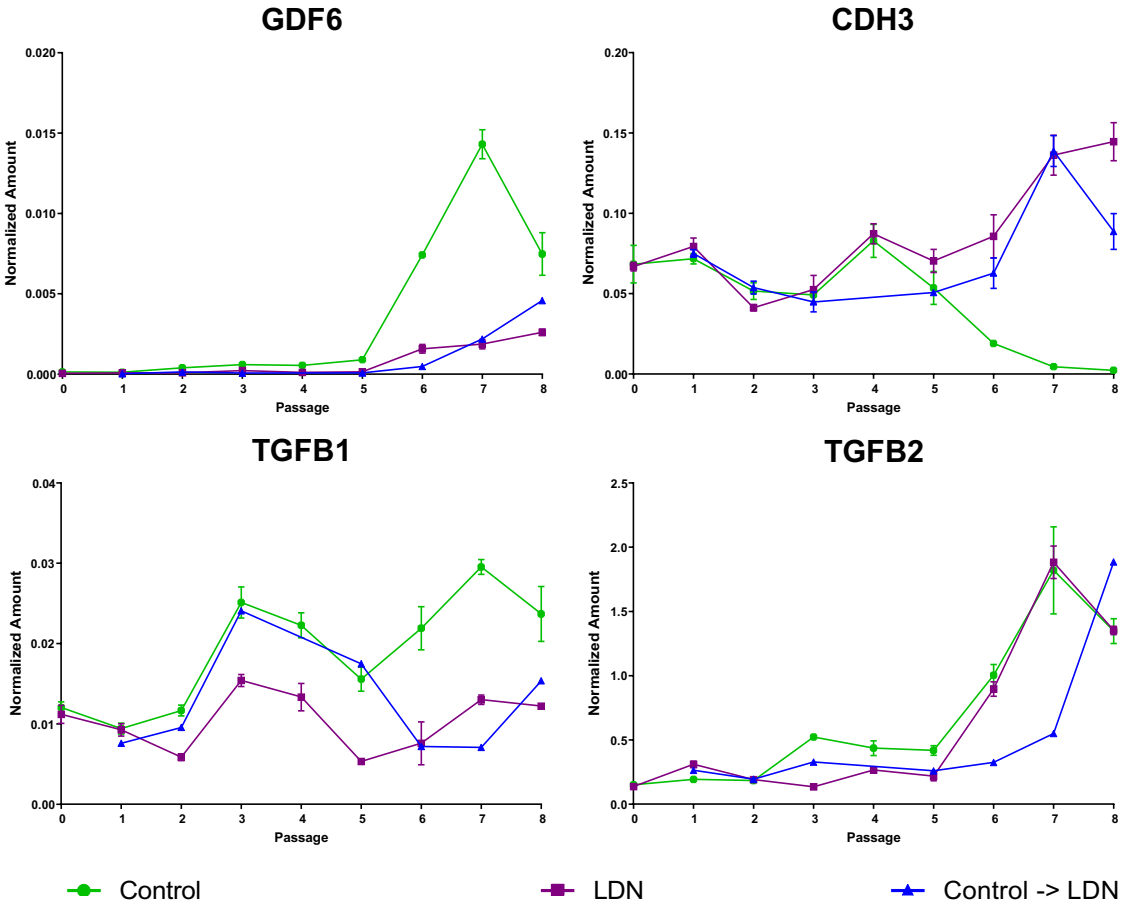

Figure 4.2. RT-qPCR analysis of RPE passaged in the presence or absence of LDN. Cells were passaged under a persistent wounding model and allowed to differentiate for 32 days. Genes that were different between the treatments are highlighted. LDN is able to prevent *GDF6* from reaching control levels. *CDH3* levels remain high in cells treated with LDN while *TGFβ1* levels remain lower than control cells. *TGFβ2* levels remain unchanged, with a slight decrease in expression seen in cells grown in DMSO but allowed to differentiate in LDN.

4.2.2: LDN-193189 Rescues RPE Treated with GDF6

Though LDN was unable to prevent RPE from undergoing EMT, it did show an inhibitory effect on *GDF6*. We examined the potential for LDN to prevent the drastic effects seen when RPE cells are treated with GDF6. Passage 2 (P2) and passage 3 (P3) RPE were treated with recombinant mouse Gdf6 (rmGdf6) for two weeks, resulting in a distinct phenotype in both passages, as evidenced in Figure 4.3-A. However, supplementation with

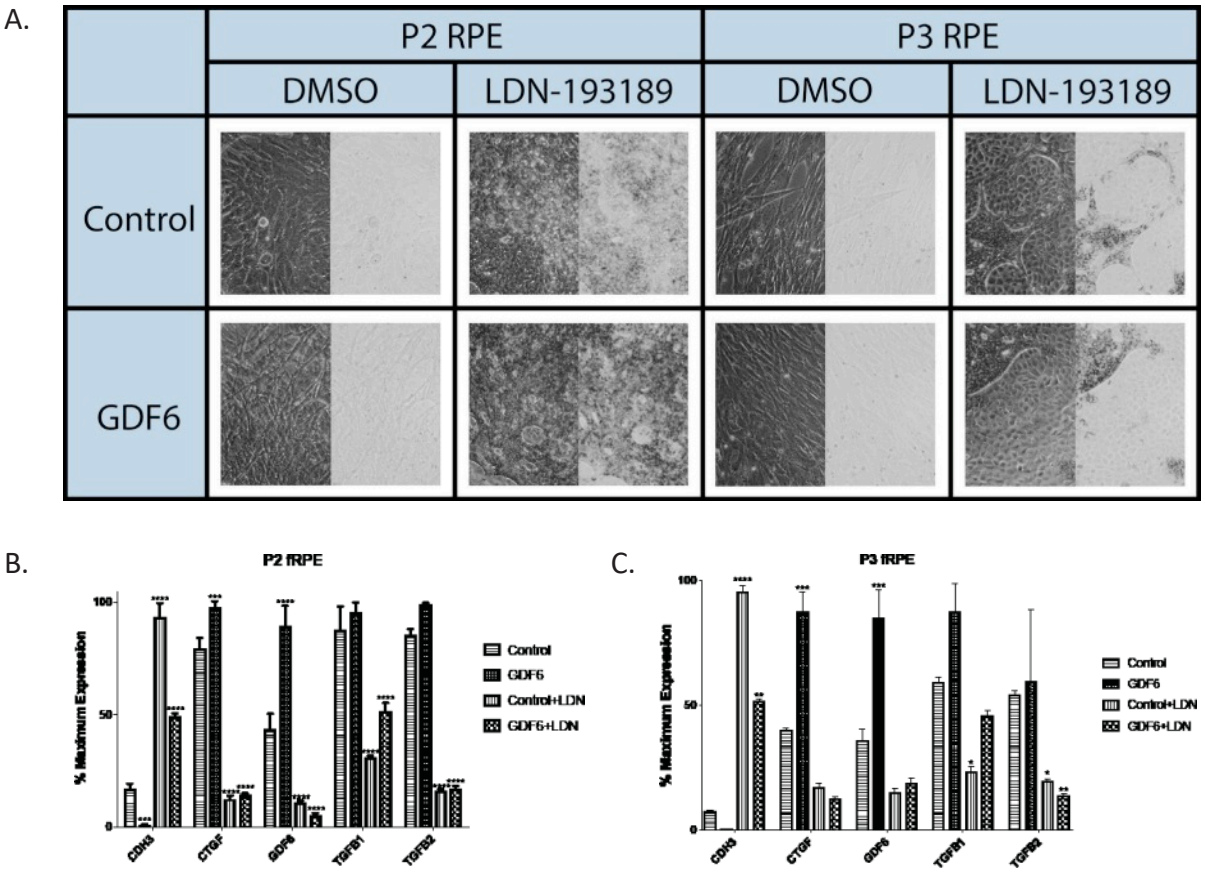

Figure 4.3. Treatment of passaged RPE with rmGdf6 and LDN-193189 (LDN). (A) Phase contrast (left) and brightfield (right) 10x images of passage 2 (P2) and passage 3 (P3) RPE. RPE were plated at high density and treated with 219nM rmGdf6 and 200nM LDN for 14 days. (B-C) RT-qPCR analysis of a subset of genes most affected by GDF6 in P2 and P3 RPE, respectively. Statistical significance with respect to the control DMSO sample was determined using a 2-way ANOVA with a Bonferroni post-test (* ≤ 0.05, ** ≤ 0.005, *** ≤ 0.0005, **** ≤ 0.0001).

LDN prevented the mesenchymal phenotype and allowed the RPE to pigment in the presence of rmGdf6, with P2 cells displaying a more substantial rescue than P3 RPE. This restoration of the phenotype extended to the genotype. Looking at a subset of genes most affected by passage, rmGdf6 treatment exacerbates the mesenchymal phenotype through upregulation of genes found in highly passaged cells like connective tissue growth factor (*CTGF*) (Figure 4.3-B). Treatment with LDN resulted in downregulation of these genes and upregulation of genes found in healthy RPE like *CDH3*. The passaged RPE already begin to express *GDF6* naturally, as P2 and P3 cells are beginning to undergo EMT (as evidenced by the lack of pigmentation and cobblestone morphology in control cells), and GDF6 treatment further upregulates endogenous *GDF6* in both passages. Treatment of the control cells with LDN significantly reduces the expression of *GDF6* in P2 cells and brings it below control levels in P3 cells, resulting in an improved phenotype in both passages. P2 cells show a more drastic reduction of *GDF6* expression with LDN treatment and thus a better rescue of the phenotype. LDN-193189 can effectively rescue the phenotype of externally applied and internally produced GDF6 in RPE.

Full inhibition of the BMP signaling pathway is unable to occur if the concentration of LDN is too low. To investigate the optimal concentration of LDN for full inhibition, we challenged low-density RPE with 1 μg/mL rmGdf and various amounts of LDN (Figure 4.4). RPE show phosphorylation of Smad1/5/9 with no LDN present, but every concentration of LDN examined prevented phosphorylation of Smad1/5/9. The concentration of LDN typically used is 200 nM, which is more than sufficient to prevent any Smad1/5/9 phosphorylation due to GDF6 signaling [5].

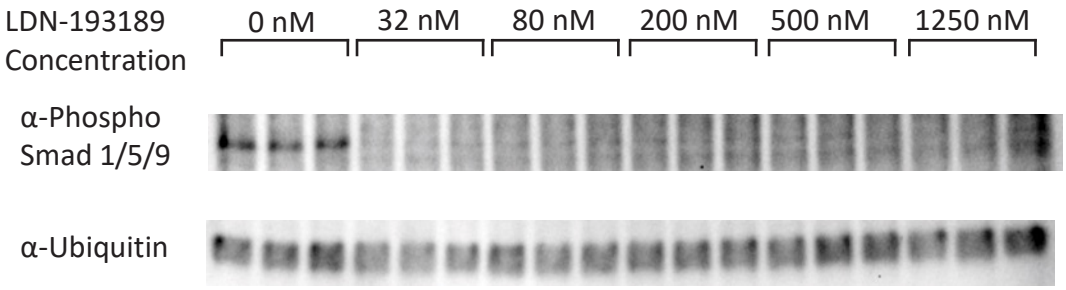

Figure 4.4. LDN-193189 is able to effectively inhibit GDF6 induced Smad1/5/9 signaling. Passage 0 RPE were incubated with the various concentrations of LDN-193189 for one hour. Cells were then challenged with 1 μg/mL rmGdf6 for 30 minutes, at which time the cells were harvested for Smad phosphorylation analysis. GDF6 can induce Smad1/5/9 phosphorylation in cells not treated with LDN-193189 but is prevented from initiating phosphorylation in all concentrations of LDN-193189 assayed. α-Ubiquitin is used as a loading control.

4.2.3: Inhibition of TGFβ Receptors Rescues RPE Overexpressing GDF6

Given the potential for mouse and human GDF6 to behave differently, we investigated if RPE could be rescued using LDN while overexpressing human *GDF6*. Data from P2 and P3 RPE, which begin to express *GDF6* naturally, suggested LDN could rescue the phenotype, but *GDF6* still had relatively low expression (Figure 4.3). We transfected RPE with *GDF6* or an empty control vector and let the cultures differentiate in the presence of LDN, RepSox (an Alk5 or Smad2/3 inhibitor), or a combination of both. After 32 days of differentiation, the untreated cells behaved as expected, while the *GDF6* overexpressing cells appeared mesenchymal-like and the control cells differentiated into a healthy monolayer (Figure 4.5-A). Treatment of RPE with the BMP receptor inhibitor LDN resulted in a rescue of the mesenchymal phenotype. The RPE regained their cuboidal morphology and pigmented, similar to healthy RPE (Figure 4.5-B). There were no overt morphological

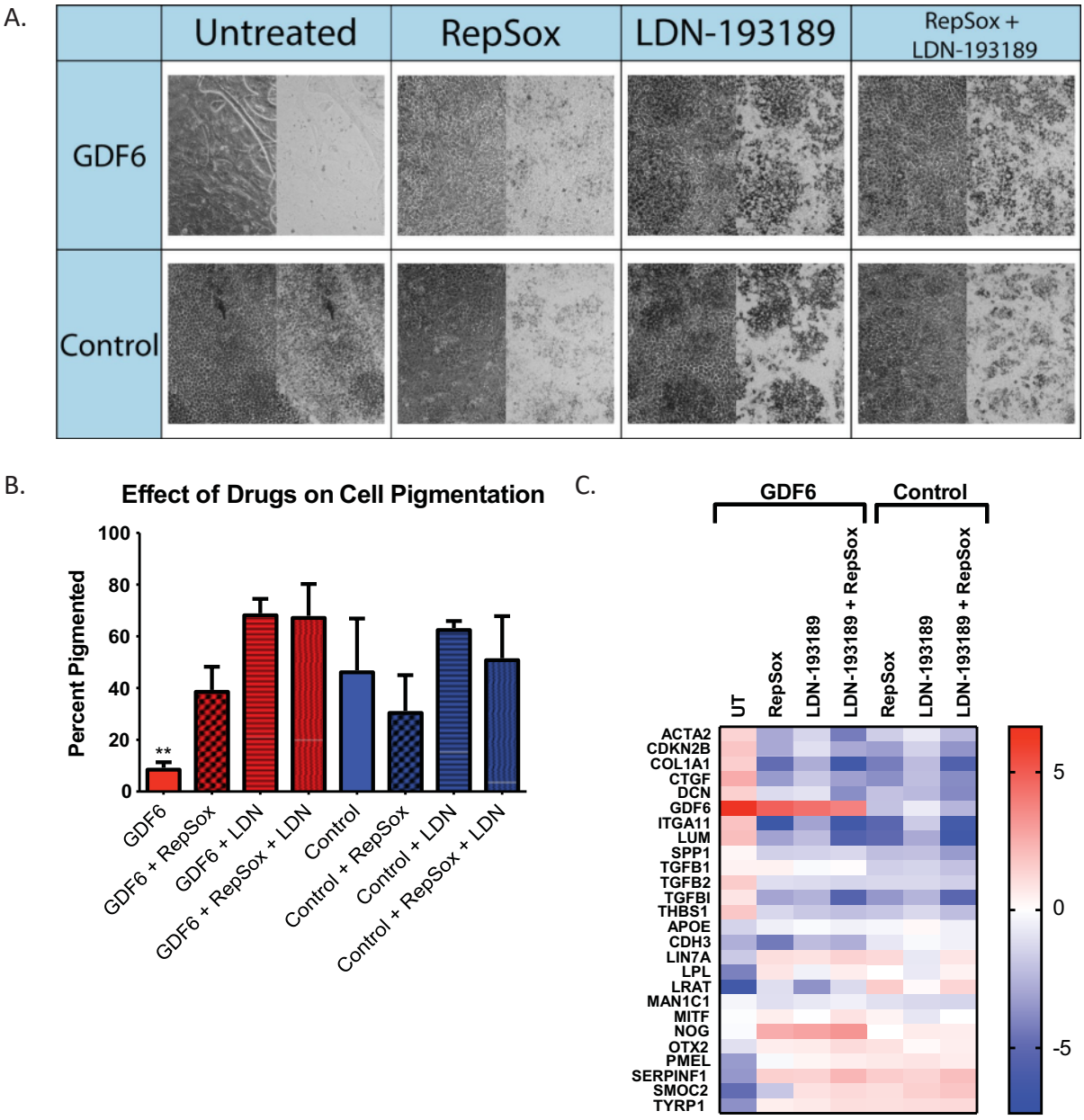

Figure 4.5. Effect of Smad phosphorylation inhibitors on RPE. (A) Phase contrast (left) and brightfield (right) 10X images of RPE overexpressing *GDF6* or an empty control vector. Cells were fed approximately every other day with RepSox, LDN-193189, or a combination of the two for 32 days. (B) Effect of Smad phosphorylation inhibitors on RPE pigmentation after 32 days. Displayed is the percentage of an image that is pigmented. Statistical significance was determined using a one-way ANOVA (** ≤ 0.005). (C) Heat map displaying RT-qPCR results. The log fold change of experimental value to control was determined. Genes higher than control are shown in red, while genes lower than control are shown in blue.

differences between cells overexpressing *GDF6* and treated with LDN and the control group. This similarity in appearance continues into similar gene expression when comparing a subset of genes found in healthy and passaged RPE. LDN restores the levels of healthy RPE genes like *CDH3* and lecithin retinol acyltransferase (*LRAT*) while reducing expression levels of genes found in highly passaged RPE like *CTGF* and collagen type I alpha 1 chain (*COL1A1*) (Figure 4.5-C). Interestingly, the TGFβ receptor inhibitor RepSox displays a similar rescue of the phenotype and genotype. RPE overexpressing *GDF6* can return to their normal morphology if Smad2/3 phosphorylation is inhibited. Inhibition of the TGFβ pathway prevents GDF6 from affecting the cellular phenotype, suggesting one of the downstream targets of GDF6 may operate through the Smad2/3 pathway.

4.2.4: CRISPR Knockdown of GDF6

We have shown *GDF6* to be sufficient in causing RPE to undergo EMT, but its necessity in the process has yet to be determined. Clustered regularly interspaced short palindromic repeats (CRISPR)/Cas9 (CRISPR-associated protein 9) is a useful tool in editing and altering gene function in cells [10-12]. CRISPR interference (CRISPRi) uses a catalytically inactive Cas9 protein (dCas9) to prevent transcription of a gene instead of initiating double-stranded breaks, thus reducing the potential for off-target effects [13-15]. RPE were transfected with dCas9 and two guide RNAs (gRNA) targeting different regions of the *GDF6* transcription start site (TSS). Passaged RPE that either have no gRNA or a gRNA targeting a control gene (ubiquitination Factor E4A; *UBE4A*) have a typical EMT morphology: mainly a loss of pigmentation and lack of a cobblestone appearance, favoring a larger, more stretched out appearance (Figure 4.6-A). RPE transfected with either gRNA targeting the TSS

of *GDF6* retain a more typical appearance, with *GDF6* gRNA 2 producing the healthiest phenotype with pigmentation. Looking at a subset of genes most affected by passaging of RPE, RPE transfected with either *GDF6* gRNA downregulate genes found in highly passaged RPE and upregulate genes found in healthy RPE (Figure 4.6-B). Knocking down *GDF6* appears to delay RPE EMT; however, this effect is short-lived as the RPE transfected with a *GDF6* gRNA undergo EMT by the next passage (Figure 4.7). *GDF6* is sufficient, but not necessary, for RPE to undergo EMT.

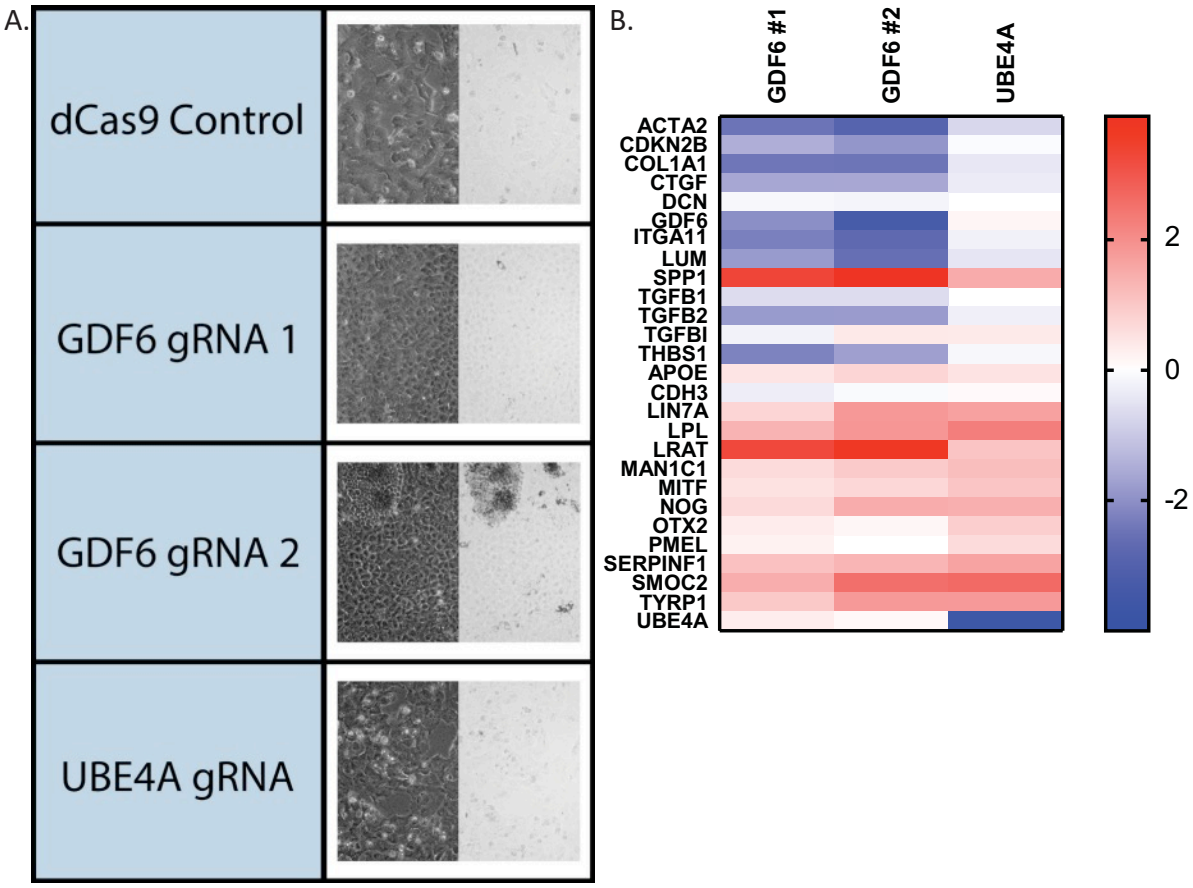

Figure 4.6. CRISPRi knockdown of *GDF6* in passage 5 RPE. (A) Phase contrast (left) and brightfield (right) 10X images of iPS-RPE infected with dCas9 and a gRNA directed to *GDF6* or a control gene (*UBE4A*). Images are of passage 5 iPS-RPE that were allowed to differentiate for 32 days. (B) Heat map of RT-qPCR results displaying the effect of *GDF6* knockdown on RPE. The log fold change the experimental gRNA samples to the dCas9 alone sample was determined. Expression levels higher than the dCas9 control are displayed in red whereas levels lower than control are in blue. *UBE4A* was used as a positive control.

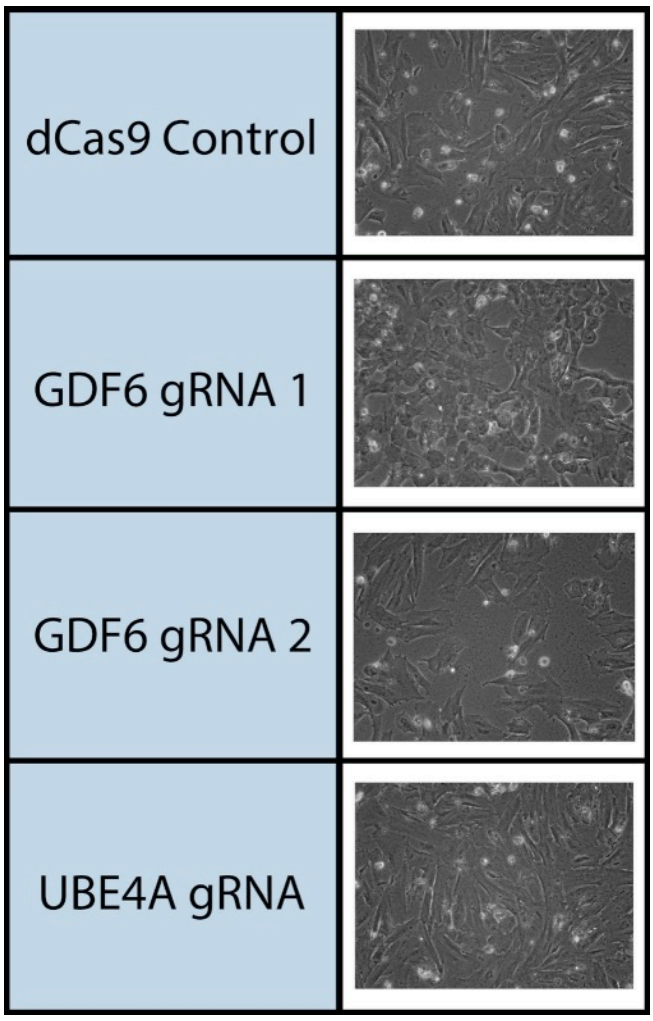

Figure 4.7. CRISPRi knockdown in passage 6 RPE. Phase Contrast 10X images of passage 6 iPS-RPE infected with dCas9 and a gRNA directed to *GDF6* or a control gene (*UBE4A*). iPS-RPE were differentiated for 32 days before imaging.

4.3: Discussion

4.3.1: GDF6 is not necessary for RPE to undergo EMT

In the previous chapter, we showed *GDF6* to be sufficient in initiating EMT in RPE. However, blocking the signal transduction pathway of BMP genes through inhibition of the Alk2, 3, and 6 receptors does not prevent RPE from undergoing EMT. This same phenomenon has been observed with TGFβ signaling, as TGFβ signaling is sufficient to induce EMT in RPE [3, 16, 17]. A delay in EMT was seen when RPE were passaged in the

presence of the Alk5 inhibitor RepSox, as the cells retained a normal phenotype for more passages than usual [5]. Nevertheless, the RPE ultimately succumbed to their fate and underwent EMT independent of TGFβ, suggesting TGFβ is sufficient, but not necessary for RPE EMT [5]. Attempted prevention of healthy RPE seems futile, as blocking one type of EMT (such as TGFβ or GDF6 mediated) only results in another form of EMT, possibly through hepatocyte growth factor (HGF) signaling, the Hippo pathway, platelet derived growth factor (PDGF) signaling, or the Wnt/ β-catenin pathway [18, 19].

The multitude of ways RPE can undergo EMT may explain why RPE passaged with LDN undergo EMT but have a different appearance and gene expression from untreated RPE. The EMT seen in LDN treated RPE may be due to *TGFβ2* (but not *TGFβ1*) expression as LDN treatment does not affect *TGFβ2* expression. Coupled with the increase in *CTGF*, as well as the fact that CTGF increases binding of TGFβ2 to TGFβ receptor 2 (TGFβRII), it is plausible LDN treated RPE have undergone this other form of EMT [19]. Often, there are antagonistic effects of TGFβ and BMP proteins [20, 21]. TGFβ proteins are known inducers of EMT; therefore, there may be BMP proteins acting antagonistically. By blocking the BMP pathway, we prevent possible antagonists from operating, thus letting TGFβ act on the RPE uncontrollably, causing the EMT observed in LDN treated RPE.

Knocking down *GDF6* allows us to determine the effects *GDF6* alone has on RPE EMT. If *GDF6* were necessary for RPE EMT, knocking down the gene would prevent RPE from undergoing EMT. However, RPE still undergo EMT with knockdown of *GDF6*, it is just delayed. Knocking down instead of knocking out a gene can create leakiness and still allow some gene expression. This phenomenon is seen in other CRISPRi knockdowns, especially

when dCas9 stem cells have been directed to differentiate into a cell type, as was done here [14]. It may be that a low level of *GDF6* is all that is necessary to initiate EMT and incomplete knockdown may provide the necessary expression levels. Another possibility is that not all the cells integrated the gRNA for *GDF6*. These cells may proliferate faster than the rest of the culture and express *GDF6*, reducing the effect of the knockdown.

The inability for *GDF6* knockdown to prevent EMT may be due to other factors as well. There is known redundancy in both the TGFβ and BMP pathways, as there are many proteins that signal through just a few receptors [22, 23]. For example, bone morphogenic protein (BMP) 7 is a known inducer of bone formation; however, there is no noticeable effect on formation when *BMP7* is conditionally deleted from the limb [24, 25]. GDF6 is very similar to GDF5 and growth differentiation factor 7 (GDF7), sharing 80-86% identity in the C-terminus region and making up a unique subtype in the BMP protein group [26, 27]. It is highly plausible that by inhibiting *GDF6*, a similar protein (like GDF5 or GDF7) may be compensating for its loss and taking its place, causing RPE to undergo EMT. One of the only successful ways to prevent EMT in RPE is to transfect the RPE with *MYCN* and orthodenticle homeobox 2 (*OTX2*), key RPE transcription factors [28].

4.3.2: GDF6 has an inhibitory effect on CDH3

RPE treated with GDF6 appear to ignore traditional contact inhibition pathways, resulting in a net-like layer of overlapping cells instead of a monolayer. It is possible the loss of the critical cadherin maintaining the epithelial state (*CDH3*), when *GDF6* is expressed, may be initiating the Hippo pathway, causing increased cell proliferation and EMT in otherwise healthy RPE [18]. Cadherins play an essential role in both cell-cell adhesion and

transfer of information intracellularly through interactions with the cytoskeleton [29]. E-cadherin (*CDH1*) is an epithelial marker, and as cells undergo EMT *CDH1* expression decreases, with the loss of CDH1 function simultaneously promoting EMT [30]. CDH1 is an upstream modulator of the Hippo pathway and is critical in controlling cell proliferation through contact inhibition; without CHD1 cell proliferation is unimpeded, resulting in aberrant growth similar to tumor cells [31]. In RPE the dominant cadherin is p-cadherin (CDH3), not CDH1 as in most epithelial cells [32]. It is plausible for CDH3 to assume the same role as CDH1 in RPE, maintaining the RPE in a healthy epithelial state. When RPE undergo EMT, there is a decrease in both *CDH1* and *CDH3* levels, a phenomenon that is accelerated by *GDF6* expression.

TGFβ expression in epithelial cells has been linked to dedifferentiation of the epithelial state as well as a decrease in *CDH1* [33]. In RPE a similar effect is seen, as increased expression of *GDF6* correlates with a decrease in expression of *CDH3*. It is unknown whether this decrease in *CDH3* expression is a direct effect of *GDF6* expression or a bystander effect from RPE undergoing EMT. The data suggests the former: *GDF6* has an inhibitory effect on *CDH3* expression. By preventing *GDF6* expression by passaging RPE in the presence of LDN, *CDH3* levels remain high, even after the cells have undergone an apparent mesenchymal transition. Other BMP/GDF6 proteins—like the closely related GDF5 and GDF7—may also have an inhibitory effect on *CDH3*. Blocking BMP signaling in healthy RPE using LDN results in higher *CDH3* expression levels, thus proposing other members of the pathway participate in inhibiting the gene. Furthermore, knockdown of *GDF6* does not elevate *CDH3* levels but instead results in *CDH3* levels lower than control counterparts. This

lowered expression is likely due to similar GDF/BMP proteins compensating for the loss of *GDF6*.

Non-canonical signaling has been well documented for members of the TGFβ family, specifically TGFβ1 and TGFβ2 [34-36]. Additionally, members of the BMP family demonstrate Smad-independent signaling, with BMP-2 activating the p38 mitogen-activated protein kinase (MAPK) pathway as well as its canonical Smad1/5/9 signaling pathway [37]. However, non-canonical pathway activation due to GDF6 has yet to be identified, with canonical Smad1/5/9 the only pathway of note [26]. We found GDF6 protein treatment to inhibit *CDH3* expression, and inhibition of its signaling pathway using LDN rescues expression; however, *CDH3* is unable to reach the same levels as RPE not exposed to GDF6 and treated with LDN. This negative regulation of *CDH3* by GDF6 may be occurring in a non-canonical, Smad-independent manner, as GDF6 appears always to effect *CDH3* levels. Further investigation is needed to determine if the decrease in *CDH3* due to GDF6 is what makes RPE undergo irreversible EMT. One possible way to achieve this is to overexpress *CDH3* in RPE and see if the cells still undergo EMT; the RPE will probably still undergo EMT with the overexpression of *CDH3*, as LDN treated RPE retain high levels of *CDH3* but still undergo EMT. A more useful approach would be to determine if GDF6 can initiate EMT in the presence of CDH3.

4.3.3: Downstream targets of GDF6 operate through TGFβ receptors

GDF6 has been shown to only activate the Smad1/5/9 pathway and bind to BMP—not TGFβ—receptors [6, 26]. However, GDF6 RPE given the TGFβ receptor inhibitor RepSox exhibited an avoidance of the mesenchymal phenotype, much like GDF6 RPE treated with

LDN. RepSox is an extremely selective and potent inhibitor of TGFβ type I receptors and therefore effectively inhibits canonical TGFβ signaling [38]. GDF6 itself cannot be affected by RepSox, and Smad1/5/9 phosphorylation still occurs in its presence; yet, GDF6 appears to be affected by RepSox. This reaction indicates that something downstream of GDF6 operates through the TGFβ pathway, and it is this gene that promotes an EMT phenotype in RPE. In order to determine what gene this is and the mechanism of action for GDF6, a more in-depth sequencing analysis needs to be performed.

4.4: Conclusion

GDF6 has previously shown to be sufficient in inducing EMT in RPE, but its necessity remained unknown. Inhibition of the BMP signaling pathway failed to extend the epithelial phenotype in RPE, and knockdown of *GDF6* only slightly extended the phenotype, indicating *GDF6* is not necessary for EMT in RPE. GDF6 did have an inhibitory effect on *CDH3* expression, a phenomenon seen with TGFβ and *CDH1*. However, its method of inhibition may be through a non-canonical Smad-independent pathway. Canonical signaling of GDF6 has downstream targets that operate through TGFβ receptors, as the Alk5 inhibitor RepSox can maintain an epithelial phenotype in the presence of GDF6. In order to determine the mechanistic properties of GDF6, deeper sequencing and pathway analysis is needed.

4.5: References

1. Casaroli-Marano, R.P., R. Pagan, and S. Vilaro, *Epithelial-mesenchymal transition in proliferative vitreoretinopathy: intermediate filament protein expression in retinal pigment epithelial cells.* Invest Ophthalmol Vis Sci, 1999. **40**(9): p. 2062-72.
2. Ohlmann, A., et al., *Epithelial-mesenchymal transition of the retinal pigment epithelium causes choriocapillaris atrophy.* Histochem Cell Biol, 2016. **146**(6): p. 769-780.

3. Xu, J., S. Lamouille, and R. Derynck, *TGF-beta-induced epithelial to mesenchymal transition.* Cell Res, 2009. **19**(2): p. 156-72.
4. Saika, S., *TGFbeta pathobiology in the eye.* Lab Invest, 2006. **86**(2): p. 106-15.
5. Radeke, M.J., et al., *Restoration of mesenchymal retinal pigmented epithelial cells by TGFβ pathway inhibitors: implications for age-related macular degeneration.* Genome Med, 2015. **7**(1): p. 58.
6. Berasi, S.P., et al., *Divergent activities of osteogenic BMP2, and tenogenic BMP12 and BMP13 independent of receptor binding affinities.* Growth Factors, 2011. **29**(4): p. 128-39.
7. Yu, P.B., et al., *Dorsomorphin inhibits BMP signals required for embryogenesis and iron metabolism.* Nat Chem Biol, 2008. **4**(1): p. 33-41.
8. Boergermann, J.H., et al., *Dorsomorphin and LDN-193189 inhibit BMP-mediated Smad, p38 and Akt signalling in C2C12 cells.* Int J Biochem Cell Biol, 2010. **42**(11): p. 1802-7.
9. Vogt, J., R. Traynor, and G.P. Sapkota, *The specificities of small molecule inhibitors of the TGFss and BMP pathways.* Cell Signal, 2011. **23**(11): p. 1831-42.
10. Doetschman, T. and T. Georgieva, *Gene Editing With CRISPR/Cas9 RNA-Directed Nuclease.* Circ Res, 2017. **120**(5): p. 876-894.
11. Jiang, F. and J.A. Doudna, *CRISPR-Cas9 Structures and Mechanisms.* Annu Rev Biophys, 2017. **46**: p. 505-529.
12. Ma, Y., L. Zhang, and X. Huang, *Genome modification by CRISPR/Cas9.* Febs j, 2014. **281**(23): p. 5186-93.
13. Larson, M.H., et al., *CRISPR interference (CRISPRi) for sequence-specific control of gene expression.* Nat Protoc, 2013. **8**(11): p. 2180-96.
14. Mandegar, M.A., et al., *CRISPR Interference Efficiently Induces Specific and Reversible Gene Silencing in Human iPSCs.* Cell Stem Cell, 2016. **18**(4): p. 541-53.
15. Gilbert, L.A., et al., *CRISPR-mediated modular RNA-guided regulation of transcription in eukaryotes.* Cell, 2013. **154**(2): p. 442-51.
16. Roberts, A.B., et al., *Smad3 is key to TGF-beta-mediated epithelial-to-mesenchymal transition, fibrosis, tumor suppression and metastasis.* Cytokine Growth Factor Rev, 2006. **17**(1-2): p. 19-27.
17. Li, H., et al., *Snail involves in the transforming growth factor β1-mediated epithelial-mesenchymal transition of retinal pigment epithelial cells.* PLoS One, 2011. **6**(8): p. e23322.
18. Chen, Z., Y. Shao, and X. Li, *The roles of signaling pathways in epithelial-to-mesenchymal transition of PVR.* Mol Vis, 2015. **21**: p. 706-10.
19. Yang, S., et al., *Mechanisms of epithelial-mesenchymal transition in proliferative vitreoretinopathy.* Discov Med, 2015. **20**(110): p. 207-17.
20. Keller, B., et al., *Interaction of TGFbeta and BMP signaling pathways during chondrogenesis.* PLoS One, 2011. **6**(1): p. e16421.
21. Candia, A.F., et al., *Cellular interpretation of multiple TGF-beta signals: intracellular antagonism between activin/BVg1 and BMP-2/4 signaling mediated by Smads.* Development, 1997. **124**(22): p. 4467-80.

22. Munger, J.S. and D. Sheppard, *Cross talk among TGF-beta signaling pathways, integrins, and the extracellular matrix.* Cold Spring Harb Perspect Biol, 2011. **3**(11): p. a005017.
23. Wolfman, N.M., et al., *Ectopic induction of tendon and ligament in rats by growth and differentiation factors 5, 6, and 7, members of the TGF-beta gene family.* J Clin Invest, 1997. **100**(2): p. 321-30.
24. Sampath, T.K., et al., *Recombinant human osteogenic protein-1 (hOP-1) induces new bone formation in vivo with a specific activity comparable with natural bovine osteogenic protein and stimulates osteoblast proliferation and differentiation in vitro.* J Biol Chem, 1992. **267**(28): p. 20352-62.
25. Wang, R.N., et al., *Bone Morphogenetic Protein (BMP) signaling in development and human diseases.* Genes Dis, 2014. **1**(1): p. 87-105.
26. Mazerbourg, S., et al., *Identification of receptors and signaling pathways for orphan bone morphogenetic protein/growth differentiation factor ligands based on genomic analyses.* J Biol Chem, 2005. **280**(37): p. 32122-32.
27. Storm, E.E., et al., *Limb alterations in brachypodism mice due to mutations in a new member of the TGF beta-superfamily.* Nature, 1994. **368**(6472): p. 639-43.
28. Shih, Y.H., et al., *Restoration of Mesenchymal RPE by Transcription Factor-Mediated Reprogramming.* Invest Ophthalmol Vis Sci, 2017. **58**(1): p. 430-441.
29. Angst, B.D., C. Marcozzi, and A.I. Magee, *The cadherin superfamily: diversity in form and function.* J Cell Sci, 2001. **114**(Pt 4): p. 629-41.
30. Zeisberg, M. and E.G. Neilson, *Biomarkers for epithelial-mesenchymal transitions.* J Clin Invest, 2009. **119**(6): p. 1429-37.
31. Kim, N.G., et al., *E-cadherin mediates contact inhibition of proliferation through Hippo signaling-pathway components.* Proc Natl Acad Sci U S A, 2011. **108**(29): p. 11930-5.
32. Yang, X., et al., *Cadherins in the retinal pigment epithelium (RPE) revisited: P-cadherin is the highly dominant cadherin expressed in human and mouse RPE in vivo.* PLoS One, 2018. **13**(1): p. e0191279.
33. Vogelmann, R., et al., *TGFbeta-induced downregulation of E-cadherin-based cell-cell adhesion depends on PI3-kinase and PTEN.* J Cell Sci, 2005. **118**(Pt 20): p. 4901-12.
34. Mu, Y., S.K. Gudey, and M. Landstrom, *Non-Smad signaling pathways.* Cell Tissue Res, 2012. **347**(1): p. 11-20.
35. Zhang, Y.E., *Non-Smad Signaling Pathways of the TGF-beta Family.* Cold Spring Harb Perspect Biol, 2017. **9**(2).
36. Guo, X. and X.F. Wang, *Signaling cross-talk between TGF-beta/BMP and other pathways.* Cell Res, 2009. **19**(1): p. 71-88.
37. Hassel, S., et al., *Initiation of Smad-dependent and Smad-independent signaling via distinct BMP-receptor complexes.* J Bone Joint Surg Am, 2003. **85-A Suppl 3**: p. 44-51.
38. Gellibert, F., et al., *Identification of 1,5-naphthyridine derivatives as a novel series of potent and selective TGF-beta type I receptor inhibitors.* J Med Chem, 2004. **47**(18): p. 4494-506.

CHAPTER V: The Mechanism of Action of GDF6

5.1: Introduction

We have shown growth differentiation factor 6 (GDF6) to have an inhibitory effect on p-cadherin (*CDH3*), even in the presence of the Smad1/5/9 inhibitor LDN-193189 (LDN). This effect on gene expression is surprising, as GDF6 is not reported to act through any other signaling pathway [1]. In this final experimental chapter, we aim to investigate if GDF6 can signal through a Smad-independent pathway in retinal pigmented epithelial (RPE) cells by utilizing RNA-sequencing (RNA-seq) techniques and receptor binding assays.

5.2: Results

5.2.1: GDF6 Affects Gene Expression in the Presence of Inhibitors

Initially, inhibition of the bone morphogenic protein (BMP) or transforming growth factor β (TGFβ) receptor signaling cascades restored the phenotype of RPE cells to a healthy state, as evidenced in the previous chapter (Figure 4.5). To ensure the RPE were, in fact, healthy, RNA-seq was used to validate this claim. However, a closer look at the gene expression revealed the RPE, while phenotypically normal, were not the same as RPE not exposed to *GDF6*. AutoSOME, an unbiased clustering software, found 171 unique clusters which we manually placed into 18 subgroups (Supplemental Figure 5.1). We then selected four of the most interesting clusters for further analysis (Figure 5.1). RPE that overexpress *GDF6* up-regulate genes found in extracellular matrix organization and cardiovascular development (Cluster A) while down-regulating genes related to pigmentation and melanin biosynthesis (Cluster B). Clusters C and D are of more interest as they include genes that are

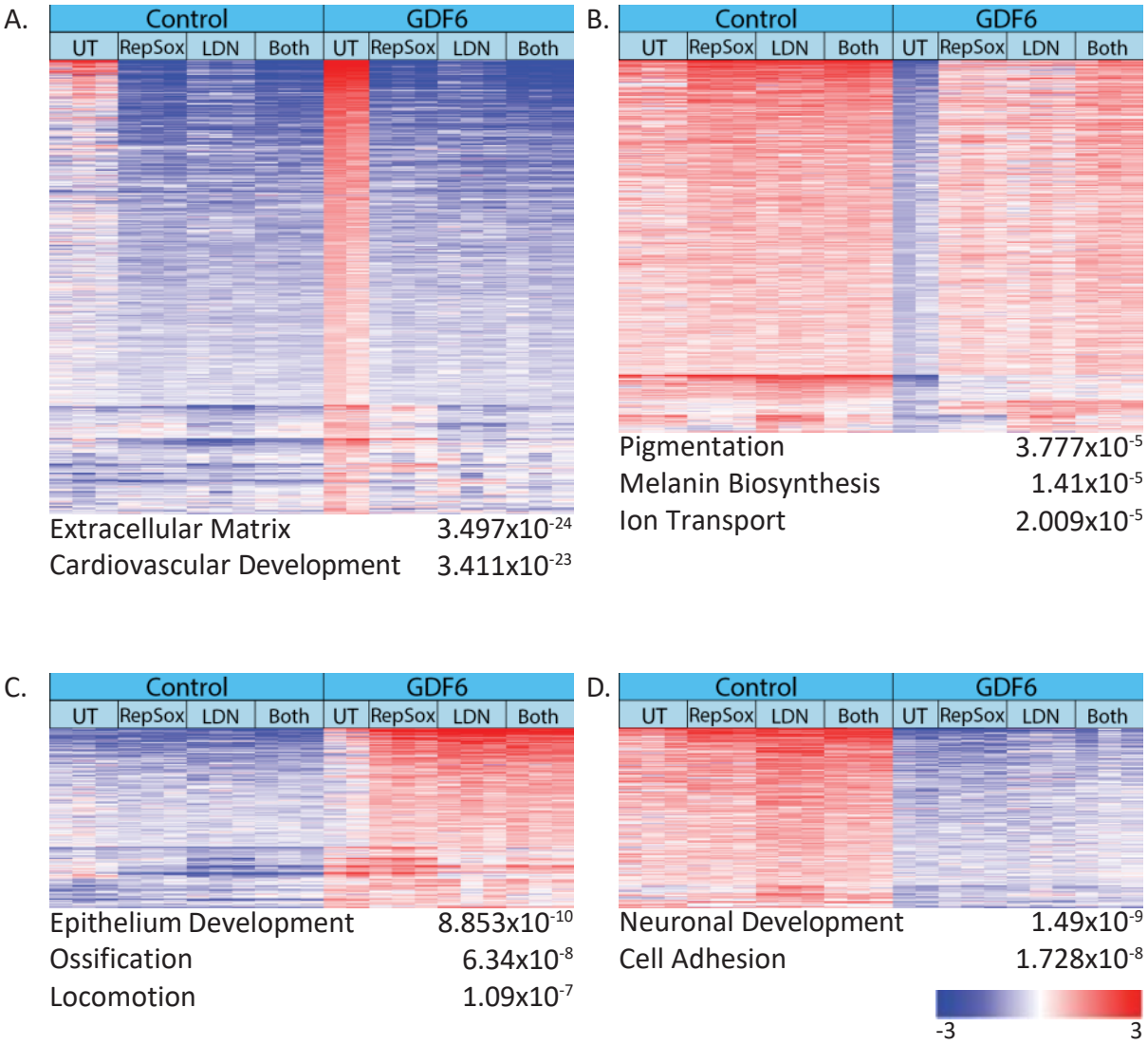

Figure 5.1. RNA-Seq clustering and gene ontology (GO) analysis of RPE treated with Smad phosphorylation inhibitors. Data was range-centered and Log2 transformed prior to cluster analysis using AutoSOME 2.1. Clusters were manually placed into larger subgroups based on their expression profile (Supplemental Figure 5.1.1). Shown here are four prominent clusters with interesting expression patterns wherein (A) represents genes up-regulated in untreated GDF6 RPE, (B) shows genes down-regulated in untreated GDF6 RPE, (C) highlights genes up-regulated in GDF6 RPE irrespective of inhibitor treatment, and (D) portrays genes that are down-regulated in GDF6 RPE regardless of inhibitor treatment. The color scale represents the $\log_2$ expression level of the gene. Below each cluster are the ontology groups associated with each cluster along with the associated enrichment *P* value. Each column of the cluster represents a replicate, and each row represents a gene.

sensitive to *GDF6* but do not respond to the inhibitory drugs LDN-193189 (LDN) or RepSox.

Up-regulation of genes related to ossification and locomotion always occur when RPE overexpress *GDF6*, even in the presence of its inhibitor LDN (Cluster C), whereas neuronal development genes and cell adhesion genes remain down-regulated in every treatment (Cluster D).

We compared each treatment with its control (e.g., GDF6 with RepSox to control with RepSox) to determine what genes were up or down-regulated. We then looked across treatments to see if there were any similarities in what genes were being affected. Figure 5.2 highlights the similarities in the up and down-regulated genes across treatments, with 109 genes remaining up-regulated (A) and 184 genes staying down-regulated (B). The key epithelial-to-mesenchymal transition (EMT) genes, inhibitor of DNA Binding 1 (*ID1*), snail family transcriptional repressor 1 (*SNAI1*), and msh homeobox 2 (*MSX2*), populate the top 20 genes that remained up-regulated regardless of treatment (C). The genes that are always down-regulated are involved in neural function and cell adhesion (D). Notably, *TGFβ1* displayed an increase in transcript number when exposed to *GDF6* in all conditions when compared to control cells, though treatment with LDN appeared to lessen this effect (Figure 5.3). While there is a restoration of morphology and pigmentation, there is still a difference when compared to control.

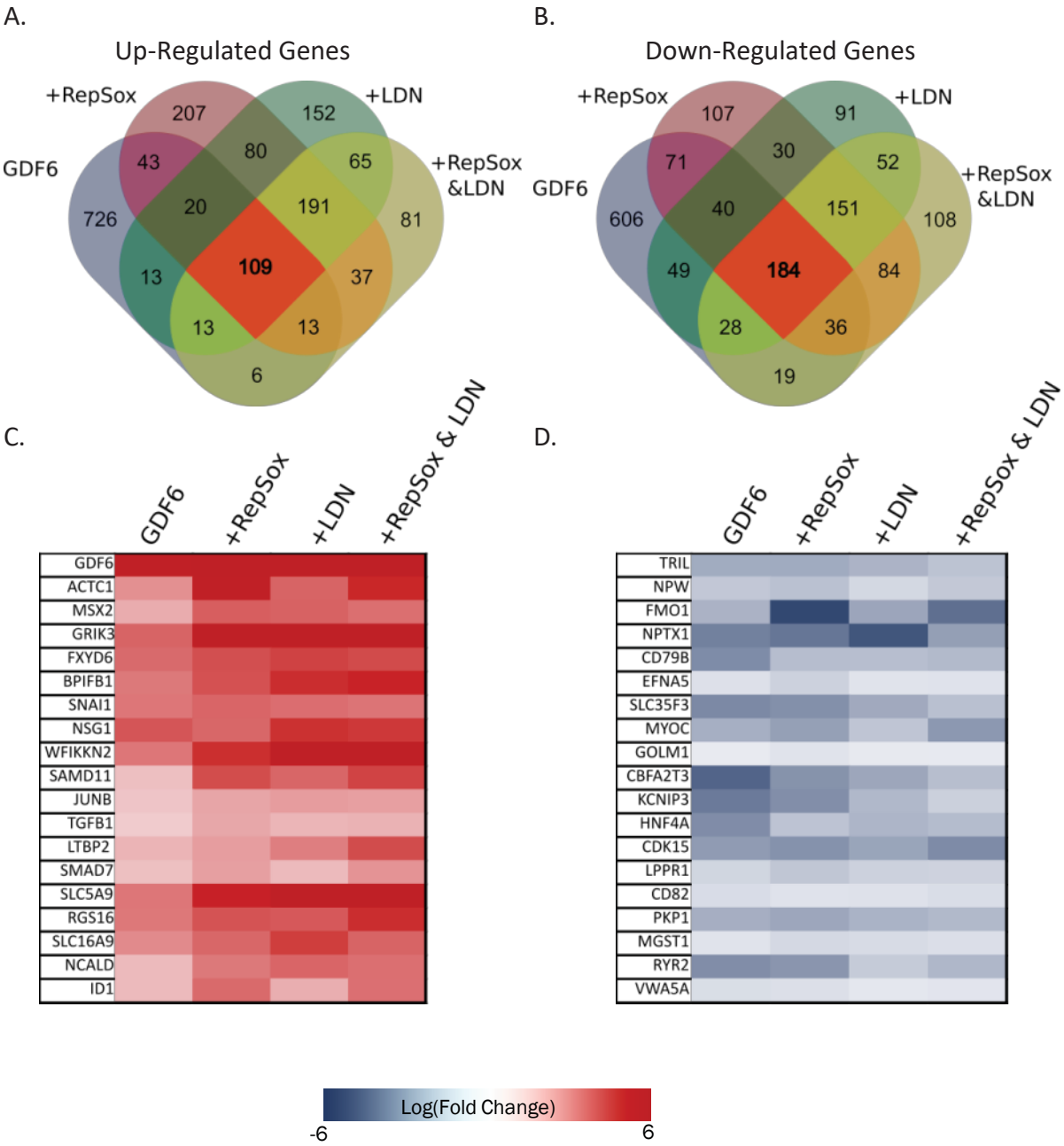

Figure 5.2. Determination of genes that remain unchanged during Smad inhibition treatment. (A&B) Venn diagram depicting the number of genes either up-regulated (A) or down-regulated (B) that are unique to each treatment. 109 genes remain up-regulated and 184 genes remain down-regulated across all treatments. (C&D) Heat maps showing the top 20 up-regulated (C) and down-regulated (D) genes across all treatments. Gene order was determined using the FDR of each gene. The color bar represents the Log (Fold Change) of each gene, with red representing genes that are up-regulated compared to control cells, and blue representing down-regulated genes.

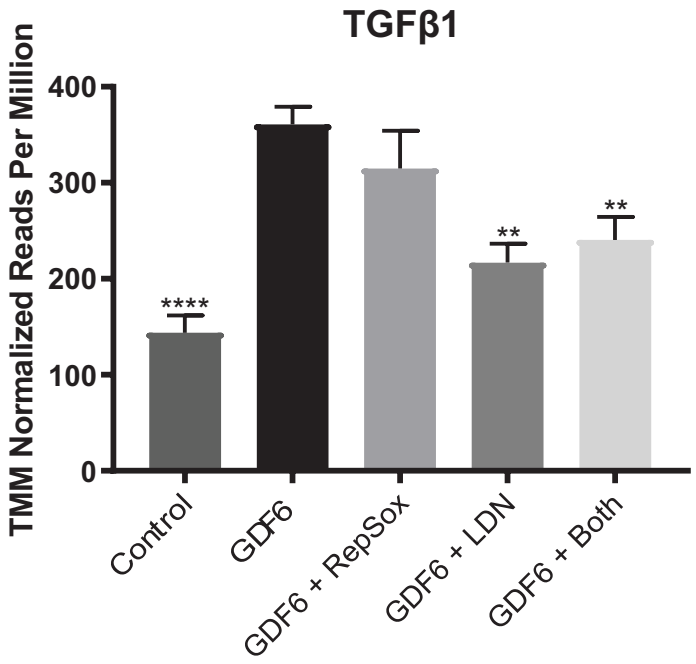

Figure 5.3. Trimmed mean of M-values (TMM) normalized reads per million of *TGFβ1* in control RPE or RPE exposed to *GDF6* along with LDN or RepSox. Statistical significance was determined using a one-way ANOVA with respect to *GDF6* over expressing cells (****≤0.0001, **≤0.007).

5.2.2: GDF6 Does not Interact with Kinase Receptors

GDF6's ability to affect gene expression in the presence of inhibitors suggests that it may be acting through a non-canonical Smad signaling pathway. Since the canonical GDF6 pathway involves protein phosphorylation, we hypothesized its non-canonical pathway receptors might do the same, leading to an evaluation of common receptor kinases. A phospho-array on 43 different receptor kinases and two related total proteins was performed to elucidate the potential pathway. P0 RPE were plated the at a low density and the next day exposed to combination of RepSox and LDN for an hour, followed by addition of recombinant mouse Gdf6 (rmGdf6) for another hour. A combination of the small

molecules was used to ensure complete blockage of the Smad signaling pathway, and the resulting protein lysate was analyzed to determine any changes in phosphorylation (Figure 5.4). After normalizing the integrated pixel density for each treatment, there were no significant changes in the phosphorylation states of any of the kinases (Table 5.1).

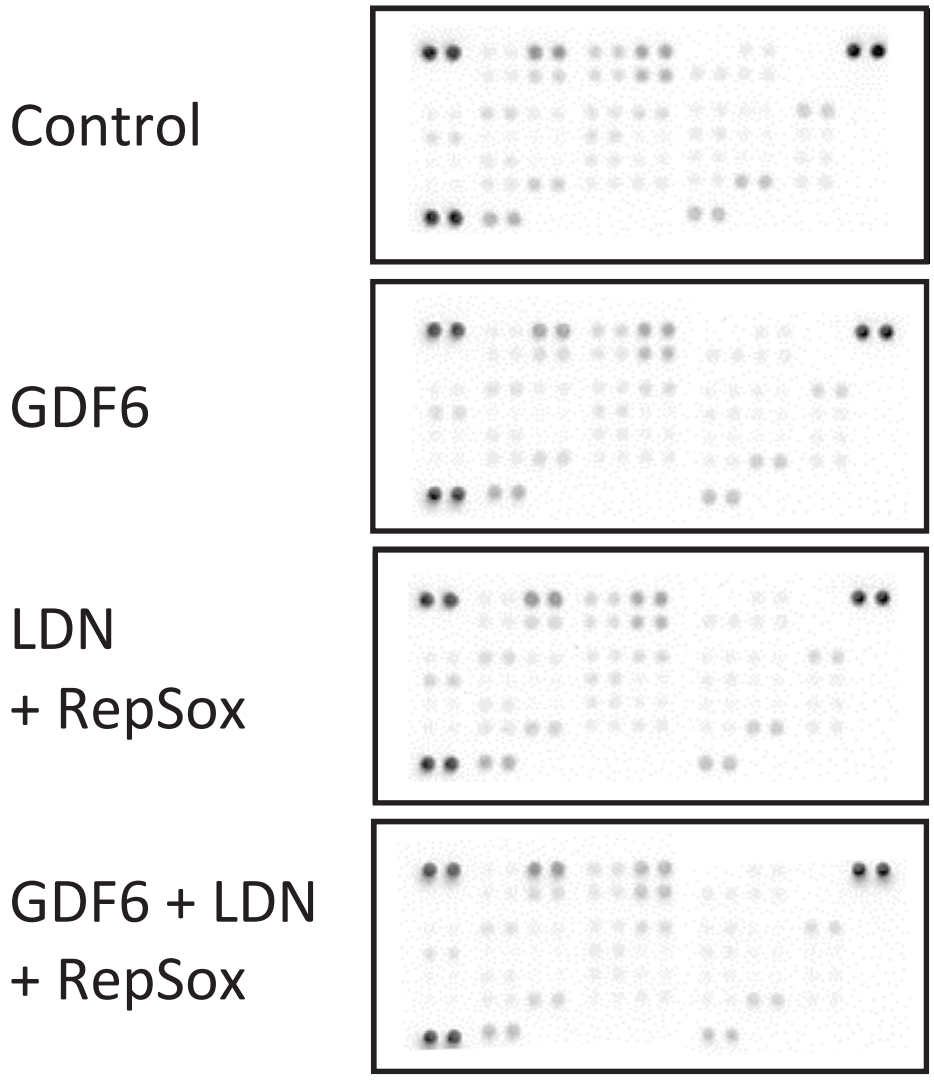

Figure 5.4. Western blot images of a phosphokinase array. Each pair of dots represents either one of 43 receptor kinases or 2 total proteins. RPE were treated with rmGdf6 and the SMAD inhibitor drugs LDN-193189 and RepSox. The protein lysate was harvested, exposed to membranes containing antibodies to the receptor kinases and developed using chemiluminescence.

Standardized to Reference (Ratio)				
	Control	LDN + RepSox	GDF6	GDF6 + LDN + RepSox
Reference	0.99804605	0.99140143	0.98157545	0.93707416
p38a	0.02698045	0.02829993	0.02792849	0.02059155
ERK 1/2	0.31834259	0.39910442	0.29148681	0.40488961
JNK 1/2/3	0.07907245	0.07656647	0.07642833	0.06131416
GSK-3a/B	0.22220927	0.24211414	0.24796915	0.19733902
EGF R	0.02777449	0.03060782	0.03069831	0.02481901
MSK 1/2	0.07402574	0.08316838	0.07721224	0.08641883
AMPKa1	0.05425344	0.05418471	0.04571454	0.04638054
Akt 1/2/3	0.14852789	0.15951077	0.16699027	0.16206969
TOR	0.01898327	0.02516273	0.02449864	0.01527471
CREB	0.06129778	0.07421836	0.05682671	0.05480988
HSP27	0.02463345	0.02969424	0.02530965	0.01983048
AMPKa2	0.03892273	0.03760427	0.03426752	0.03095447
B-Catenin	0.05119767	0.0618515	0.06153017	0.06986927
Src	0.04789114	0.0807494	0.06621621	0.05178265
Lyn	0.01323948	0.01402739	0.01176639	0.01000904
Lck	0.00797378	0.00989999	0.00806944	0.00709906
STAT2	0.0480349	0.05169486	0.04897986	0.0397313
STAT5a	0.01217798	0.01523017	0.0138994	0.01410432
Fyn	0.01112317	0.01634485	0.01670987	0.01057824
Yes	0.0327861	0.03872662	0.03247323	0.03003351
Fgr	0.00773306	0.00876807	0.00676679	0.00668975
STAT6	0.03198538	0.03612186	0.03319908	0.03086707
STAT5b	0.01544271	0.01988809	0.01951646	0.01655808
Hck	0.01146084	0.01704393	0.01677761	0.01080422
Chk-2	0.03771914	0.04472714	0.03984586	0.03120603
FAK	0.08568718	0.0961711	0.07757226	0.08996197
PDGF RB	0.0227027	0.02650341	0.02346311	0.0168203
STAT5a/b	0.02867384	0.03321641	0.03015054	0.02604908
Reference	1.00195395	1.00859857	1.01842455	1.06292584
PRAS40	0.1851287	0.20489292	0.20966789	0.17558136
PBS	0	0	0	0
p53	0.02864716	0.02345409	0.03179839	0.0210295
Reference	1	1	1	1
Akt 1/2/3	0.03601812	0.02965853	0.02862979	0.02551217
p53	0.02685309	0.02549085	0.0289526	0.02170853
p70 S6 Kinase	0.02196164	0.01815469	0.01709565	0.02347877
p53	0.01417072	0.01346038	0.01133179	0.00497399
c-Jun	0.08745557	0.0677675	0.07747245	0.06287137
p70 S6 Kinase	0.03187487	0.02618139	0.02606183	0.02524902
RSK 1/2/3	0.0134	0.01338365	0.01336014	0.01101896
eNOS	0.018248	0.0186848	0.01813311	0.01186912
STAT3	0.01946443	0.01392597	0.01816202	0.01500662
p27	0.00959303	0.00852892	0.00979487	0.00677184
PLC-y1	0.02177017	0.01930211	0.02098533	0.01093063
STAT3	0.02256663	0.01900043	0.01899071	0.01750373
WNK1	0.11551864	0.09843219	0.09888336	0.07923419
PYK2	0.0313455	0.02901332	0.02842102	0.01671982
HSP60	0.13175214	0.13402487	0.11268194	0.11591621
PBS	0	0	0	0

Table 5.1. Ratio of integrated pixel density of each receptor kinase or total protein to its reference gene.

5.3: Discussion

5.3.1: GDF6 can Act Through a Non-Canonical Smad Pathway

In the previous chapter, GDF6 was shown to affect p-cadherin (*CDH3*) gene expression in the presence of its inhibitor LDN, suggesting GDF6 possibly operated through a non-canonical pathway in addition to its traditional Smad1/5/9 phosphorylation pathway. Some TGFβ and BMP proteins have been shown to have additional non-canonical pathways, but none had been previously reported for GDF6 [1-5]. By looking at changes in gene expression when using inhibitors, we show here that GDF6 has a robust effect on gene expression, suggesting it can operate through a non-canonical pathway.

Although our screen to determine novel GDF6 receptor binding did not pick up any hits, it is possible that GDF6 could be acting through an unassayed receptor kinase or another receptor type. Alternatively, GDF6 could be directly signaling through the BMP Type II Receptor (BMPRII), which has shown direct signaling with the assistance of LIM domain kinase 1 (LIMK1) [6]. A protein pull-down assay would be needed to determine what other receptors GDF6 may be binding. GDF6 has an extremely high affinity for BMPRII, so depletion of the receptor from the lysate is necessary prior to analysis [1]. GDF6 has also been found to bind to Activin Receptor 2 A/B (ActRII), and depletion of these receptors as well could help ensure the end product is not oversaturated with known ligand-receptor pairs. If no novel receptors are found to be interacting with GDF6, then we can assume it is directly signaling through BMPRII.

Another possibility is that LDN may not be fully inhibiting GDF6 signaling, allowing for some Smad1/5/9 signaling to occur. This leakiness may account for the subset of genes

that remain unchanged regardless of treatment. As previously reported in chapter 4, nanomolar amounts of LDN inhibit GDF6 Smad1/5/9 phosphorylation, so it would be surprising for LDN not to block the pathway effectively (Figure 4.4). Additionally, if LDN were leaky, we would expect the RPE to exhibit a phenotype and genotype more similar to those of RPE overexpressing *GDF6*. Instead, the cells showed a normal phenotype, and most of the highly affected genes returned to normal (Figure 4.5). We believe GDF6 is likely acting through a novel, non-canonical pathway, but to confirm this, the receptor it binds to needs to be identified.

5.3.2: GDF6 is Priming RPE to Undergo EMT

We previously showed that *GDF6* is not necessary for RPE to undergo EMT and blockage of the TGFβ signaling pathway alone prevented EMT in RPE [7]. However, it appears that *GDF6* is having an extensive effect on the RPE as evidenced by the number of genes that are altered by *GDF6* expression. Regardless of inhibitory drugs, *GDF6* upregulates genes related to EMT. *MSX2* is one of the most affected genes due to *GDF6* expression. It is integral in the early differentiation of mesenchyme and is directly activated by BMP protein binding [8]. Additionally, *MSX2* can induce EMT in epithelial cells and, when combined with *BMP4*, promotes mesodermal cell fate [9, 10]. *GDF6* induces *MSX2* expression but may not necessarily interact with it; LDN and RepSox likely inhibit the gene(s) that bind to *MSX2* and are responsible for the mesenchymal phenotype (along with its subsequent signaling pathway). Therefore, we see an increase in expression without induction of a mesenchymal state.

In the previous chapters, we linked *GDF6* to a decrease in both *CDH1* (E-cadherin) and *CDH3* (P-cadherin) expression. SNAI1 is a well-studied inducer of EMT in epithelial cells, often present in invasive cancerous tumors [11]. It is also a known repressor of *CDH1* [12]. The decrease in both *CDH1* and *CDH3* expression may not be a direct consequence of *GDF6*, but instead be due to *SNAI1* expression. Another gene well associated with both EMT and reduction of epithelial cadherin is *ID1* [13, 14]. *ID1*, as well as *TGFβ1*, is upregulated in the presence of *GDF6*. TGFβ-induced EMT is dependent on not only Smad2/3 signaling but also Smad1/5/9, with *ID1* being an early transcriptional target of the latter pathway [15]. *GDF6* is affecting the necessary genes required for RPE to undergo EMT, but the phenotype is not occurring in the presence of LDN or RepSox because the mesenchymal transition requires both pathways.

The changes in gene expression suggest priming of the RPE to undergo EMT, even in the presence of inhibitors. LDN is an effective inhibitor of activin-like kinase (Alk) 1, 2, 3, and 6 (inhibiting Smad1/5/9 signaling), and, while more potent and stable than dorsomorphin, LDN still has a large number of off-target effects, including inhibition of several kinases [16, 17]. Additionally, LDN has been shown to inhibit the type II receptor ActRIIA, preventing Smad2/3 signaling as well [18]. This promiscuity of the inhibitor may be why we see an effect on gene expression; it may not be GDF6 itself eliciting this response. Inhibitors with fewer off-target effects are available, but they have a higher selectivity for Alk2 over the other type I receptor kinases[19, 20]. GDF6 has been shown to not bind to Alk 1 or 2 but to Alk6 and Alk3 instead, rendering these newer inhibitors ineffective [21]. A more potent pan-

inhibitor of Smad1/5/9 phosphorylation needs to be discovered to block signaling with no off-target effects.

5.4: Conclusion

The mechanism of GDF6 in RPE EMT has not previously been studied. In this chapter, we looked at what genes *GDF6* affected, specifically those that remained unchanged in the presence of Smad phosphorylation inhibitors LDN and RepSox. Importantly, GDF6 can alter gene expression without signaling through its traditional Smad1/5/9 pathway. This novel signaling pathway may be a secondary pathway initiated through binding of the same receptors, similar to Smad-independent TGFβ signaling. There could also be direct signaling through binding and activation of the BMPRII receptor. Though we were unable to detect binding of a novel receptor by GDF6, it is still a possibility.

The genes affected by signaling through the non-canonical pathway are genes related to EMT, essentially priming the RPE to undergo EMT. Genes like *MSX2*, *TGFβ1*, *SNAI1* and *ID1* are all upregulated in the presence of *GDF6* and are strongly linked to EMT. Studies have shown TGFβ-induced EMT requires phosphorylation of both Smad pathways, so blocking one or more pathway with inhibitors is likely preventing the mesenchymal phenotype while still upregulating genes related to EMT.

5.5: References

1. Mazerbourg, S., et al., *Identification of receptors and signaling pathways for orphan bone morphogenetic protein/growth differentiation factor ligands based on genomic analyses.* J Biol Chem, 2005. **280**(37): p. 32122-32.
2. Mu, Y., S.K. Gudey, and M. Landstrom, *Non-Smad signaling pathways.* Cell Tissue Res, 2012. **347**(1): p. 11-20.
3. Zhang, Y.E., *Non-Smad Signaling Pathways of the TGF-beta Family.* Cold Spring Harb Perspect Biol, 2017. **9**(2).

4. Guo, X. and X.F. Wang, *Signaling cross-talk between TGF-beta/BMP and other pathways.* Cell Res, 2009. **19**(1): p. 71-88.
5. Hassel, S., et al., *Initiation of Smad-dependent and Smad-independent signaling via distinct BMP-receptor complexes.* J Bone Joint Surg Am, 2003. **85-A Suppl 3**: p. 44-51.
6. Foletta, V.C., et al., *Direct signaling by the BMP type II receptor via the cytoskeletal regulator LIMK1*, in *J Cell Biol*. 2003. p. 1089-98.
7. Radeke, M.J., et al., *Restoration of mesenchymal retinal pigmented epithelial cells by TGFβ pathway inhibitors: implications for age-related macular degeneration.* Genome Med, 2015. **7**(1): p. 58.
8. Davidson, D., *The function and evolution of Msx genes: pointers and paradoxes.* Trends Genet, 1995. **11**(10): p. 405-11.
9. di Bari, M.G., et al., *Msx2 induces epithelial-mesenchymal transition in mouse mammary epithelial cells through upregulation of Cripto-1.* J Cell Physiol, 2009. **219**(3): p. 659-66.
10. Richter, A., et al., *BMP4 promotes EMT and mesodermal commitment in human embryonic stem cells via SLUG and MSX2.* Stem Cells, 2014. **32**(3): p. 636-48.
11. Kaufhold, S. and B. Bonavida, *Central role of Snail1 in the regulation of EMT and resistance in cancer: a target for therapeutic intervention.* J Exp Clin Cancer Res, 2014. **33**: p. 62.
12. Barrallo-Gimeno, A. and M.A. Nieto, *The Snail genes as inducers of cell movement and survival: implications in development and cancer.* Development, 2005. **132**(14): p. 3151-61.
13. Hu, H., et al., *A novel role of Id-1 in regulation of epithelial-to-mesenchymal transition in bladder cancer.* Urol Oncol, 2013. **31**(7): p. 1242-53.
14. Zhang, X., et al., *Identification of a novel inhibitor of differentiation-1 (ID-1) binding partner, caveolin-1, and its role in epithelial-mesenchymal transition and resistance to apoptosis in prostate cancer cells.* J Biol Chem, 2007. **282**(46): p. 33284-94.
15. Ramachandran, A., et al., *TGF-beta uses a novel mode of receptor activation to phosphorylate SMAD1/5 and induce epithelial-to-mesenchymal transition.* Elife, 2018. **7**.
16. Boergermann, J.H., et al., *Dorsomorphin and LDN-193189 inhibit BMP-mediated Smad, p38 and Akt signalling in C2C12 cells.* Int J Biochem Cell Biol, 2010. **42**(11): p. 1802-7.
17. Yadin, D., P. Knaus, and T.D. Mueller, *Structural insights into BMP receptors: Specificity, activation and inhibition.* Cytokine Growth Factor Rev, 2016. **27**: p. 13-34.
18. Horbelt, D., et al., *Small molecules dorsomorphin and LDN-193189 inhibit myostatin/GDF8 signaling and promote functional myoblast differentiation.* J Biol Chem, 2015. **290**(6): p. 3390-404.
19. Kausar, T. and S.M. Nayeem, *Identification of small molecule inhibitors of ALK2: a virtual screening, density functional theory, and molecular dynamics simulations study.* J Mol Model, 2018. **24**(9): p. 262.
20. Mohedas, A.H., et al., *Structure-activity relationship of 3,5-diaryl-2-aminopyridine ALK2 inhibitors reveals unaltered binding affinity for fibrodysplasia ossificans progressiva causing mutants.* J Med Chem, 2014. **57**(19): p. 7900-15.

21. Berasi, S.P., et al., *Divergent activities of osteogenic BMP2, and tenogenic BMP12 and BMP13 independent of receptor binding affinities.* Growth Factors, 2011. **29**(4): p. 128-39.

CHAPTER VI: Discussion

The retinal pigmented epithelium (RPE) play an important role in the establishment and maintenance of the blood-retinal barrier, and breaking this barrier can lead to various eye diseases [1]. In order for this barrier function to be reestablished after disruption, RPE must undergo an epithelial-to-mesenchymal transition (EMT) to heal the wound, and subsequently, undergo a mesenchymal-to-epithelial transition (MET) to reform the barrier [2]. However, with repeated and/or prolonged wounding, RPE tend to undergo a terminal EMT, become fibrotic, and are incapable of reforming a healthy monolayer [3-6]. Previous investigations in our lab, using an in vitro model of wound healing, identified *GDF6* as one of the top candidates to be involved in the failure of RPE to repair. This current body of work sets out to investigate *GDF6* and its relationship with RPE EMT.

Radeke *et al*. (2015) examined the effect of EMT in RPE along with potential causes and preventions [7]. Repeated passaging was used as an *in vitro* model of wound healing or EMT. They found RPE that had undergone a terminal EMT were able to revert to a normal, epithelial state in the presence of the transforming growth factor beta (TGFβ) inhibitor A83-01. Their results indicated the TGFβ pathway affected EMT. However, it is unlikely that TGFβ alone was the cause for a terminal fibrotic differentiation, as passage 0 (P0) RPE express *TGFβ1* and these cells can freely undergo both EMT and MET. They compared gene expression profiles between healthy P0 RPE and mesenchymal passage 5 (P5) RPE, looking for a gene only expressed in P5 RPE, to determine what caused this fibrotic switch to happen. Growth differentiation factor 6 (*GDF6*), a member of the TGFβ superfamily, matched this expression profile. *GDF6* displayed one of the most dramatic gene expression

changes in healthy versus passaged RPE. This led to our initial hypothesis: *GDF6* causes irreversible EMT in RPE and by inhibiting *GDF6*, we can prevent fibrotic RPE.

In this report we found *GDF6* plays a major role in RPE EMT. In chapter three we demonstrated that *GDF6* is sufficient to induce EMT in RPE. Exposing p0 RPE to *GDF6* induces a mesenchymal state as if the RPE have undergone EMT without passaging. This mesenchymal change was apparent in both the phenotype and gene expression of treated RPE. However, *GDF6* is not necessary for RPE EMT. In chapter 4 we inhibited GDF6 signaling using a Smad1/5/9 phosphorylation inhibitor LDN-193189 (LDN). Prevention of its signaling cascade neither prevented nor delayed RPE EMT. Additionally, knocking down *GDF6* failed to stop RPE EMT, though there was a slight delay. While the RPE still succumbed to a mesenchymal phenotype, the cells had a different appearance and gene expression, suggesting this switch was due to another pathway. In chapter five we investigated the idea that GDF6 may be operating through a novel, non-canonical pathway as *GDF6* affects the expression of specific genes in the presence of Smad phosphorylation pathway inhibitors. To help determine this pathway, we performed a phospho-kinase array analysis but were unable to elucidate a novel receptor. We have since modified our hypothesis and now believe *GDF6* may play a role in RPE EMT by inducing *TGFβ1* expression, leading to the EMT phenotype, as well as preventing the return back to an epithelial cell by inhibiting MET.

6.1: Mechanism of GDF6

The mechanism of GDF6 action on RPE was previously unknown. Prior studies observed a canonical Smad1/5/9 signaling in mesenchymal cells, with GDF6 showing affinity for the type one activin-like kinase (Alk) receptors 3 and 6, as well as affinity to the type two

receptors activin receptor two (ActRII) A/B and the bone morphogenic protein (BMP) receptor two (BMPRII) [8, 9]. Based on the results shown in chapters three, four, and five, we have developed a model for how GDF6 signals in RPE (Figure 6.1).

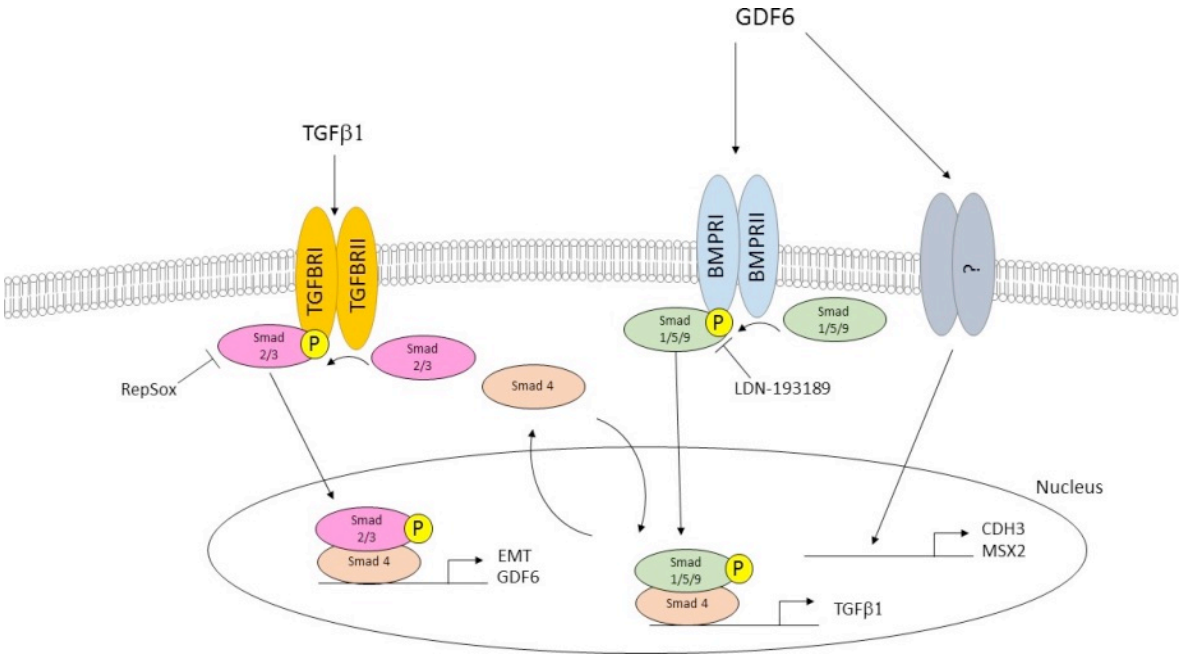

Figure 6.1. Model of GDF6 mechanism of action in RPE. GDF6 binds to the BMP receptors, initiating phosphorylation of Smad1/5/9. This phosphorylated Smad protein is then translocated to the nucleus with the assistance of Smad 4, where it affects *TGFβ1* expression. TGFβ1 then binds to the TGFβ receptors, triggering phosphorylation of Smad2/3. Once co-localized with Smad 4 and translocated to the nucleus, genes relating to RPE EMT are affected. Additionally, a protein acting through the TGFβ receptors activates *GDF6* transcription. GDF6 affects gene expression of a subset of genes, like *CDH3* and *MSX2*, through a non-canonical pathway, possibly through binding of another receptor complex.

We believe that EMT in RPE is not caused directly by GDF6, but instead by a protein operating through the TGFβ pathway that is induced by GDF6. When we administer GDF6 to RPE, RPE become mesenchymal; however, the use of RepSox, a Smad2/3 Alk5 inhibitor, restores the phenotype of RPE. Since GDF6 itself does not phosphorylate Smad2/3 (Figure 3.5), RepSox should not be able to suppress the mesenchymal phenotype induced by the

addition of GDF6. The fact that it does suggests that GDF6 is acting on something that binds to the TGFβ receptors to phosphorylate Smad2/3. We hypothesize the gene GDF6 is acting on is *TGFβ1*. In order to conclude this, the gene in question must be unaffected by RepSox treatment but down-regulated by LDN and the gene must act directly on GDF6 and not by some other downstream effector. As shown in Figure 5.3, *TGFβ1* fits this profile. Additionally, GDF6 affects *TGFβ1* expression in a dose-dependent manner, suggesting that GDF6 directly influences *TGFβ1* expression (Figure 3.1).

We believe a protein operating through the TGFβ receptor activates *GDF6*. Previously, Radeke *et. al* (2015) passaged RPE in the presence of a TGFβ inhibitor, A-83-01, and *GDF6* expression never occurred [7]. This suggests that something operating through the TGFβ pathway initiates expression of *GDF6*. This activation of the pathway could be due to high, constant TGFβ1 expression causing chromatin modification at the promoter site of *GDF6*. The passage model of wounding used to initiate RPE EMT is a constant source of stress on the RPE, and stress is known to induce transcriptional regulation changes in plant chromatin [10]. Stress, in the form of hypoxia or a tumor environment, can induce chromatin remodeling and epigenetic reprogramming of the genome in mammalian cells [11, 12]. TGFβ is a known cell stressor through its induction of EMT in epithelial cells, and treatment of epithelial mammary cells and lens epithelial cells with TGFβ resulted in vast chromatin modifications, especially around mesenchymal gene promoter sites [13, 14]. However, the list of potential genes that are involved in Smad2/3 phosphorylation is exhaustive, and it could be difficult to tease out exactly what is activating *GDF6*.

Finally, when RPE are exposed to *GDF6*, we always see the regulation of specific genes—like a down-regulation of *CDH3* and an up-regulation of *MSX2* (Figure 5.2). This regulation remains true when the RPE are grown in the presence of both small molecule inhibitors, RepSox and LDN, suggesting GDF6 may be acting through some non-canonical signaling pathway. This non-canonical pathway may be due to direct signaling of BMPRII or by another unknown receptor complex [15]. The pathway can potentially be elucidated by performing receptor-ligand pull-down experiments, baiting the receptors with GDF6.

6.2: Epithelial-to-Mesenchymal Transition (EMT)

EMT is an essential process in both development and wound healing, allowing cells to migrate to their necessary location to become a different cell type or to fill a gap [16]. Aberrant wound healing can cause RPE and other epithelial cells to become fibrotic and form scar tissue, leading to various issues [17]. Additionally, when cells undergo EMT they become migratory—an issue when the cells are cancerous. It is important to understand the underlying mechanisms of EMT and cell fibrosis in order to potentially reverse and prevent this transformation.

6.2.1: GDF6

The research displayed in the previous chapters informs us that *GDF6* is a key player in RPE EMT. This phenomenon is not specific to RPE cells; other epithelial cell types that have undergone a fibrotic transformation show evidence of increased *GDF6*. Renal epithelial cells exposed to TGFB1 have increased *GDF6* transcripts and form fibrotic mesenchymal cells, similar to the fibrotic cells seen in RPE [18]. Also, lung epithelial cells with a *TGFBR2* knockout exhibited a decrease in *GDF6* transcripts and a subsequent

decrease in fibrosis [19]. It may be that *GDF6* does not directly cause the mesenchymal phenotype, as is the case in RPE. Instead, *GDF6* may be preventing the cells from returning to an epithelial state by inhibiting important cell junction genes.

GDF6 is also a natural inducer of mesenchyme. Embryonic stem cells treated with BMP12/13 resulted in tendon precursor cells, indicating GDF6 is a natural inducer of mesenchymal fate [20]. Older mesenchymal stem cells (MSCs) are rejuvenated in the presence of GDF6, reinstating their osteogenic potential [21]. GDF6 also induces adipose-derived MSCs (AD-MSCs) into a nucleus pulposus (NP)-like phenotype, and these cells may be useful in therapies for intervertebral disc regeneration [22]. GDF6 appears to participate in the EMT process in many epithelial cells and targeting GDF6 may help prevent the fibrotic diseases that occur due to the inability of the cells to undergo MET.

6.2.2: TGFβ

TGFβ is one of the most well-known inducers of EMT in RPE as well as many other epithelial cell types [23]. However, *TGFβ* expression can be both beneficial and harmful to cells in what is known as the "TGFβ Paradox" [24]. This phenomenon was first seen in cancer: *TGFβ* initially acts as a tumor suppressor but switches to a tumor promoter in later stages of the disease, primarily when cells have undergone EMT [24, 25]. *TGFβ* expression is common in metastatic breast cancer, promoting mesenchymal cell differentiation and migration through the lymphatic system [26, 27]. Gastric cancer cells exposed to TGFβ also show increased EMT, lung metastasis, and tumor formation [28]. Inhibiting TGFβ at later stages of disease could be beneficial in preventing the spread of cancer, but it is necessary to understand its early anti-tumor properties as well.

The TGFβ paradox is observed in the eye as well. Complications of dysregulated wound healing in lens epithelial cells can lead to cataract formation. This cataract formation is due to TGFβ-induced transdifferentiation of epithelial cells into myofibroblasts [29, 30]. The myofibroblasts cause scarring and vision loss, but TGFβ has also demonstrated an ability to induce the beneficial lens fiber cell from lens epithelial cells [31]. RPE also exhibit the TGFβ paradox, as *TGFβ* is present in healthy P0 RPE that can undergo both EMT and MET, but at some point *TGFβ* becomes a main inducer of irreversible EMT in RPE [7]. This switch from a beneficial to a malevolent protein may be due to an increased concentration from prolonged activation. Initially, when RPE (or other epithelial cells) are healthy, TGFβ signaling provides the beneficial effects previously noted. Continuous activation of the TGFβ pathway leads to increased concentrations, signaling the cells are in a stressful environment and thus must change in order to survive, causing EMT, proliferation, and migration. While blocking TGFβ signaling can rescue RPE that have undergone EMT, the cells ultimately succumb to a mesenchymal fate [7].

6.2.3: Other Potential Pathways

While TGFβ is one of the most well-known and well-documented inducers of EMT in epithelial cells, other pathways and mechanisms can also lead to a mesenchymal state. Blockage of TGFβ-mediated Smad2/3 signaling in RPE delays EMT in RPE and can rescue mesenchymal RPE, but the cells ultimately lose their epithelial phenotype [7]. As demonstrated in chapter 4, RPE treated with the Smad1/5/9 inhibitor LDN still undergo a morphological change when passaged. *TGFβ1* and *GDF6* expression levels remain low, yet

the RPE still lose their characteristic cobblestone morphology. This loss of an epithelial state is likely due to alternative pathways or non-canonical TGFβ/BMP pathways.

6.2.3.A: Wnt/β-catenin and Hippo Pathways

The Wnt signaling pathway is responsible for regulating proliferation, differentiation, and cell polarity [32]. This pathway comes in 2 forms: the canonical, β-catenin dependent pathway and the non-canonical, β-catenin independent pathway. The β-catenin independent pathway has been shown to play a role in EMT, specifically in cancers such as melanoma, but the interaction of β-catenin to cadherins makes the canonical pathway more interesting and applicable [33, 34]. In the canonical pathway, Wnt ligands bind to Frizzled and lipoprotein receptor-related protein receptors, leading to activation of Dishevelled (Dvl) and inhibition of the GSK-3/APC/Axin-degradation complex. This leads to β-catenin accumulation in the cytoplasm and its subsequent translocation to the nucleus where it can interact with transcription factor T-cell factor (TCF) and lymphoid enhancer factor (LEF). β-catenin translocation to the nucleus is thought to be a vital molecular event leading to EMT [35]. RPE that have undergone EMT upregulate members of the Wnt signaling cascade, suggesting activation of the Wnt pathway [7]. Wnt signaling has also been found to induce EMT and increase proliferation in RPE that have lost contact inhibition, independent of TGFβ presence [36]. Initiation of the Wnt signaling cascade in RPE may prove useful in regenerating a healthy RPE layer or repairing a wound, as the pathway can increase proliferation in the normally senescent cell. Wnt-induced EMT is seen after laser photocoagulation of RPE, with the RPE showing an increase in proliferation as well as key RPE transcription factors *MITF* and *OTX2* [37, 38]. Importantly, the EMT phenotype after

this treatment is transient, with the RPE undergoing MET and returning to a healthy state [37]. Stimulation of the Wnt pathway and use of Wnt inhibitors may prove useful in repairing the RPE monolayer after injury or disease.

The Hippo pathway is also involved in cell proliferation, differentiation, and survival [39-42]. Unlike other similar signaling pathways, the Hippo pathway does not have any dedicated signaling peptides or receptors, but it does maintain a core pathway comprised of serine/threonine kinases: Mammalian Sterile 20-like 1 and 2 (MST 1/2) and Large tumor suppressor 1/2 (LATS1/2) [39]. Phosphorylation of LATS1/2 leads to interaction and phosphorylation of the transcription regulators yes-associated protein 1 and transcriptional coactivator with PDZ-binding motif (YAP/TAZ), resulting in cytoplasmic retention and degradation [43]. The Hippo pathway can be regulated through four upstream branches of signaling: the Crumbs complex, regulators of MST kinases, the actin cytoskeleton, and adherens junctions [39]. Inhibition of the pathway through a mechanism such as loss of cell polarity causes translocation of YAP/TAZ to the nucleus, allowing for interaction with the TEA-domain-containing (TEAD) transcription factor family and induction of genes related to cell proliferation. Both YAP and TAZ have been shown to promote EMT when the Hippo pathway is inhibited [44, 45].

YAP/TAZ is also known to be affiliated with Wnt signaling. YAP/TAZ can associate with β-catenin in the Wnt-OFF state, leading to the degradation of the complex but in the Wnt-ON state, the complex is disassembled and YAP/TAZ, along with β-catenin, translocate to the nucleus [43, 46, 47]. Preventing YAP/TAZ accumulation in the nucleus can help avoid EMT, thus maintaining activation of the Hippo pathway is crucial. However, other pathways

like Wnt can regulate YAP/TAZ, so direct inhibition of YAP/TAZ is a more favorable approach to preventing EMT.

6.2.3.B: Connective Tissue Growth Factor (CTGF)

Connective tissue growth factor (CTGF) is a matricellular protein, acting through unknown receptors as well as modifying other growth factors and cytokines, such as TGFβ1, Wnt integrins, epidermal growth factor receptor (EGFR), among others [48]. It is strongly linked to the pathology of fibrotic diseases in many different cell types, from liver cells to heart and lung cells [48, 49]. CTGF dysregulation has also been found in various age-related vascular pathologies, including those in the eye like diabetic retinopathy [50]. CTGF can interact with TGFβ to promote a fibrotic lineage but can also operate independently of TGFβ through induction of p38, extracellular signal-regulated kinase 1/2mM (Erk1/2), Jun N-terminal inase (JNK), and Akt [51]. Additionally, CTGF has been shown to cause an EMT-like cell fate change both *in vitro* and *in vivo* [52]. RPE subjected to TGFβ/BMP inhibitors still eventually lose their epithelial fate, as evidenced in chapter four and previous work by our lab [7]. Since CTGF can initiate EMT and tissue fibrosis without signaling from TGFβ, it becomes a probable answer as to how RPE can still undergo EMT. CTGF-induced EMT may also account for the differences in the appearance of passage 7 RPE in chapter four. RPE passaged with LDN have low levels of *TGFβ1* and still undergo EMT, but their appearance is markedly different from control cells, suggesting EMT is mediated from a factor other than TGFβ. Inhibition of CTGF using neutralizing antibodies has been successful in reducing proangiogenic and profibrotic genes in RPE, and combination treatment with TGFβ inhibitors may be necessary to prolong the RPE phenotype *in vitro* [53].

6.2.3.C: Redundancy

The TGFβ superfamily is comprised of over 35 protein-encoding genes that fall into four subfamilies: the TGFβ subfamily, the BMP/GDF6 subfamily, the activin and inhibin subfamilies, and divergent members. These proteins operate through a handful of receptors and phosphorylate either Smad2/3 or Smad1/5/9. The complexity of the pathways makes it likely that there is some redundancy in the family and even within the subfamilies themselves [54]. TGFβ1 and TGFβ3 arefound to be partially redundant in developmental processes, like the creation of brain vasculature, where both isoforms are present and bind to integrins [55]. GDF11 and myostatin (GDF8) both regulate muscle growth and skeletal patterning, and redundancy has been seen in their skeletal patterning function, suggesting the redundancy is tissue dependent [56]. Redundancy of GDF6 has also been suggested due to its high homology with other family members, such as GDF5 and GDF7 [57]. In chapter four, we discovered that knocking down *GDF6* still resulted in RPE EMT. It is possible that, due to the high levels of homology, GDF5 or GDF7 could be replicating GDF6 signaling and influencing RPE EMT. Targeting GDF6 for the prevention of a terminal, fibrotic EMT will likely not be sufficient; a broader inhibition of GDF/BMP family members is needed. As observed in chapter 4, LDN, a broad inhibitor of GDF/BMP, failed to delay EMT in RPE. However, the RPE in this situation may be undergoing EMT mediated by other previously mentioned pathways.

6.2.4: Prevention

EMT and subsequent fibrosis of epithelial cells have been linked to the pathogenesis of various diseases, including cancer and organ fibrosis [58]. It is imperative to understand

the underlying mechanism in order to prevent EMT from occurring. Small molecules targeting multiple potential pathways of EMT have been synthesized and show promise in inhibiting EMT in cancerous cells [59].

While preventing EMT may avoid disease pathology, EMT is a necessary process in development and wound healing. EMT stimulates both migration and proliferation which are necessary for normally senescent cells such as RPE [60]. In order to repair the RPE monolayer, EMT needs to be initiated to heal the wound, and then the cells need to be instructed to undergo MET to reform the barrier layer. Stimulation of EMT in RPE can be achieved using laser photocoagulation or addition of known EMT induction factors like TGFβ [7, 37, 38]. Once the wound is repaired, the RPE need to undergo MET in order to reform the epithelial layer and prevent disease. BMP7 has been shown to promote MET and help cells regain an epithelial phenotype [61]. Inhibition of GDF6 may also promote MET, as evidenced in chapter four. Passaging RPE caused EMT by passage six but the addition of the inhibitor LDN restored the epithelial phenotype. This effect was short-lived as the addition of LDN to cells at passage seven resulted in only a partial restoration of the phenotype. The timing of EMT inhibition appears crucial both to the response of the cell and survival of the cell fate.

6.3: Implication in Disease

The ability for *GDF6* to induce EMT in RPE suggests that it may have a role in various eye diseases where EMT is involved in the pathogenesis of disease. This logic extends to other epithelial cells as well; *GDF6* is likely involved in the pathology of other diseases

related to a change in epithelial morphology. Understanding and potentially inhibiting *GDF6* could prevent the progression of disease in tissues in addition to the eye.

6.3.1: Age-Related Macular Degeneration (AMD)

Age-related macular degeneration (AMD) is the leading cause of blindness in the developed world among those aged 55 and older [62]. AMD is characterized by a loss of central vision in the macula region due to photoreceptor and RPE death. Accumulation of drusen, a yellow deposit of lipids, is a hallmark characteristic of AMD. Advanced AMD is divided into two types: wet AMD or choroidal neovascularization (CNV), and dry AMD or geographic atrophy (GA). In CNV, new blood vessels form in the sub-RPE space and leak fluid and blood, resulting in swelling and damage of the macula and RPE layer. GA is the gradual degeneration of RPE and photoreceptors, resulting in clearly demarcated lesions in the retina. Over 80% of all AMD cases are classified as dry AMD, but wet AMD results in 90% of blindness in all AMD cases [63, 64]. There is currently no cure for dry AMD, and CNV can only be treated with anti-VEGF treatments for so long before they stop working [65, 66]. Stem cell-based therapies are attempting to treat both types of AMD by transplanting derived RPE into the areas of cell death with positive responses, such as improvement in visual acuity, starting to be reported [67, 68]. While these therapies may prove useful in stopping disease progression, it would be better to prevent the disease entirely.

EMT of the RPE is a common occurrence in both GA and CNV. RPE in the GA transition zone (cells on the edges of the lesions) are commonly found to have undergone EMT, forming a fibrotic mesh [69-71]. In CNV, subretinal fibrosis is caused by RPE that have undergone EMT [3, 72]. RPE EMT is not sufficient to cause CNV, as blood vessel formation is

driven by an increase in VEGF [73]. As shown in previous chapters, *GDF6* has a negative effect on cadherin 3 (*CDH3*) expression. This downregulation of a critical cell adhesion molecule can result in a loss of adherens junctions, leading to a breakdown of the barrier and allowing blood and other fluid from the sub-retinal space to leak onto the retina. There are reports of a slight increase of *GDF6* transcripts in the macular age-matched RPE-choroid sample of patients with GA and CNV (personal communication with Monte Radeke). The RPE are likely undergoing EMT to repair the lesion in GA or the barrier function in CNV. Inhibition of *GDF6* may enable RPE to undergo MET and reform the necessary epithelial barrier.

6.3.2: Proliferative Vitreoretinopathy (PVR)

Proliferative Vitreoretinopathy (PVR) is a complication of retinal detachment surgery, occurring in 5-10% of all repairs [74]. PVR is the formation of a fibrous membrane on either or both sides of the retina, eventually causing retinal detachment and loss of vision. There are two main cell types involved in the formation of the membranes: RPE and Müller glia. Upon retinal detachment these cells undergo EMT or a glial-mesenchymal transition (GMT), initiating proliferation and migration into the subretinal or periretinal space [75]. The cells then transform to a myofibroblast cell, causing contractile forces that pull at the retina causing detachment.

We have shown in chapter 3 that *GDF6* can induce EMT in RPE. Additionally, our lab has seen increased *GDF6* expression in fibrotic RPE [7]. This suggests *GDF6* may be involved in the RPE formation of epiretinal membranes. Müller glial cells also play an active part in PVR pathogenesis. Glial cells that have undergone GMT produce inflammatory cytokines

and elevate traditional mesenchymal markers [76, 77]. Similar to RPE, passaged Müller glia display increased *GDF6* expression *in vitro* (personal communication with Monte Radeke and Rachael Warrington). Inhibition of *GDF6* may prove useful in preventing fibrotic membrane accumulation after retinal detachment surgery.

6.3.3: Cancer

Metastasis may be responsible for as much as 90% of cancer-related deaths, and EMT of the cancerous cells is a likely culprit in transforming the cells from a stationary state to a proliferative, invasive one [78]. Melanoma is regarded as one of the deadliest types of cancer and EMT is a well-studied phenomenon in disease progression [79]. It arises when melanocytes, pigmented cells within the skin, mutate and become cancerous. These cells are more likely to metastasize and spread throughout the body. Melanocytes and RPE share the ability to pigment using melanin, but melanocytes are of a neural crest origin whereas RPE originate from neuroectodermal cells [80]. Recently, *GDF6* has been implicated in the pathogenesis of melanoma as it is found in cancerous melanomas but not the non-cancerous precursor melanocyte [81]. The authors suggest that *GDF6* promotes melanoma progression through inhibition of pro-apoptotic genes to increase proliferation and promote invasiveness. This is similar to what is seen when cancerous cells undergo EMT to metastasize and spread. We have shown *GDF6* to play a role in EMT of an epithelial cell and combined with their new cancer-promoting role in melanomas, *GDF6* may be involved in other cancers where cells undergo EMT and metastasize. Examination of *GDF6* expression levels in other epithelial cancers is needed, and inhibition of *GDF6* could prove useful in future treatments.

6.4: Conclusions

Understanding RPE EMT is critical in understanding various diseases of the eye. If we can control RPE EMT, we can help treat and prevent these diseases. In my Ph.D. research, I investigated the role *GDF6* has in RPE EMT, revealing it can induce EMT in healthy cells but is not necessary for RPE EMT. Additionally, I showed that GDF6 could act through a novel, non-canonical pathway to affect gene expression. The work presented in this dissertation provides insight into the underlying mechanisms of RPE EMT and the conversion into a fibrotic cell, specifically the role *GDF6* has in the process of RPE EMT. We believe *GDF6* promotes EMT through upregulation of TGFβ proteins. It drives fibrosis of the RPE through prevention of MET by negatively regulating important adherens proteins, preventing the RPE from reforming a healthy, polarized monolayer. Future work is needed to determine the role of cadherins in MET as well as their relationship with *GDF6*.

6.5: References

1. Cunha-Vaz, J., R. Bernardes, and C. Lobo, *Blood-retinal barrier.* Eur J Ophthalmol, 2011. **21 Suppl 6**: p. S3-9.
2. Sugino, I.K., H. Wang, and M.A. Zarbin, *Age-related macular degeneration and retinal pigment epithelium wound healing.* Mol Neurobiol, 2003. **28**(2): p. 177-94.
3. Ishikawa, K., R. Kannan, and D.R. Hinton, *Molecular mechanisms of subretinal fibrosis in age-related macular degeneration.* Exp Eye Res, 2016. **142**: p. 19-25.
4. Little, K., et al., *Myofibroblasts in macular fibrosis secondary to neovascular age-related macular degeneration - the potential sources and molecular cues for their recruitment and activation.* EBioMedicine, 2018. **38**: p. 283-291.
5. Roberts, A.B., et al., *Smad3 is key to TGF-beta-mediated epithelial-to-mesenchymal transition, fibrosis, tumor suppression and metastasis.* Cytokine Growth Factor Rev, 2006. **17**(1-2): p. 19-27.
6. Friedlander, M., *Fibrosis and diseases of the eye.* J Clin Invest, 2007. **117**(3): p. 576-86.
7. Radeke, M.J., et al., *Restoration of mesenchymal retinal pigmented epithelial cells by TGFβ pathway inhibitors: implications for age-related macular degeneration.* Genome Med, 2015. **7**(1): p. 58.

8. Mazerbourg, S., et al., *Identification of receptors and signaling pathways for orphan bone morphogenetic protein/growth differentiation factor ligands based on genomic analyses.* J Biol Chem, 2005. **280**(37): p. 32122-32.
9. Berasi, S.P., et al., *Divergent activities of osteogenic BMP2, and tenogenic BMP12 and BMP13 independent of receptor binding affinities.* Growth Factors, 2011. **29**(4): p. 128-39.
10. Pecinka, A. and O. Mittelsten Scheid, *Stress-induced chromatin changes: a critical view on their heritability.* Plant Cell Physiol, 2012. **53**(5): p. 801-8.
11. Johnson, A.B. and M.C. Barton, *Hypoxia-induced and stress-specific changes in chromatin structure and function.* Mutat Res, 2007. **618**(1-2): p. 149-62.
12. Karpinets, T.V. and B.D. Foy, *Tumorigenesis: the adaptation of mammalian cells to sustained stress environment by epigenetic alterations and succeeding matched mutations.* Carcinogenesis, 2005. **26**(8): p. 1323-34.
13. Arase, M., et al., *Dynamics of chromatin accessibility during TGF-beta-induced EMT of Ras-transformed mammary gland epithelial cells.* Sci Rep, 2017. **7**(1): p. 1166.
14. Ganatra, D.A., et al., *Association of histone acetylation at the ACTA2 promoter region with epithelial mesenchymal transition of lens epithelial cells.* Eye (Lond), 2015. **29**(6): p. 828-38.
15. Foletta, V.C., et al., *Direct signaling by the BMP type II receptor via the cytoskeletal regulator LIMK1*, in *J Cell Biol*. 2003. p. 1089-98.
16. Thiery, J.P., et al., *Epithelial-mesenchymal transitions in development and disease.* Cell, 2009. **139**(5): p. 871-90.
17. Stone, R.C., et al., *Epithelial-mesenchymal transition in tissue repair and fibrosis.* Cell Tissue Res, 2016. **365**(3): p. 495-506.
18. Brennan, E.P., et al., *Next-generation sequencing identifies TGF-beta1-associated gene expression profiles in renal epithelial cells reiterated in human diabetic nephropathy.* Biochim Biophys Acta, 2012. **1822**(4): p. 589-99.
19. Degryse, A.L., et al., *TGFbeta signaling in lung epithelium regulates bleomycin-induced alveolar injury and fibroblast recruitment.* Am J Physiol Lung Cell Mol Physiol, 2011. **300**(6): p. L887-97.
20. Dale, T.P., et al., *Tenogenic Differentiation of Human Embryonic Stem Cells.* Tissue Eng Part A, 2018. **24**(5-6): p. 361-368.
21. Hisamatsu, D., et al., *Growth differentiation factor 6 derived from mesenchymal stem/stromal cells reduces age-related functional deterioration in multiple tissues.* Aging (Albany NY), 2016. **8**(6): p. 1259-75.
22. Clarke, L.E., et al., *Growth differentiation factor 6 and transforming growth factor-beta differentially mediate mesenchymal stem cell differentiation, composition, and micromechanical properties of nucleus pulposus constructs.* Arthritis Res Ther, 2014. **16**(2): p. R67.
23. Xu, J., S. Lamouille, and R. Derynck, *TGF-beta-induced epithelial to mesenchymal transition.* Cell Res, 2009. **19**(2): p. 156-72.
24. Roberts, A.B. and L.M. Wakefield, *The two faces of transforming growth factor beta in carcinogenesis.* Proc Natl Acad Sci U S A, 2003. **100**(15): p. 8621-3.

25. Principe, D.R., et al., *TGF-beta: duality of function between tumor prevention and carcinogenesis.* J Natl Cancer Inst, 2014. **106**(2): p. djt369.
26. Johansson, J., et al., *TGF-beta1-Induced Epithelial-Mesenchymal Transition Promotes Monocyte/Macrophage Properties in Breast Cancer Cells.* Front Oncol, 2015. **5**: p. 3.
27. Pang, M.F., et al., *TGF-beta1-induced EMT promotes targeted migration of breast cancer cells through the lymphatic system by the activation of CCR7/CCL21-mediated chemotaxis.* Oncogene, 2016. **35**(6): p. 748-60.
28. Peng, X., et al., *SOX4 contributes to TGF-beta-induced epithelial-mesenchymal transition and stem cell characteristics of gastric cancer cells.* Genes Dis, 2018. **5**(1): p. 49-61.
29. de Iongh, R.U., et al., *Transforming growth factor-beta-induced epithelial-mesenchymal transition in the lens: a model for cataract formation.* Cells Tissues Organs, 2005. **179**(1-2): p. 43-55.
30. Shu, D.Y. and F.J. Lovicu, *Myofibroblast transdifferentiation: The dark force in ocular wound healing and fibrosis.* Prog Retin Eye Res, 2017. **60**: p. 44-65.
31. Boswell, B.A., et al., *Dual function of TGFbeta in lens epithelial cell fate: implications for secondary cataract.* Mol Biol Cell, 2017. **28**(7): p. 907-921.
32. MacDonald, B.T., K. Tamai, and X. He, *Wnt/beta-catenin signaling: components, mechanisms, and diseases.* Dev Cell, 2009. **17**(1): p. 9-26.
33. Zhan, T., N. Rindtorff, and M. Boutros, *Wnt signaling in cancer.* Oncogene, 2017. **36**(11): p. 1461-1473.
34. Chen, Z., Y. Shao, and X. Li, *The roles of signaling pathways in epithelial-to-mesenchymal transition of PVR.* Mol Vis, 2015. **21**: p. 706-10.
35. Hill, T.P., et al., *Canonical Wnt/beta-catenin signaling prevents osteoblasts from differentiating into chondrocytes.* Dev Cell, 2005. **8**(5): p. 727-38.
36. Chen, H.C., et al., *Wnt signaling induces epithelial-mesenchymal transition with proliferation in ARPE-19 cells upon loss of contact inhibition.* Lab Invest, 2012. **92**(5): p. 676-87.
37. Han, J.W., et al., *Wnt/beta-Catenin Signaling Mediates Regeneration of Retinal Pigment Epithelium After Laser Photocoagulation in Mouse Eye.* Invest Ophthalmol Vis Sci, 2015. **56**(13): p. 8314-24.
38. Cho, I.H., et al., *The role of Wnt/beta-catenin signaling in the restoration of induced pluripotent stem cell-derived retinal pigment epithelium after laser photocoagulation.* Lasers Med Sci, 2018.
39. Johnson, R. and G. Halder, *The two faces of Hippo: targeting the Hippo pathway for regenerative medicine and cancer treatment.* Nat Rev Drug Discov, 2014. **13**(1): p. 63-79.
40. Yu, F.X. and K.L. Guan, *The Hippo pathway: regulators and regulations.* Genes Dev, 2013. **27**(4): p. 355-71.
41. Genevet, A. and N. Tapon, *The Hippo pathway and apico-basal cell polarity.* Biochem J, 2011. **436**(2): p. 213-24.
42. Halder, G. and R.L. Johnson, *Hippo signaling: growth control and beyond.* Development, 2011. **138**(1): p. 9-22.

43. Totaro, A., T. Panciera, and S. Piccolo, *YAP/TAZ upstream signals and downstream responses.* Nat Cell Biol, 2018. **20**(8): p. 888-899.
44. Lei, Q.Y., et al., *TAZ promotes cell proliferation and epithelial-mesenchymal transition and is inhibited by the hippo pathway.* Mol Cell Biol, 2008. **28**(7): p. 2426-36.
45. Lamar, J.M., et al., *The Hippo pathway target, YAP, promotes metastasis through its TEAD-interaction domain.* Proc Natl Acad Sci U S A, 2012. **109**(37): p. E2441-50.
46. Azzolin, L., et al., *YAP/TAZ incorporation in the beta-catenin destruction complex orchestrates the Wnt response.* Cell, 2014. **158**(1): p. 157-70.
47. Varelas, X., et al., *The Hippo pathway regulates Wnt/beta-catenin signaling.* Dev Cell, 2010. **18**(4): p. 579-91.
48. Toda, N., et al., *CTGF in kidney fibrosis and glomerulonephritis.* Inflamm Regen, 2018. **38**: p. 14.
49. Lipson, K.E., et al., *CTGF is a central mediator of tissue remodeling and fibrosis and its inhibition can reverse the process of fibrosis.* Fibrogenesis Tissue Repair, 2012. **5**(Suppl 1): p. S24.
50. Ungvari, Z., et al., *Connective tissue growth factor (CTGF) in age-related vascular pathologies.* Geroscience, 2017. **39**(5-6): p. 491-498.
51. Sonnylal, S., et al., *Selective expression of connective tissue growth factor in fibroblasts in vivo promotes systemic tissue fibrosis.* Arthritis Rheum, 2010. **62**(5): p. 1523-32.
52. Sonnylal, S., et al., *Connective tissue growth factor causes EMT-like cell fate changes in vivo and in vitro.* J Cell Sci, 2013. **126**(Pt 10): p. 2164-75.
53. Bagheri, A., et al., *Simultaneous application of bevacizumab and anti-CTGF antibody effectively suppresses proangiogenic and profibrotic factors in human RPE cells.* Mol Vis, 2015. **21**: p. 378-90.
54. Munger, J.S. and D. Sheppard, *Cross talk among TGF-beta signaling pathways, integrins, and the extracellular matrix.* Cold Spring Harb Perspect Biol, 2011. **3**(11): p. a005017.
55. Mu, Z., et al., *TGFbeta1 and TGFbeta3 are partially redundant effectors in brain vascular morphogenesis.* Mech Dev, 2008. **125**(5-6): p. 508-16.
56. McPherron, A.C., T.V. Huynh, and S.J. Lee, *Redundancy of myostatin and growth/differentiation factor 11 function.* BMC Dev Biol, 2009. **9**: p. 24.
57. Williams, L.A., D. Bhargav, and A.D. Diwan, *Unveiling the bmp13 enigma: redundant morphogen or crucial regulator?* Int J Biol Sci, 2008. **4**(5): p. 318-29.
58. Kalluri, R. and R.A. Weinberg, *The basics of epithelial-mesenchymal transition.* J Clin Invest, 2009. **119**(6): p. 1420-8.
59. Basu, D., et al., *Identification, mechanism of action, and antitumor activity of a small molecule inhibitor of hippo, TGF-beta, and Wnt signaling pathways.* Mol Cancer Ther, 2014. **13**(6): p. 1457-67.
60. Tamiya, S., L. Liu, and H.J. Kaplan, *Epithelial-mesenchymal transition and proliferation of retinal pigment epithelial cells initiated upon loss of cell-cell contact.* Invest Ophthalmol Vis Sci, 2010. **51**(5): p. 2755-63.

61. Wang, Y., et al., *Bone morphogenetic protein-7 prevented epithelial-mesenchymal transition in RLE-6TN cells.* Toxicol Res (Camb), 2016. **5**(3): p. 931-937.
62. Wong, W.L., et al., *Global prevalence of age-related macular degeneration and disease burden projection for 2020 and 2040: a systematic review and meta-analysis.* Lancet Glob Health, 2014. **2**(2): p. e106-16.
63. Kahn, H.A., et al., *The Framingham Eye Study. I. Outline and major prevalence findings.* Am J Epidemiol, 1977. **106**(1): p. 17-32.
64. Ferris, F.L., 3rd, S.L. Fine, and L. Hyman, *Age-related macular degeneration and blindness due to neovascular maculopathy.* Arch Ophthalmol, 1984. **102**(11): p. 1640-2.
65. Tranos, P., et al., *Resistance to antivascular endothelial growth factor treatment in age-related macular degeneration.* Drug Des Devel Ther, 2013. **7**: p. 485-90.
66. Zarbin, M., I. Sugino, and E. Townes-Anderson, *Concise Review: Update on Retinal Pigment Epithelium Transplantation for Age-Related Macular Degeneration.* Stem Cells Transl Med, 2019.
67. da Cruz, L., et al., *Phase 1 clinical study of an embryonic stem cell-derived retinal pigment epithelium patch in age-related macular degeneration.* Nat Biotechnol, 2018. **36**(4): p. 328-337.
68. Kashani, A.H., et al., *A bioengineered retinal pigment epithelial monolayer for advanced, dry age-related macular degeneration.* Sci Transl Med, 2018. **10**(435).
69. Ghosh, S., et al., *A Role for betaA3/A1-Crystallin in Type 2 EMT of RPE Cells Occurring in Dry Age-Related Macular Degeneration.* Invest Ophthalmol Vis Sci, 2018. **59**(4): p. Amd104-amd113.
70. Zanzottera, E.C., et al., *Visualizing Retinal Pigment Epithelium Phenotypes In The Transition To Geographic Atrophy In Age-Related Macular Degeneration.* Retina, 2016. **36 Suppl 1**: p. S12-s25.
71. Sarks, J.P., S.H. Sarks, and M.C. Killingsworth, *Evolution of geographic atrophy of the retinal pigment epithelium.* Eye (Lond), 1988. **2 (Pt 5)**: p. 552-77.
72. Hirasawa, M., et al., *Transcriptional factors associated with epithelial-mesenchymal transition in choroidal neovascularization.* Mol Vis, 2011. **17**: p. 1222-30.
73. Ohlmann, A., et al., *Epithelial-mesenchymal transition of the retinal pigment epithelium causes choriocapillaris atrophy.* Histochem Cell Biol, 2016. **146**(6): p. 769-780.
74. Khan, M.A., C.J. Brady, and R.S. Kaiser, *Clinical management of proliferative vitreoretinopathy: an update.* Retina, 2015. **35**(2): p. 165-75.
75. Kanda, A., et al., *TGF-beta-SNAIL axis induces Muller glial-mesenchymal transition in the pathogenesis of idiopathic epiretinal membrane.* Sci Rep, 2019. **9**(1): p. 673.
76. Eastlake, K., et al., *Muller glia as an important source of cytokines and inflammatory factors present in the gliotic retina during proliferative vitreoretinopathy.* Glia, 2016. **64**(4): p. 495-506.
77. Zhou, T., et al., *Mesenchymal marker expression is elevated in Muller cells exposed to high glucose and in animal models of diabetic retinopathy.* Oncotarget, 2017. **8**(3): p. 4582-4594.

78. Chaffer, C.L. and R.A. Weinberg, *A perspective on cancer cell metastasis.* Science, 2011. **331**(6024): p. 1559-64.
79. Yan, S., et al., *Epithelial-Mesenchymal Expression Phenotype of Primary Melanoma and Matched Metastases and Relationship with Overall Survival.* Anticancer Res, 2016. **36**(12): p. 6449-6456.
80. Bharti, K., S.S. Miller, and H. Arnheiter, *The new paradigm: retinal pigment epithelium cells generated from embryonic or induced pluripotent stem cells.* Pigment Cell Melanoma Res, 2011. **24**(1): p. 21-34.
81. Venkatesan, A.M., et al., *Ligand-activated BMP signaling inhibits cell differentiation and death to promote melanoma.* J Clin Invest, 2017.

APPENDIX

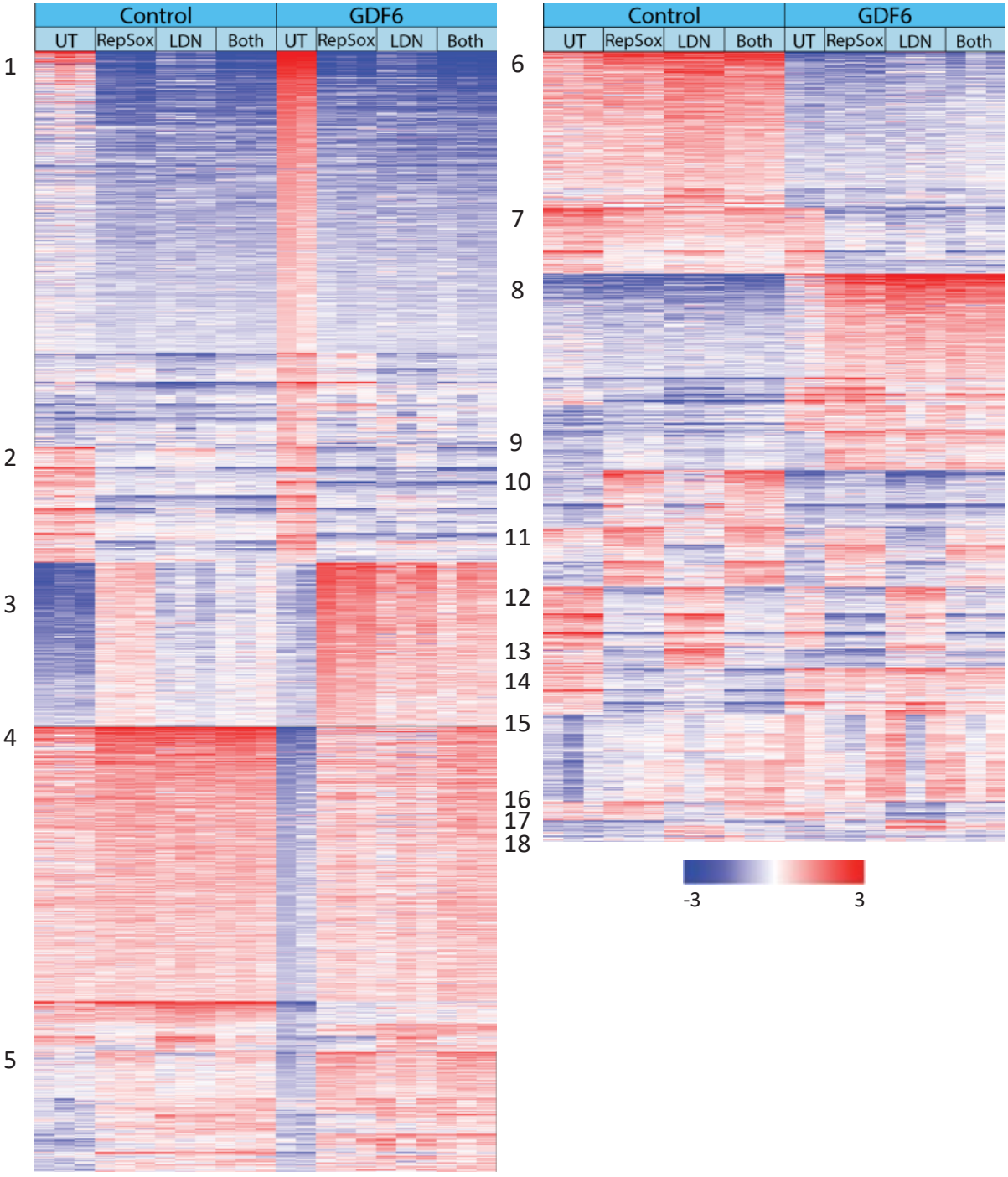

Supplemental Figure 5.1. Complete RNA-Seq AutoSOME Clustering of RPE treated with Smad phosphorylation inhibitors. Clusters were manually placed into 18 larger subgroups from 171 unique clusters. Color bar represents the Log (Fold Change) of the gene, with blue representing down-regulated genes and red representing up-regulated genes.

Description for Supplemental Files

- Supplemental File 5-1. Normalized Reads Per Million (RPM) of all differentially expressed genes.
- Supplemental File 5-2. Gene expression information of the 4 clusters presented in Figure 5.1.
- Supplemental File 5-3. Genes up or down-regulated in RPE exposed to *GDF6*, regardless of treatment (Figure 5.2).

ACRONYM LIST

ActRI	Activin Receptor 1
ActRII	Activin Receptor 2
AD-MSC	Adipose-Derived Mesenchymal Stem Cells
Alk	Activin-like Kinase
AMD	Age-Related Macular Degeneration
AMH	Anti-Mullerian Hormone
BM	Bruch's Membrane
BMP	Bone Morphogenic Protein
BMP4	Bone Morphogenic Protein 4
BMP7	Bone Morphogenic Protein 7
BMPRI	BMP Receptor 1
BMPRII	Bone Morphogenic Protein Receptor 2
Cas9	CRISPR-associated Protein 9
CDH1	Epithelial Cadherin (E-cadherin)
CDH11	Cadherin 11
CDH2	Mesenchymal Cadherin (N-cadherin)
CDH3	Placental Cadherin (P-cadherin)
CFP	Cyan Fluorescent Protein
CNV	Choroidal Neovascularization
COL1A1	Collagen Type I Alpha 1 Chain
Co-Smads	Common-Mediator Smads

CRISPR	Clustered Regularly Interspaced Short Palindromic Repeats
CRISPRi	CRISPR Interference
CTGF	Connective Tissue Growth Factor
DAN	Differential Screening-Selected Gene in Neuroblastoma
dCas9	Catalytically Inactive Cas9 Protein
DCN	Decorin
DMSO	Dimethyl Sulfoxide
Dvl	Dishevelled
ECM	Extracellular Matrix
EGF	Epidermal Growth Factor
EGFR	Epidermal Growth Factor Receptor
EMT	Epithelial-to-Mesenchymal Transition
Erk	Extracellular Signal-related Kinase
FACS	Fluorescent-Activated Cell Sorting
FGF-2	Fibroblast Growth Factor 2
FGF-5	Fibroblast Growth Factor 5
FN	Fibronectin
FST	Follistatin
GA	Geographic Atrophy
GDF	Growth Differentiation Factor
GDF5	Growth Differentiation Factor 5
GDF6 RPE	RPE overexpressing GDF6 transcripts

GDF6	Growth and Differentiation Factor 6
GDF7	Growth Differentiation Factor 5
GDF8	Myostatin
GDNF	Glial Cell-Derived Neurotrophic Factor
GMT	Glial-to-Mesenchymal Transition
gRNA	Guide RNA
HGF	Hepatocyte Growth Factor
ID1	Inhibitor of DNA Binding 1
IGF-IR	Insulin-Like Growth Factor Receptor I
iPSC	Induced Pluripotent Stem Cell
I-Smads	Inhibitory Smads
JNK	Jun N-terminal Kinase
LAP	Latency Associated Peptide
LATS1/2	Large Tumor Suppressor 1/2
LDN	LDN-193189
LEF	Lymphoid Enhancer Factor
LIMK1	LIM Domain Kinase 1
LRAT	Lecithin Retinol Acyltransferase
MAPK	Mitogen-activated Protein Kinase
Met	Hepatocyte Growth Factor Receptor
MET	Mesenchymal-to-Epithelial Transition
MOI	Multiplicity of Infection

MSC	Mesenchymal Stem Cells
MST 1/2	Mammalian Sterile 20-like 1 and 2
MSX2	Msh Homeobox 2
NEHJ	Non-Homologous End Joining
NP	Nucleus Pulposus
oBRB	Outer Blood-Retina Barrier
ORF	Open Reading Frame
OTX2	Orthodenticle Homeobox 2
P0	Passage 0
P1	Passage 1
P2	Passage 2
P3	Passage 3
P5	Passage 5
P7	Passage 7
PBS	Phosphate Buffered Saline
PDGF	Platelet Derived Growth Factor
PEDF	Pigment Epithelium-Derived Factor
PMEL	Premelanosome Protein
PVDF	Polyvinylidene Fluoride
PVR	Proliferative Vitreoretinopathy
rmGdf6	Recombinant Mouse GDF6
RNA-seq	RNA-sequencing

RPE	Retinal Pigmented Epithelium
RPE65	Retinoid Isomerase
RPM	Read Counts Per Million
R-Smad	Receptor-Activated Smad
RTK	Receptor Tyrosine Kinase
RT-qPCR	Real-Time Quantitative Polymerase Chain Reaction
SARA	Smad Anchor for Receptor Activation
SDS-PAGE	Sodium Dodecyl Sulfate-Polyacrylamide Gel Electrophoresis
SNAI1	Snail Family Transcriptional Repressor 1
SOST	Sclerostin
SPP1	Osteopontin
TAZ	Transcriptional Coactivator with PDZ-Binding Motif
TBST	0.1% Tween 20
TCF	Transcription Factor T-Cell Factor
TEAD	TEA-Domain Containing Transcription Factor
TGFβ	Transforming Growth Factor β
TGFβ1	Transforming Growth Factor β1
TGFβ2	Transforming Growth Factor β2
TGFβRI	Transforming Growth Factor β Receptor 1
TGFβRII	Transforming Growth Factor β Receptor 2
TSP-1	Thrombospondin-1
TSS	Transcription Start Site

UBE4A	Ubiquitination Factor E4A
USAG-1	Uterine Sensitization-Associated Gene 1
VEGF	Vascular Endothelial Growth Factor
VIM	Vimetin
YAP	Yes-Associated Protein 1
YFP	Yellow Fluorescent Protein